Institutional Repository - Research Portal
Dépôt Institutionnel - Portail de la Recherche
researchportal.unamur.be
University of Namur

THESIS / THÈSE

MASTER IN BIOCHEMISTRY AND MOLECULAR AND CELLULAR BIOLOGY

Characterization of immune response against brucella melitensis following an intra-dermal infection in mice

Demars, Aurore

Award date:
2016

Awarding institution:
University of Namur

Link to publication

General rights
Copyright and moral rights for the publications made accessible in the public portal are retained by the authors and/or other copyright owners and it is a condition of accessing publications that users recognise and abide by the legal requirements associated with these rights.

- Users may download and print one copy of any publication from the public portal for the purpose of private study or research.
- You may not further distribute the material or use it for any profit-making activity or commercial gain
- You may freely distribute the URL identifying the publication in the public portal ?

Take down policy
If you believe that this document breaches copyright please contact us providing details, and we will remove access to the work immediately and investigate your claim.

Download date: 02. May. 2026



UNIVERSITE DE NAMUR

Faculté des Sciences

CHARACTERIZATION OF IMMUNE RESPONSE AGAINST *BRUCELLA MELITENSIS* FOLLOWING AN INTRA-DERMAL INFECTION IN MICE

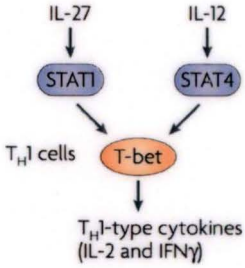
Mémoire présenté pour l'obtention

du grade académique de master 120 en biochimie et biologie moléculaire et cellulaire

Aurore DEMARS

Janvier 2016

Other deficient mice



STAT-1$^{-/-}$: STAT-1/T-bet pathway is activated by IL-27. Mice deficient for STAT-1 can not induce IFN-γ by this pathway.

IL-12p35$^{-/-}$: Mice deficient for IL-12p35 are deficient for the IL-12 cytokine and are thus unable to produce IFN-γ by the STAT-4/T-bet pathway.

T-bet$^{-/-}$: Mice deficient for T-bet are unable to produce IFN-γ by T-bet pathway.

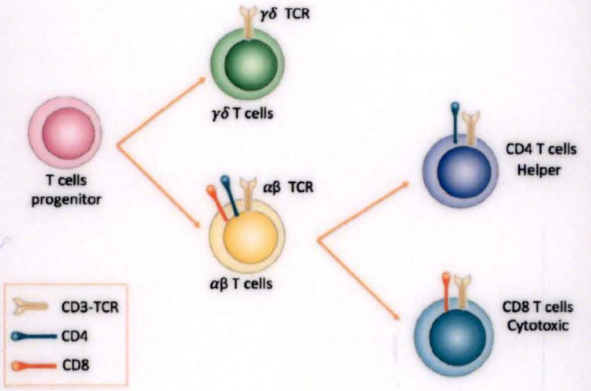
IFN-γR$^{-/-}$: the receptor of IFN-γ is present at the surface of infected cells and is involved in the induction of effector mechanisms and activation of monocytes. Mice deficient for IFN-γR are so in the impossibility to induce effector mechanisms to fight ***Brucella***.

IL-17RA$^{-/-}$: IL-17RA-deficient mice are deficient for the receptor of IL-17, the cytokine released by a T_H17 immune response. IL-17RA-deficient mice have thus a failure in the T_H17 response.

CCR2$^{-/-}$: Mice deficient for this receptor attract monocytes at the place of infection with a delay time.

MuMT$^{-/-}$: Mice deficient for MuMT are devoid of all B cells.

Mice deficient for T cells



$CD3^{-/-}$: CD3-deficient mice are devoid of all T lymphocytes (T cells).

$\alpha\beta TCR^{-/-}$ and $\gamma\delta TCR^{-/-}$: In 95 % of cases, the TCR is composed of α/β chains. These cells possess two co-receptors: CD4 and CD8. The αβTCR-deficient mice are so deficient for $CD8^+$ and $CD4^+$ T cells. In 5 % of the cases, the TCR is composed of γ/δ chains. γδTCR-deficient mice are thus devoid of this peculiar type of T cells.

$MHCII^{-/-}$ (≈$CD4^{-/-}$): Mice deprived of $CD4^+$ T cells are obtained by using MHCII-deficient mice unable to present peptides and to select $CD4^+$ T cells differentiation in the thymus.

$TAP\text{-}1^{-/-}$ (≈$CD8^{-/-}$): Mice deprived of $CD8^+$ T cells are obtained by using TAP1-deficient mice unable to load peptides in the MHCI of the antigen-presenting cells (APC) and to select $CD8^+$ T cells differentiation in the thymus.

Université de Namur
FACULTE DES SCIENCES
Secrétariat du Département de Biologie
Rue de Bruxelles 61 - 5000 NAMUR
Téléphone: + 32(0)81.72.44.18 - Téléfax: + 32(0)81.72.44.20
E-mail: joelle.jonet@unamur.be - http://www.unamur.be

Caractérisation de la réponse immunitaire contre *Brucella melitensis* dans un modèle d'infection intra-dermique en souris

DEMARS Aurore

Résumé

Brucellae spp. (α-proteobactéries) sont des bactéries Gram-négatives intracellulaires qui causent la brucellose, une zoonose à échelle mondiale. Chez les animaux, la maladie est caractérisée par l'avortement chez les femelles et l'infertilité chez les mâles. L'humain est un hôte accidentel pouvant être infecté de manière chronique. Dans ce mémoire, nous étudions la souche *Brucella melitensis* 16M qui infecte les chèvres et les moutons. Nous étudions la réponse immunitaire chez la souris après une infection intra-dermique (ID). Ce modèle expérimental imite l'infection naturelle de *Brucella* par contact direct entre une lésion cutanée et des tissus ou liquides infectés, cas ayant été rapportés chez les fermiers, vétérinaires ou bouchers.
Les principaux objectifs de ce mémoire sont (i) la caractérisation de la cinétique de l'infection ID par *B. melitensis* dans des souris C57BL/6 sauvages, (ii) la caractérisation phénotipique des cellules infectées dans la peau et le ganglion drainant, (iii) l'identification de la sous-classe "T helper" contrôlant l'infection intra-dermique et (iv) l'identification des cellules lymphoïdes impliquées dans le contrôle de l'infection ID primaire et secondaire.
Nos résultats suggèrent qu'après infection en ID, *B. melitensis* se multiplie activement dans la peau et dissémine dans le ganglion lymphatique drainant et dans la rate pour atteindre le pic de charge bactérienne après 3 jours d'infection. Après 50 jours, *B melitensis* est presque entièrement éliminée de la peau et du ganglion, mais persiste dans la rate, suggérant que le système immunitaire est capable de contrôler efficacement sa croissance dans la peau. Dans la lésion, quelques cellules infectées sont positives pour les marqueurs MHCII, CD11c et Ly-6G, suggérant que les cellules infectées aux temps précoces de l'infection ne sont ni des monocytes activés, ni des cellules dendritiques, ni des neutrophiles. En utilisant une batterie de souris rendues génétiquement déficientes pour des éléments clés du système immunitaire, nous observons que la réponse T_H1 médiée par l'IFN-γ est indispensable pour contrôler l'infection dans la peau. Lors de l'infection primaire, les lymphocytes $CD4^+$ semblent être les principales cellules contrôlant l'infection. Cependant, nous démontrons que l'absence de lymphocytes $\alpha\beta TCR^+$ peut être compensée par les lymphocytes $\gamma\delta TCR^+$ après une infection secondaire. En plus, un rôle important des cellules B a été observé pour contrôler l'infection secondaire, mais pas la primaire.

Mémoire de master 120 en biochimie et biologie moléculaire et cellulaire

Janvier 2016

Promoteur: E. Muraille, **Co-Promoteur:** J.-J. Letesson

Université de Namur
FACULTE DES SCIENCES
Secrétariat du Département de Biologie
Rue de Bruxelles 61 - 5000 NAMUR
Téléphone: + 32(0)81.72.44.18 - Téléfax: + 32(0)81.72.44.20
E-mail: joelle.jonet@unamur.be - http://www.unamur.be

Characterization of immune response against *Brucella melitensis* following an intra-dermal infection in mice

DEMARS Aurore

Abstract

Brucellae spp. (α-proteobacteria) are Gram-negative intracellular bacteria that cause brucellosis, a worldwide zoonosis. In animals, the disease is characterized by abortion in females and infertility in males. Human is an accidental host who can be chronically infected. In this master thesis, we study the *Brucella melitensis* 16M strain, that infects goat and sheep. We investigate the immune response of mice following intra-dermal (ID) infection. This experimental model mimics the natural *Brucella* infection by direct contact between skin lesion and infected tissue or fluid, which has been reported in farmers, vets or butchers.

The main objectives of this master thesis are (i) the characterization of the course of the intra-dermal (ID) *B. melitensis* infection in wild type C57BL/6 mice, (ii) the phenotypic characterization of infected cells in the skin and draining lymph node, (iii) the identification of the T helper subclasses of immune response controlling the intra-dermal infection and (iv) the identification of lymphoid cells involved in the control of primary and secondary ID infections.

Our results showed that following ID infection, *B. melitensis* actively multiplies in skin lesion and disseminate in draining lymph node (dLN) and spleen to reach a peak of bacterial load at 3 days post-infection. At 50 days, *B. melitensis* is almost completely eliminated from skin lesion and dLN but persists in spleen, suggesting that the immune system is able to efficiently control its growth in skin tissues. In the lesion, only a few fraction of infected cells appears to be positive for MHCII, CD11c and Ly-6G markers, suggesting that infected cells at early times post-infection are neither activated monocytes, nor dendritic cells, nor neutrophils, respectively. Using a battery of mice genetically deficient for key elements of immune system, we observed that the IFN-γ-mediated T helper (T_H)1 response is indispensable to control skin infection. During a primary infection, $CD4^+$ T lymphocytes seem be the main cells controlling the infection. However, we demonstrate that the absence of $\alpha\beta TCR^+$ lymphocytes can be compensated by $\gamma\delta TCR^+$ lymphocytes after a secondary infection. In addition, an important role of B cells has been observed to control the bacteria during secondary, but not primary, infection.

Master Thesis 120 in molecular and cellular biochemistry and biology

January 2016

Supervisor: E. Muraille, **Co-supervisor**: J.-J. Letesson

ACKNOWLEDGEMENTS

Le mémoire représente nos premiers mois de travail dans un laboratoire. C'est la découverte de méthodes de travail, de rigueur, de la vie au sein d'une communauté. C'est également la remise d'un travail final, reflétant le travail effectué tout au long de ces 10 mois, mais aussi l'aboutissement de 5 années d'études.

Tout d'abord, j'aimerais remercier mon promoteur, le Docteur Eric Muraille de m'avoir donné le goût à l'immunologie, mais aussi pour ses conseils, son savoir et pour sa grande disponibilité, ainsi que mon co-promoteur, le Professeur Jean-Jacques Letesson, pour ses précieux conseils et le temps qu'il m'a consacré. Merci à vous deux pour le suivi apporté tout au long du mémoire.

Je remercie également l'ensemble des membres de mon jury, Mme Elodie Lobet, les Professeurs Yves Poumay et Benoit Muylkens, ainsi que le Docteur Matthieu Terwagne, pour le temps et l'attention consacrés à la lecture de ce travail.

Ensuite, j'aimerais remercier bien évidemment tout le labo qui m'a accueilli le temps de cette belle aventure. Merci à Arnaud, Simon, Kévin, Jérôme, Georges, Eme, Nayla, Mathilde, Phuong, Vicky, Katty, Séverin, Lio, J-F, Dunia, Christian, … et tous les autres! Merci aux personnes que j'ai côtoyées au BL3 pour l'aide et les échanges.

Merci à toi Popo, fidèle compagnon Bio, pour le temps que tu as consacré à la relecture de ce manuscrit. Promis, je ferai des efforts pour ne plus confondre les "." et les ",".

Merci aux mémorants de choc de cette année: Rosa, Manon, Gwen, Hélène et Nico! Je garderai de très bons souvenirs de ce bureau partagé! Merci pour votre soutien et tous ces moments de joie et de folies! On recommence l'année prochaine?

Manon (K******), je tenais à te remercier particulièrement. Un grand merci pour tout: l'aide dans le travail, le soutien, les moments de fous rire, les discussions, … Je pense qu'on a formé un duo parfait! P.S.: Je confirme, j'aurais dû t'inscrire à l'émission concernant les lubies alimentaires.

Arnaud, je commencerai par te dire merci pour avoir su changer ma vision du travail en labo et avoir su me donner goût à la recherche! Ensuite, merci pour ton aide, ton temps, ta patience, ton partage de connaissances, les nombreuses discussions et tout simplement ta façon d'être. Merci! Je crois qu'on n'aurait pas su tomber sur meilleur encadrant! Manon et toi avez été de très belles rencontres, on se reverra (désolée pour vous…).

Merci à la team Gémo (Julie, Clément, Carlo et Popo) pour l'organisation de la « Beer hour », que Gwen, et son horloge biologique programmée à 16h chaque vendredi, ne manquait pas de nous rappeler.

Je n'oublierai pas de remercier mes parents pour m'avoir permis de réaliser ces études et pour leur soutien tout au long de ces années! Merci à toi papy pour ton intérêt pour la brucellose et merci Cédric pour ta patience, ton aide précieuse et ton soutien au quotidien!

Merci aux souris sacrifiées pour le travail, sans qui rien n'aurait été possible!
De manière générale, un tout grand merci à toutes les personnes qui auront contribué, de loin ou de près, à la réalisation de ce projet.

LIST OF ABBREVIATIONS

aBCV	Autophagy *Brucellae*-containing vacuole
AD	Anno Domini
APC	Antigenic presenting cells
ATP	Adenosine Triphosphate
B.	*Brucellae*
BCR	B cell receptors
BCV	*Brucellae*-containing vacuole
BtpB	*Brucellae* TIR-containing protein B
C57BL/6	C57 black 6
CCR2	C-C chemokine receptor type 2
CD	Cluster of differentiation
CD4/CD8	CD4/8 αβTCR T cells
CFU	Colony forming units
CLIP	Class II-associated invariant chain peptide
CpG	Cytosine phosphate Guanine
d.	Day
DAMPs	Damage associated molecular patterns
DC	Dendritic cells
DETC	Dendritic epidermal T cells
dLN	Draining lymph node
DNA	Deoxyribonucleic acid
eBCV	Endosomal *Brucellae*-containing vacuole
EE	Early endosome
ELISA	Enzyme-linked immunosorbent assay
ER	Endoplasmic reticulum
ERES	Endoplasmic reticulum exit site
HEV	High endothelial venule
HK	Heat-killed
ID	Intra-dermal
IFN-γ	Interferon-gamma
Ig	Immunoglobulin
IL	Interleukin
ILC	Innate lymphoid cells
IN	Intra-nasal
iNOS	Inducible nitric oxide synthase
IP	Intra-peritoneal
ITAM	Immunoreceptor Tyrosine-based Activation Motif
JAK	Janus kinases
Kan	Kanamycin
LAMP1	Lysosomal-associated membrane proteins
LB	Luria-Bertani

LC	Langerhans cells
LE	Late endosome
li	Invariant chain
LPS	Lipopolysaccharides
Lys	Lysosomes
MHC	Major histocompatibility complex
MyD88	Myeloid differentiation primary response gene 88
NADPH	Nicotinamide adenine dinucleotide phosphate
Nal	Nalidixic
NETs	Neutrophils extracellular traps
NK	Natural killer
NKT	Natural killer T cells
NO	Nitric oxide
ns	Non significant
OD	Optical density
P	P-value
p.i.	Post-infection
PAMPs	Pathogen-associated molecular patterns
PBS	Phosphate Buffer Sodium
PFA	Paraformaldehyde
pH	Hydrogen Potential
PRR	Pattern recognition receptors
rBCV	Replicative *Brucellae*-containing vacuole
RNI	Reactive nitrogen intermediate
ROI	Reactive oxygen intermediate
rpm	Revolution per minute
RPMI	Roswell Park Memorial Institute medium
RT	Room Temperature
spp	Species pluralis
STAT	Signal Transducers and Activators of Transcription
T-bet	T-box expressed T cells
T4SS	Type IV secretion system
TAP1	Antigen peptide transporter 1
TCR	T cell receptor
TGF	Transforming Growth Factor
TH	T helper
TLR	Tool-like receptors
TMB	Tetramethylbenzidine
TNF-α	Tumor necrosis factor alpha
Treg	T regulatory
WHO	World Health Organization
WT	Wild type
YT	Yeast Extract Tryptone

TABLE OF CONTENTS

ACKNOLEDGMENTS 4
LIST OF ABBREVIATIONS 5
INTRODUCTION 10
1 Biological interactions 11
2 The *Brucella* genus 11
2.1 Discovery of *Brucella* 11
2.2 Strains and specific hosts 11
2.3 Pathology of brucellosis 12
2.3.1 Epidemiology 12
2.3.2 Pathology and transmission 12
2.3.3 Diagnosis and treatments 13
3 The immune system 13
3.1 Lymphoid organs 14
3.2 Innate immune system 14
3.2.1 The skin and mucosa: first barriers 14
3.2.2 Detection of bacterial pathogens 15
3.2.3 Innate immune defence mechanisms 15
3.3 Transition between innate and adaptive immunity: APC 18
3.4 Adaptive immune system 18
3.4.1 The T lymphocytes or T cells 18
3.4.2 The non-conventional T cells 22
3.4.3. The B lymphocytes or B cells 23
3.5 Immune memory 24
3.6 Skin immunity 25
3.6.1 Structure of the skin 25
3.6.2 Immunity of the skin 27
4 Experimental models to study *Brucellae* infection 28
4.1 Discovery from *in vitro* models: the trafficking 28
4.2 *In vivo* study models: *Mus musculus* 30
4.2.1 Intra-peritoneal (IP) infection model 30
4.2.2 Intra-nasal (IN) infection model 31
4.2.3 Intra-dermal (ID) infection model 33
OBJECTIVES 35
RESULTS 36
1 Characterization of WT C57BL/6 mice after intra-dermal infection 37
2 Phenotype of infected cells 39
3 Characterization of immune response following primary ID infection 46
4 Identification of lymphocyte cells critically involved in the control of primary and secondary *Brucella* infection 49
4.1 Primary immune response following ID infection 49
4.2 Secondary immune response following ID infection 51
DISCUSSION 54
1 Characterization of WT C57BL/6 mice after intra-dermal infection 55
2 Characterization of immune response following primary ID infection 56
3 Identification of lymphocyte cells critically involved in the control of primary and secondary *Brucella* infection 57
3.1 Primary immune response following ID infection 57
3.2 Secondary immune response following ID infection 58
CONCLUSION AND PERSPECTIVES 60
MATERIALS AND METHODS 63
1 Materials 64
1.1 Bacterial strain 64
1.2 Mice of experiments 64

1.3 Ethics statements 65
1.4 Medium, products and solutions 65
1.4.1 2 YT agar 65
1.4.2 PBS X10 (Phosphate Buffer Saline) 65
1.4.3 PBS-Triton-X100 65
1.4.4 FACS buffer 66
1.4.5 Sucrose solution (20 %) 66
1.4.6 Blocking solution 66
1.4.7 Paraformaldehyde (PFA – 4 %) 66
1.4.8 DNase/Collagenase 66
1.4.9 Products references 67
2 Methods 68
2.1 *Brucella melitensis* strain streaking 68
2.2 Liquid culture 68
2.3 Preparation of infectious dose 68
2.4 Infection of mice 68
2.5 Euthanasia of mice and dissection 69
2.6 Evaluation of bacterial load (colony forming units) 69
2.6.1 Principle 69
2.6.2 Method 69
2.7 Preparation of tissues for analysis by immunohistology 70
2.7.1 Principle 70
2.7.2 Method 70
2.8 Blood sampling 70
2.9 ELISA test 71
2.9.1 Principle 71
2.9.2 Method 71
2.10 Mice immunization and challenge 72
2.11 Antibiotic treatment 72
2.12 Measure of lesion size 72
2.13 Statistical analysis 72
APPENDIX 73
REFERENCES 76

« Il ne faut pas penser à l'objectif à atteindre, il faut seulement penser à avancer. C'est ainsi, à force d'avancer, qu'on atteint ou qu'on dépasse ses objectifs sans même s'en apercevoir ».

Bernard Werber

Introduction

Species	Host preference
Brucella abortus	Cattle
Brucella canis	Dog
Brucella ceti	Marine mammals (Cetacea)
Brucella inopinata	Isolated from a breast implant infection[1]
Brucella melitensis	Sheep, goat
Brucella microti	Common vole
Brucella neotomae	Desert woodrat
Brucella ovis	Sheep
Brucella pinnipedialis	Seal
Brucella papionis	Baboon

Table 1: Different species of *Brucella* genus and their specific hosts

Table of the different strains of *Brucellae* associated with the specific host. The most virulent strains for humans are: *B. melitensis, B. abortus, B. canis* and *B. suis* (V. L. Atluri *et al.*, 2011). *B. : Brucella.*

[1] Scholz *et al.*, 2010

INTRODUCTION

1 Biological interactions

Symbiosis (from Greek σύν "together" and βίωσις "living") is a close and often a long-term interaction between two organisms and exists since the apparition of life on Earth. These relationships between partners are based on inter-interactions. Examples of symbiosis are present everywhere: the barnacles attached to the whales to move long distances, the peak beef heron finding its food by removing the parasites from large mammals or a flower synthesizing a pheromone of a female insect to attract the male and to allow pollen dispersal.

A symbiotic relation between organisms can be beneficial for both partners (mutualism), beneficial for one partner without detriment for the second one (commensalism), or this relation can be beneficial for one partner and harmful for the second one (parasitism). Partners that cause damage are called pathogens. Most of the time, the interest of the pathogen is to keep in life its host to have a durable relation to continue to survive and to proliferate. Killing the host would have no advantage for the pathogen in this case. To successfully adapt to the environment of the host, the pathogen, which is often a microorganism (virus, bacterium, protozoan), must escape to the host's immune system and mechanisms established to fight it. This kind of interaction is very dynamic and is in constant evolution.

In this master thesis, the studied pathogen is the bacterium *Brucella melitensis*, that can cause a chronic infection in mammals, including humans. We focus on the immune system of mice during an intra-dermal infection by *Brucella melitensis*.

2 The *Brucella* genus

2.1 Discovery of *Brucella*

In 1884, the military physician David Bruce is sent to the island of Malta. There, a mysterious disease causes temperature waves and the death of soldiers. In 1887, D. Bruce realizes autopsies on spleens, livers and kidneys of dead soldiers having suffered of undulant fevers. An organism of about 3 micrometers and with a Gram-negative staining is discovered and is called *Micrococcus melitensis* (Tan S Y *et al.*, 2011).

Now, the causative agent has been renamed *Brucella melitensis* and is well described: *Brucella* spp. is a Gram-negative non-motile coccobacillus bacterium belonging to the α-proteobacteria class. This bacterium is intracellular and facultatively extracellular (E. Moreno and I. Moriyon, 2006). *Brucella* is the agent of brucellosis, a worldwide zoonosis (G. Pappas *et al.*, 2006). This disease is also called Mediterranean fever, Malta fever or undulant fever due to temperatures waves undergone by infected people (Tan S Y *et al.*, 2011). From that moment, other species of *Brucella* have been discovered.

2.2 Strains and specific hosts

Several species belong to the *Brucella* genus (**table 1**). Among the known species, there are *B. abortus, B. melitensis, B. suis, B. ovis, B. canis*. In the early 2000s, *B. ceti and B. pinnipedialis* have been described, followed by *B. inopinata* (Scholz *et al.*, 2010) *and B. microti*. More

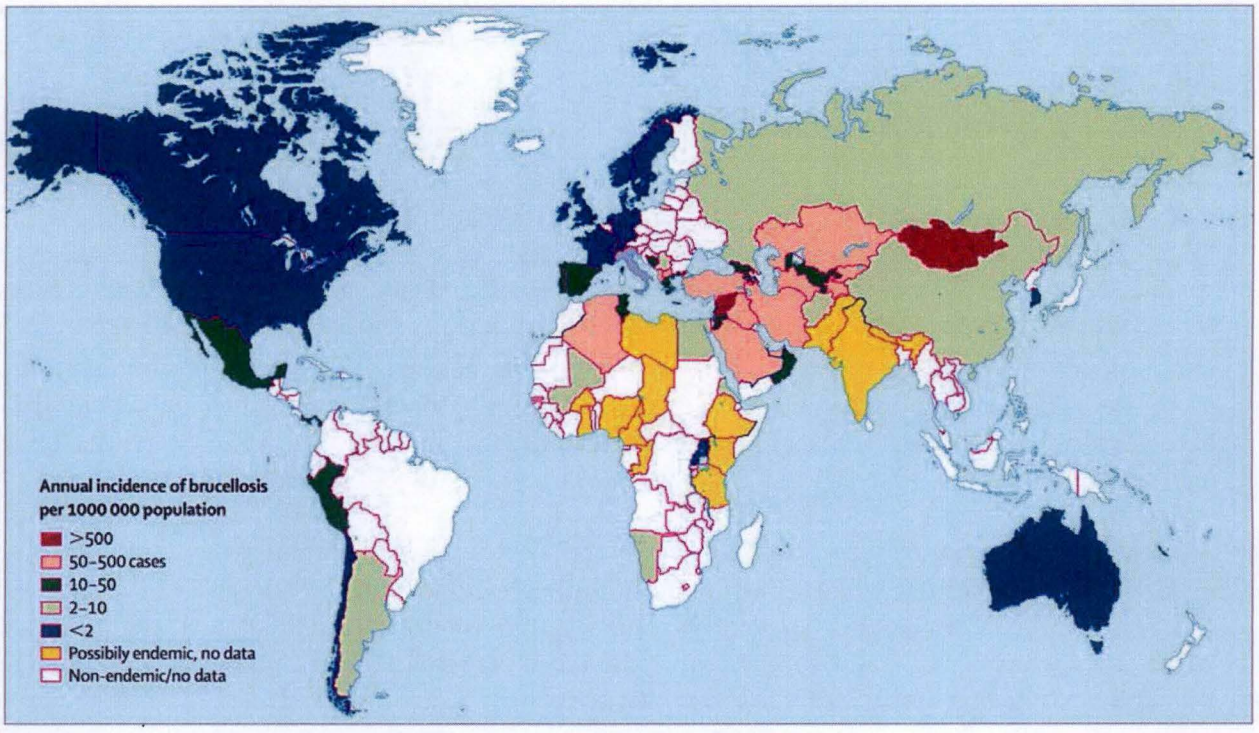


Figure 1: Worldwide incidence of human brucellosis in 2006

Brucellosis is widespread throughout the world, and more than 500,000 new cases are reported each year (Pappas *et al.*, 2006). The real number of cases of brucellosis is higher but they are not all recorded due to a lack of diagnosis.

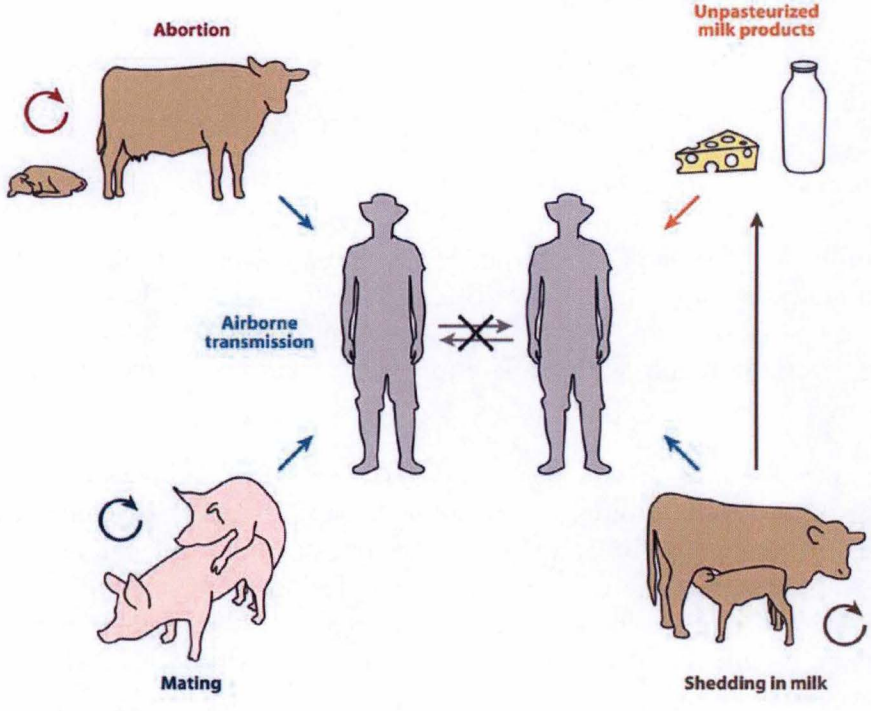


Figure 2: Different transmission paths of *Brucellae*

The transmission of *Brucellae* between animals can occur through aerosols during abortion, shedding in milk or reproduction. Humans can be infected through ingestion of unpasteurized dairy products or aerosols. The human-human transmission is rarely described and is insignificant (in terms of mode of infection) (Alturi *et al.*, 2011).

recently, new species have been discovered: the first isolated from amphibians and the second from primates, *B. papionis* (T. Eisenberg *et al.*, 2012 ; A. Whatmore *et al.*, 2014). Each species has its own specific host. For example, *B. abortus* is specific to the cattle, *B. ovis* has the sheep as specific host and *B. ceti* is able to infect marine mammals such as dolphin (D. R. Ewalt *et al.*, 1994). Some of these species are sometimes found in humans such as *B. abortus*, *B. melitensis, B. suis* biovar 1 and *B. canis* (V. L. Atluri *et al.*, 2011 ; E. M. Galinska and J. Zagorki, 2013). In these cases, human is considered as an accidental host. The most virulent strain for human seems to be *B. melitensis* (which has as specific hosts goat and sheep).

2.3 Pathology of brucellosis

Brucellosis is a frequent cause of disease in domesticated animals but also in humans. It is not an emerging disease. Indeed, an examination of skeletons of humans dead in 79 AD during the Mount Vesuvius eruption has revealed typical bones lesions of brucellosis in more than 17 % of cases (L. Capasso *et al.*, 2002). More recently, the analysis of *Australopithecus africanus* skeleton has revealed that the lesions seemed to be the same than the one of a person infected by *Brucella*. This discovery could place the origin of brucellosis to about 2.5 millions years ago (D'anastio *et al.*, 2009). However, the first real clues of brucellosis date of Middle Ages with the screening and DNA sequencing that reveal the *Brucella* DNA on skeletal from the Ancient Albanian city (Mutolo *et al.*, 2012).

2.3.1 Epidemiology

Because brucellosis is a zoonosis, the incidence of human brucellosis is linked with the frequency of the disease in animals, its natural reservoir. The incidence of human brucellosis remains very high in areas where brucellosis is endemic in domestic animals (**figure 1**), *i.e.*, Africa, Asia, Latin America and Kuwait with an average of 500,000 new reported cases each year. In Europe, northern countries have eradicated brucellosis and have a brucellosis-free status. However, several countries from the south of Europe still possess an endemic brucellosis status such as Greece, Spain or Portugal (S. J. Cutler *et al.*, 2005; G. Pappas *et al.*, 2006; P. de Figueiredo *et al.*, 2015).

2.3.2 Pathology and transmission

In the specific host, *Brucella* has a tropism for the reproductive tract that results in abortion in pregnant females and infertility in males (A. V. Carvalho Neta *et al.*, 2010; V. L. Atluri *et al.*, 2011). Consequently, the disease causes major economic damage for livestock producers. For example, the production loss of milk and meat induces annual economical shortfall of 600 million of dollars by year in Latin America (M. N. Seleem *et al.*, 2010). The horizontal transmission of bacteria occurs through aerosols (during the abortion), via genital contact during mating or via shedding in milk (**figure 2**).

As depicted above, human is an accidental host of *Brucella*. The infection is frequently transmitted from animals to human through ingestion of unpasteurized dairy products, inhalation during animal abortion or contact of conjunctiva or skin lesions with infected amniotic fluids or placenta (**figure 2**) (V. L. Atluri *et al.*, 2011; E. M. Galinska and J. Zagorki, 2013). Transmission between humans by tissue transplantation or sexual contact has occasionally been reported but is more anecdotic (B. G. Mantur *et al.*, 1996).

In humans, the infection results in undulant fevers in the acute phase whereas the chronic phase

	Innate system	Adaptive system
Cellular immunity	- Granulocytes (neutrophils, eosinophils, basophils) - Monocytes (which will give macrophages and dendritic cells) - Cytotoxic cells (Natural Killers)	- Lymphocytes (B and T)
Humoral immunity	- Complement	- Immunoglobulins (antibodies)

Table 2: Interaction of immune system and the components of immunity

Immune system is composed of the innate and the adaptive responses. These responses are possible via different partners, soluble and cellular, that interact together. The main cellular partners in the innate immunity are the granulocytes, the monocytes and the cytotoxic cells. In the adaptive response, the cellular components are the lymphocytes. Concerning the humoral immunity, the complement cascade constitutes the main humoral mechanism in the innate immunity, and the antibodies are the main humoral effectors in the adaptive response.

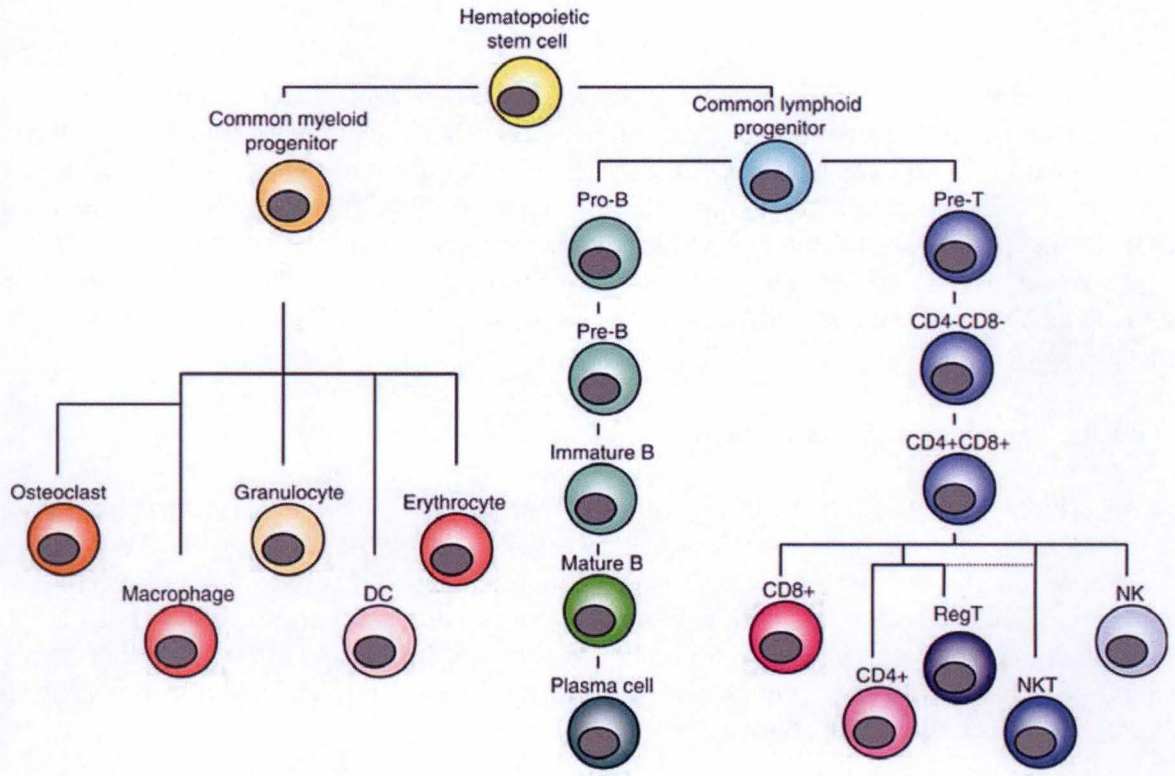


Figure 3: Hematopoietic cells

Differentiation of hematopoietic stem cells to give the progenitors of myeloid cells and lymphoid cells. Lymphoid progenitors are divided in B and T cells, and these latter cells are subdivided into $CD8^+$, $CD4^+$, regT, NKT and NK cells. Myeloid progenitors are divided into dendritic cells (DCs), macrophages, granulocytes, erythrocytes and osteoclasts (Adapted from V. Bottero *et al.*, 2006). CD: cluster of differentiation, regT : T regulatory, NKT : Natural Killer T, NK : Natural Killer.

is characterized by tiredness, muscular pain (P. de Figueiredo *et al.*, 2015), but also serious clinical manifestations such as orchitis, osteoarthritis, spondylitis, neurological disorders, etc. (M. Doganay and B Aygen, 2003). Cutaneous manifestations (rashes, papules, ulcers, abscess, erythema nodosum, ecchymosis, vasculitis or purpura) of brucellosis appear in approximately 8 % of reported cases (J. Ariza *et al.*, 1989; C. Akcali *et al.*, 2007; Z. Karaali *et al.*, 2011).

2.3.3 Diagnosis and treatments

Currently, the methods of brucellosis detection are mainly serodiagnosis. These tests are based on the detection of antibodies anti-*Brucella* such as an anti-LPS. But one major problem with this diagnosis is the impossibility to differentiate an infected animal from a vaccinated one. Another problem is the antigenic similarity between the LPS O chain of *Brucella* and other organisms such as *Yersinia enterocolitica* O9, a Gram-negative enterobacterium (Kittelberger *et al.*, 1995 ; S. J. Cutler *et al.*, 2005 ; E. Moreno and I. Moriyo, 2006).

The treatments to eliminate *Brucella* from an organism are usually a combination of antibiotics (Doxycycline - Rifampicin). The "World Health Organization" (WHO) recommends the following treatment: 600 mg of Rifampicin and 200 mg of Doxycycline a day during 6 weeks. However, this treatment is expensive and there are frequent relapses in patients. The limited number of effective antibiotics and the potential risk of resistance explain the research of alternative solutions (T. A. Ficht *et al.*, 2009). Unfortunately, a protective and safe human vaccine is still lacking although considerable progress has been achieved. The effective vaccines in animals (based on a live attenuated strain of *Brucella*) are still virulent in humans (M. Corbel, 1995; S. J. Cutler *et al.*, 2005; T. A. Ficht *et al.*, 2009). For now, two live attenuated vaccines have been efficiently used for animals: S19 *(B. abortus)* and Rev1 (*B. melitensis*) (E. Moreno and I. Moriyo, 2006).

3 The immune system

The immune system is the main defence mechanism of organisms. It is involved in the detection of foreign bodies, the response against pathogens, the adaptation to a future infection and the distinction between elements of self and non-self (K. Schultz *et al.*, 1987).
In vertebrates, the immune system is divided in two distinct responses, the innate and the adaptive responses, and is composed of a network of interaction between humoral (soluble) and cellular partners (**table 2**). The cellular immunity involves the activation of phagocytic cells, specific T cells and the release of different cytokines. The humoral immunity is mediated by secreted antibodies by activated B cells.

The cells of immunity are derived from bone marrow, containing the pluripotent hematopoietic stem cells. The division of the precursors gives the myeloid cells (innate response) and the lymphoid cells (adaptive response) (**figure 3**). The lymphoid progenitors give the B lymphocytes, that will become plasma cells once activated, and the T cells, subdivided in cluster of differentiation (CD)8 T, CD4 T, T regulatory (regT), Natural Killer T (NKT) and Natural Killer (NK) cells. All these cells will be detailed later. In the myeloid lineage, cells are notably divided in macrophages derived from monocytes, dendritic cells (DCs), erythrocytes and granulocytes (neutrophils, basophils and eosinophils) (V. Bottero *et al.*, 2006).

The efficiency of the immune system is based on the interaction between innate and adaptive responses, using different strategies to detect pathogens. While cells of innate system classically

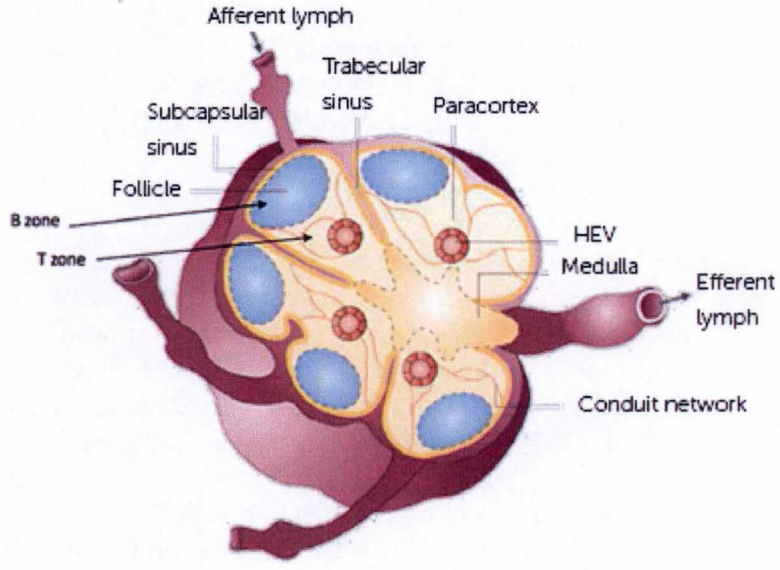


Figure 4: Structure of draining lymph node

A draining lymph node possesses two afferent lymphatic vessels and one efferent. The role of this structure is to drain the lymph circulating in tissue. It is composed of a cortex, a paracortex and a medulla zones. The follicles in the cortex are the zone of B cells. The zone of T cells is around, in the paracortex (adapted from F. Batista *et al.*, 2009).

BOX 1: PRRs

The detection of pathogens is possible through specific receptors called the Pattern Recognition Receptors (PRRs). These receptors are classified in 3 families: the secreted, cytosolic or transmembrane PRRs.

The **secreted PRRs** (collectines, ficolines and pentraxines) bind the surface of pathogens, activate the complement and induce their phagocytosis by macrophages and neutrophils.

The **cytosolic PRRs** include the RLRs (RIG1-like receptors) that recognize viruses, and the NLRs (NOD-like receptors) that detect pathogen and signals from stress conditions.

The **transmembrane PRRs** include the TLRs (Toll-like receptors) that detect a large number of PAMPs on the plasmic membrane or in the endosomes, and the CLRs (C-type lectin receptors) that detect the fungal components.

express Pattern of Recognition Receptors (PRRs) to detect molecular structures specific to micro-organisms (Pathogen Associated Molecular Patterns ; PAMPs), the adaptive system uses specific receptors expressed by B and T lymphocytes (B/T Cell Receptors ; B/TCRs). However, the limit between both systems is more and more vague. For example, lymphocytes express also PRRs and thus can be activated undependably of the T/BCRs.

3.1 Lymphoid organs

The production of immune cells and the encounter between innate immune cells and adaptive immune cells take place in specialized organs, the so-called lymphoid organs. These organs are divided in primary and secondary lymphoid organs. The first are the bone marrow and the thymus. Bone marrow is the place of production of myeloid and lymphoid cells as already said, but also the place of the maturation of B cells while the thymus ensures the maturation of T cells (C. Janeway *et al.*, 2001).

The secondary lymphoid organs are the lymph nodes and the spleen. The role of lymph nodes is to drain the lymph, the biological liquid circulating in the lymphatic vessels. The lymph node possesses two afferent lymphatic vessels and one efferent. The B cells are in follicles in periphery in the cortex and the T cells are around the B cells follicles in the paracortex. In this zone are present the HEVs (high endothelial venules) (**figure 4**). The spleen is composed of white and red pulps. A first role of the spleen is the regulation of erythrocytes formation and destruction in the red pulp. But in this case, it is the white pulp that plays a role in the immunity. Indeed, the white pulp possesses also a T zone and B follicles (Batista *et al.*,2009).

In a context of infection, the lymph containing the infected cells arrives in the lymph node by the afferent lymphatic vessels. The innate infected cells meet the T cells near the HEVs. This process allows the activation of T cells to induce the adaptive immune response (F. Batista *et al.*, 2009). The process of this activation will be detailed later. Once activated, T cells will exit by the efferent lymphatic vessel and will rejoin the blood to migrate to the site ofinfection.

3.2 Innate immune system

The innate immunity is active at early times post-infection (p.i.) because these components are immediately ready to fight pathogens. It is however a non-specific response and the repertory of PRRs is limited and invariant. In addition to the first physical and chemical barriers (*e.g.* skin, gastric pH, etc.), the innate immune system acts by different ways such as: the detection of pathogens, the recruitment of cells at the site of infection, the activation of complement cascade, the activation and orientation of a specific adaptive immune response, etc..
The innate immune response is mediated by both cellular and humoral components, interacting together. The complement belongs to the humoral immunity. Among the cellular effectors are found the granulocytes (neutrophils, eosinophils, basophiles), the monocytes (which will give after differentiation the macrophages and the DCs) and the cytotoxic cells (Natural Killers) (J. Ko and G. Splitter, 2003; A. V. Carvalho Neta *et al.*, 2010, Moser and Leo, 2010).

3.2.1 The skin and mucosa: first barriers

The skin and mucosa are natural barriers protecting an organism from injuries such as pathogen invasion. The structure and the immune role of the skin will be detailed later.

TLR	Pattern of recognition
TLR1	Peptidoglycan
TLR2	Lipoprotein
TLR3	dsRNA
TLR4	LPS
TLR5	Flagellin
TLR6	Diacyl of lipoprotein
TLR7/8	ssRNA
TLR9	Unmethylated CpG motifs

Table 3: TLRs of the innate immunity and their PAMPS

Each TLR (Tool Like Receptor) recognizes some PAMPs. PAMPs are the Pathogen-Associated Molecular Patterns present in bacteria and TLRs are present in the host cells. The recognition of PAMPs by TLRs informs the host, particularly the immune system, that a pathogen is present and what is the nature of the pathogen.
TLR: Tool Like Receptor, PAMPs: Pathogen-Associated Molecular Patterns.

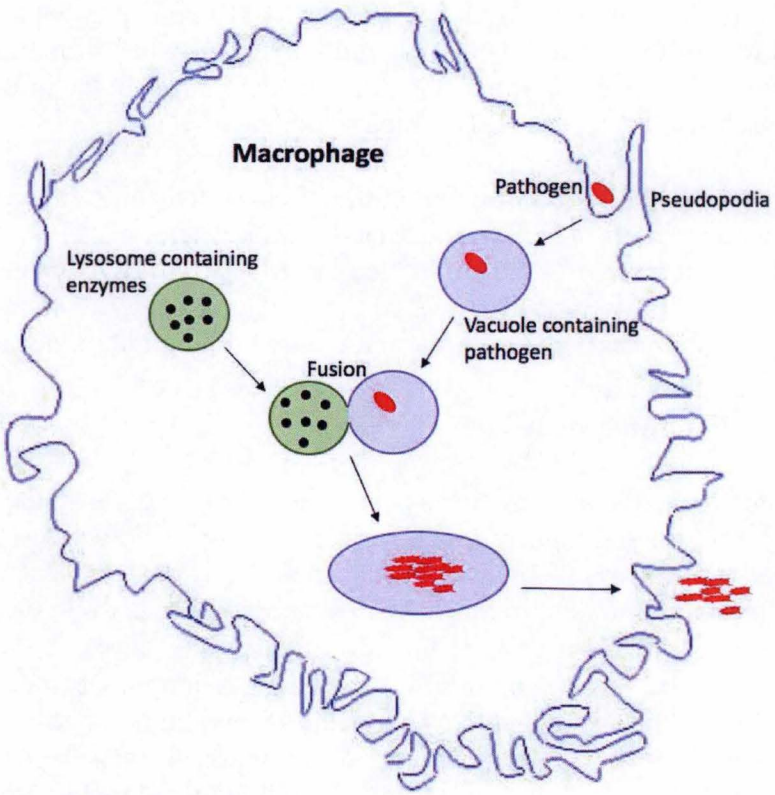


Figure 5: Phagocytosis process

Once the pathogen is at the surface of macrophage, pseudopodia surround the pathogen. Next, the pathogen is internalized into the cell. A vacuole-containing pathogen forms and fuses with lysosomes. Lysosomal enzymes degrade pathogen and finally, the debris of pathogen are released by exocytosis.

Due to their exposure to the external environment, mucosal tissues have developed mechanisms of defence. The mucosa act as barriers between the environment and the host. The mucosal epithelial cells secrete many defensive compounds such as mucins, antibodies, defensins, etc.. These compounds have an antimicrobial activity. The first barrier that pathogens encounter is the mucus, producing by the goblet cells. The mucus is composed of mucin glycoproteins, that are responsible of the viscous properties of the mucus. Mucus plays thus an important role in the protection against pathogens through the physical barrier, the secretion of antimicrobial molecules and by preventing the adhesion of pathogens on epithelial cells (SK. Linden *et al.*, 2008).

3.2.2 Detection of bacterial pathogens

As already said, bacteria possess highly conserved molecules called Pathogen-Associated Molecular Patterns (PAMPs). Among PAMPs, there are lipopolysaccharides, lipoproteins, flagellin, peptidoglycan, simple strand DNA, etc.. These PAMPs are recognized by the innate immune system via the Pattern Recognition Receptors (PRRs), a repertoire of receptors. The PRRs are conventionally classified in 3 families: the secreted, the cytosolic and the transmembrane PRRs. For more information about the different types of PRRs, consult the **BOX 1** (O. Takeuchi and
S. Akira, 2010). Among the transmembrane PRRs, there are the Toll Like Receptors (TLRs) that are usually expressed by cells playing a role in the antigens presentation (macrophages and dendritic cells (DCs)), but also by adaptive immune cells (lymphocytes) and by other cells present in tissues such as keratinocytes (L. Miller and R. Modlin, 2007) or fibroblasts (O. Takeuchi and S. Akira, 2010). Ten different TLRs are described in human and thirteen in mouse. Each TLR can recognize some PAMPs (**table 3**) (S. Akira *et al.*, 2006).
Pathogens can also induce the release of cryptic or stress molecules called Damage-Associated Molecular Patterns (DAMPs), such as ATP and heat shock proteins. These DAMPs are also recognized by PRRs.
The detection of these different molecular patterns activates the defensive mechanisms. In the case of an infection by *Brucella*, the TLRs 2, 4 and 9 recognize respectively the lipoproteins, lipopolysaccharide and DNA of bacteria (R. Copin *et al.*, 2007).

3.2.3 Innate immune defence mechanisms

Four major effector mechanisms can be involved in the innate immune response against a pathogen:

The **phagocytosis** (**figure 5**) is a mechanism of pathogens internalization. The main phagocytic cells are the macrophages, neutrophils and dendritic cells (cellular immunity). The mechanism is divided in 3 stages: (i) the recognition and the adhesion of pathogen to phagocytic cells, (ii) the internalization of pathogens via endocytosis. The membrane of phagocytic cells deforms and pseudopodia appear to form a vesicle around the pathogen and (iii) the maturation, the acidification and the fusion of vesicle with lysosomes allow to eliminate the pathogen (D. Underhill and H. Goodridge, 2012).

The **complement** belongs to the humoral immunity. It is a system of plasma proteins naturally present in the blood. It exists 3 distinct pathways that lead to the same goals: (i) the recruitment of inflammatory cells, (ii) the opsonization of pathogens (cooperation with the phagocytosis) and (iii) killing of pathogen (direct destruction). In the case of *Brucella* infection, the classical pathway seems be the dominant one (J. Ko and G. Splitter, 2003). The classical pathway is activated through the cooperation of the adaptive immunity. Indeed, the first stage of the complement is the recognition and the fixation of antibody at the surface of pathogen. The C1

BOX 2: Classical pathway of the complement

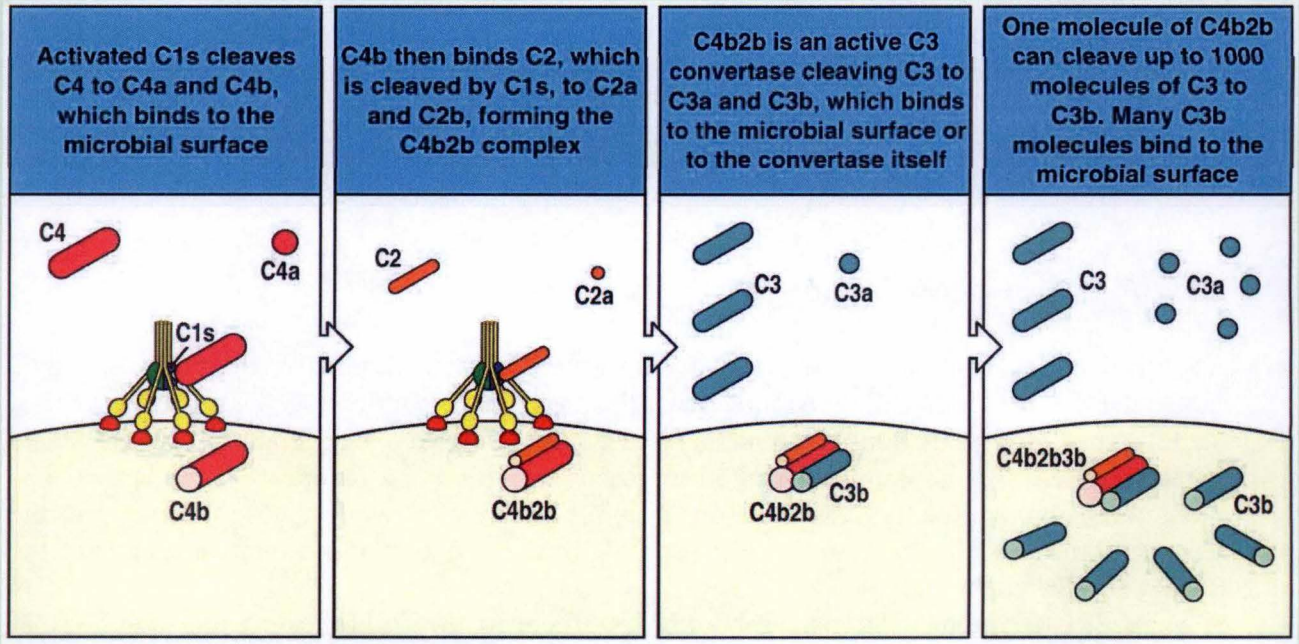
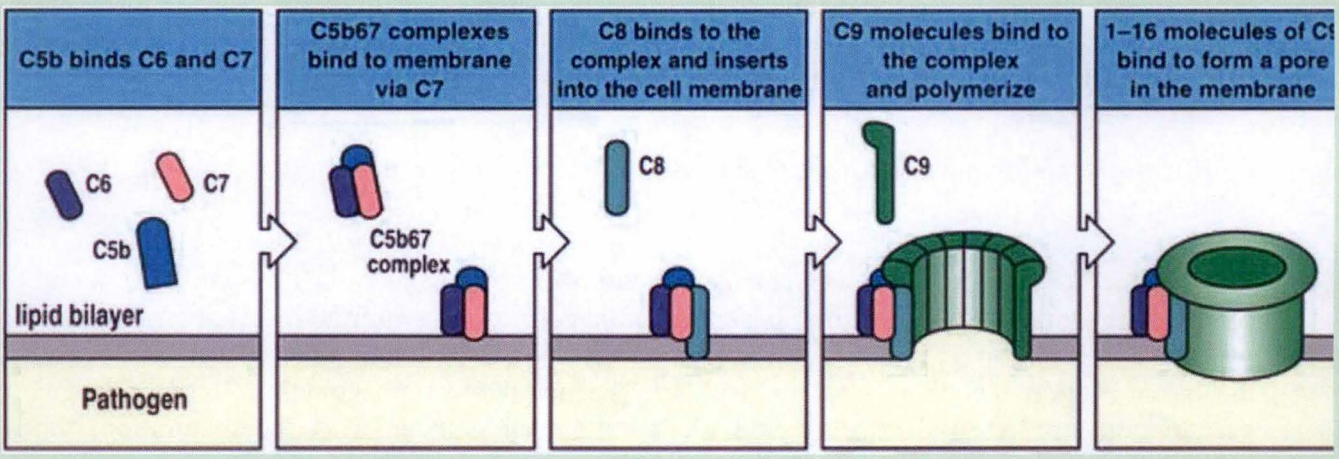


Figure 2-22 Immunobiology, 6/e. (© Garland Science 2005)

- C3b binds both C4b2b and C3b forming the active C5 convertases
- C5 binds to the C3b component of the C5 convertase enzyme
- C5 is cleaved to form C5b and C5a



plasma protein can bind the constant part of this antibody. From this stage, the different plasma proteins (C2 to C9) bind together to finally form a membrane-attack complex pore at the surface of the pathogen. See the **BOX 2** for more details about the classical complement pathway. Some of complement cleavage products[2] allow the increase of the permeability of the blood vessels. In addition, the complement allows to induce a chemotaxis[3] via the different plasma proteins, that allows the recruitment and the penetration of immune cells into the pathogen (by the pore formed) to destruct it. Finally, the opsonization process[4] is increased. It is mediated by opsonines, molecules marking a target cell to induce its phagocytose by macrophages (C. Janeway *et al.*, 2001).

The **cytotoxicity** is mediated by cytotoxic cells such as NK. These cells belong to the innate immunity and derive from lymphoid progenitor cells. NK cells recognize infected cells and use a combination of mechanisms to lyse them among which the release of cytotoxic molecules such as perforin which polymerizes to form a pore in target membrane, and granzymes which are serine proteases that use this pore to reach the cytoplasm of target cell to induce the apoptosis of infected cell (Iannello *et al.*, 2008).

Finally, **the inflammation** is a response of tissues to injuries. Injuries can be induced by PAMPs detection or by the tissue destruction and production of DAMPs. Indeed, damaged tissues and resident immune cells secrete chemokines[5] that recruit effector cells (such as phagocytic cells) from the blood vessels to the infected site.

The effectors of the innate immunity and their main functions are described in the **table 4.** Here, only the macrophages and DCs will be detailed.

The **macrophages** are present in all tissues of an organism. It is derived from blood monocytes. The main role of these cells is the detection of pathogens via the PRRs and their phagocytosis as described above. In macrophages, the bactericidal functions are reactive oxygen intermediate (ROI) and reactive nitrogen intermediate (RNI), induced by gamma-interferon (IFN-γ) and alpha-tumor necrosis factor (TNF-α). Inducible Nitric Oxide Synthase (iNOS) catalyses the production of Nitric oxide (NO) from L-arginin and NADPH. NO is able to diffuse through lipidic membranes and acts in the cytoplasm to inhibit enzymes and damage the DNA (Y. Kobayashi, 2011). In response to IFN-γ, macrophage can express major histocompatibility complex (MHC)II and become able to present antigen to T cells, a mechanism that allows the activation of adaptive immunity. Finally, these phagocytic cells are also involved in the formation of granuloma, the structure that maintains and limits the spreading of pathogens, structure that will be detailed later (T.D. Bold and J.D Ernst, 2009).

The **dendritic cells (DCs)** are derived from the myeloid lineage. They are the intermediate cells between the innate and the adaptive immunity. Indeed, these cells play an important role in the detection of pathogens but also in the initiation of adaptive response due to their role as professional antigen presenting cells (APC) (see 3.3).

---

[2] The complement cleavage products are derived from the cleavage of complement proteins via convertase during the complement cascade.

[3] Movement induced by a chemical stimulus.

[4] The opsonization process is mediated by opsonines that bind the target cell to phagocytose by macrophages or neutrophils.

[5] Chemokines are small cytokines secreted by cells and able to induce chemotaxis.

Effectors	Main function(s)
Complement	Opsonization, recruitment of macrophages/neutrophils and destruction of pathogens
Macrophages	Phagocytosis and activation of bactericidal mechanisms (ROS/RNS), antigenic presentation
Dendritic cells	Catch of antigens at the site of infection, migration to the lymph nodes and antigenic presentation
Neutrophils	Phagocytosis, degranulation, neutrophils extracellular traps (NETs), activation of bactericidal mechanisms
Eosinophils	Destruction of parasites with antibodies at the surface and degranulation
Basophils	Releasing of histamine-containing granules
Mastocytes	Releasing of histamine-containing granules and production of IL-4 (T_H2)
Natural Killers	Releasing of lytic granules, induction of the apoptosis via Fas, destruction of infected cells and production of IFN-gamma (T_H1)

Table 4: The different effectors of the innate immune response with their main functions

This table represents the main effectors of the innate immune system (Complement, macrophages, dendritic cells, neutrophils, eosinophils, basophils, mastocytes and natural killers). Each effector possesses one or several function(s). The main one are present in the table.

BOX 3: Different subpopulations of dendritic cells (DCs)

The pre-DCs can rapidly develop in functional DCs when there is an inflammatory or microbial stimulus. Among the DCs are found the monocytes and the plasmacytoid DCs (pDCs) producing IFN alpha and beta and are specialized in the anti-viral response.

The conventional DCs (detailed in the text)

The inflammatory DCs are absent in safe conditions. They differentiate from monocytes when there is inflammatory or microbial stimulus. They can produce TNF-alpha and NO.

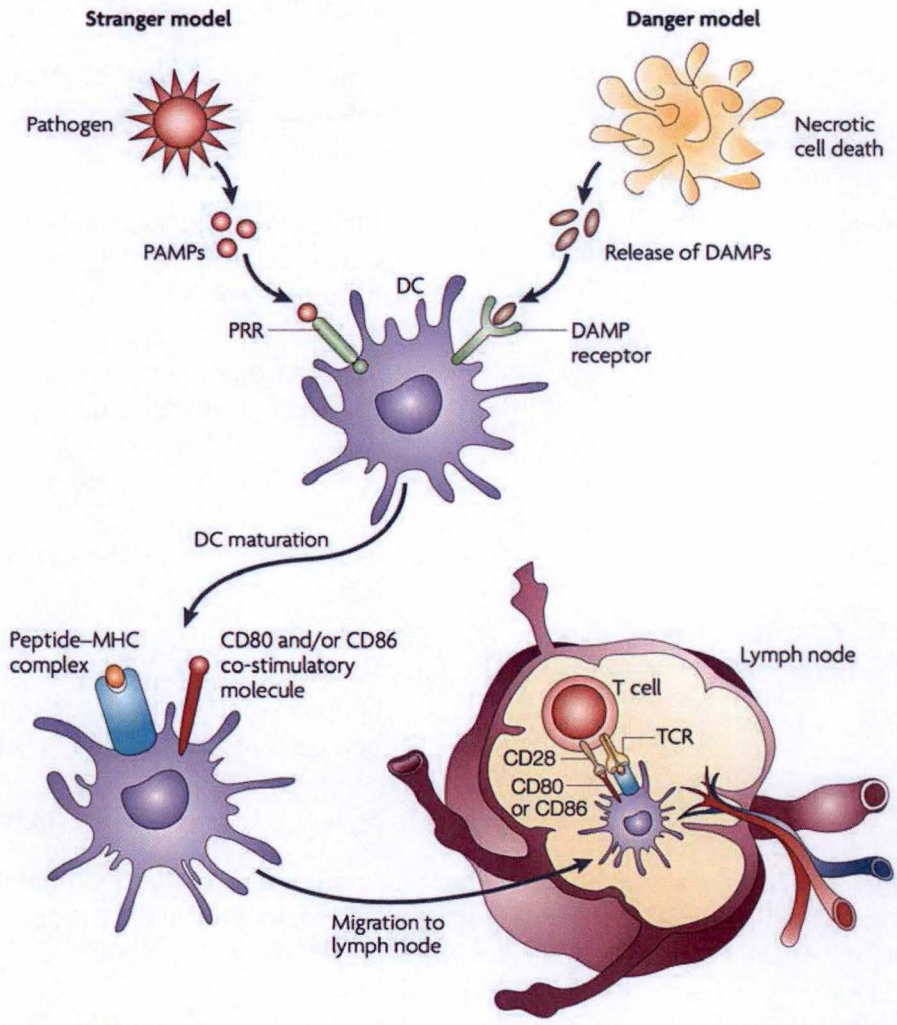


Figure 6: The role of dendritic cells as intermediate between innate and adaptive immune responses

The PAMPs (and the DAMPs caused by injuries such as the invasion of pathogens) are detected by receptors at the surface of dendritic cells. The pathogen is phagocytosed by the cell which matures towards the draining lymph node. During its migration, the DC matures and becomes an antigen presenting cell. The contact between the MHC of DC and the TCR of naive T cell occurs near the HEV (high endothelial venules). In addition to this process, cytokines are produced and co- stimulatory molecules are expressed to orientate the T response (H. Kono and K. Roch, 2008).

Different subpopulations of DCs are distinguishable, depending on their phenotype and their tissues location. The DCs can be classified in (i) pre-DCs, (ii) conventional DCs and (iii) inflammatory DCs (Shortman and Naik, 2007) (**BOX3**).
The conventional DCs are the migratory DCs (for example the Langerhans cells) and the resident DCs in lymphoid organs. The first are the sentinels of an organism. They circulate in tissues and continually interact with their environment. The detection of a pathogen constitutes a signal of maturation that induces their migration towards a lymphoid organ, where they will activate naive T cells. The second one resides in lymphoid organs where they catch and present antigens of self or non self.

3.3 Transition between innate and adaptive immunity: APCs

The dendritic cells are called the professional antigen presenting cells (APCs) because the DCs are present in all tissues and because they can activate T cells by MHCII.
In absence of infection, a part of DCs present in tissues matures and migrates towards the thymus where they present « self » antigens to T cells. T cells interacting with self-peptides presented by the MHC will be either destructed or re-programmed by the DCs that will induce the replacement of TCR (T cell receptor, see below) alpha chain (L. Klein *et al.*, 2009). Only T cells that do not react with these self-peptides-presenting DCs will escape from the thymus and become the mature patrolling T cells. It is the selection of T cells.

When a pathogen is detected via the detection of PAMPs (and DAMPs) by PRRs, DCs phagocyte the pathogen and next migrate from peripheral tissues towards draining lymph nodes. In the same time, there is the maturation process of DCs leading to its transformation from phagocytic cell to antigen presenting cell. During this process of maturation, DCs notably increase the expression of MHC and co-stimulatory signals and decrease the capacity to detect other pathogens. Once in the lymph node, DCs finally present the antigens to the T cells via MHC (ES. Trombetta, 2003). This meeting between APC and T cells takes place near the high endothelial venules (HEV) zone. In addition of the antigenic presentation, intracellular signalling cascades triggered by the PRRs induce the expression of co-stimulatory molecules and the production of pro-inflammatory mediators (**figure 6**). The variety of produced cytokines will activate the different subpopulations of T cells

3.4 Adaptive immune system

The lymphocytes (B and T) are the main actors of the adaptive response. These cells use specific receptors expressed by B and T lymphocytes (B/T Cell Receptors ; B/TCRs). They can recognize all structures and have to undergo a selection to avoid recognizing the self. This ability is absent in the innate receptors, directly encoded with a limited number in the genome. During the adaptive immunity process, the lymphocytes specific to the antigens are selected and undergo a clonal amplification. A part of these cells will differentiated to assure the establishment of an immunologic memory (**figure 7**).

3.4.1 The T lymphocytes or T cells

The TCR (T cell receptor) is a heterodimer and is responsible for recognizing antigens. It is associated to several membrane molecules, such as CD3 complex composed of γ/ε chains and

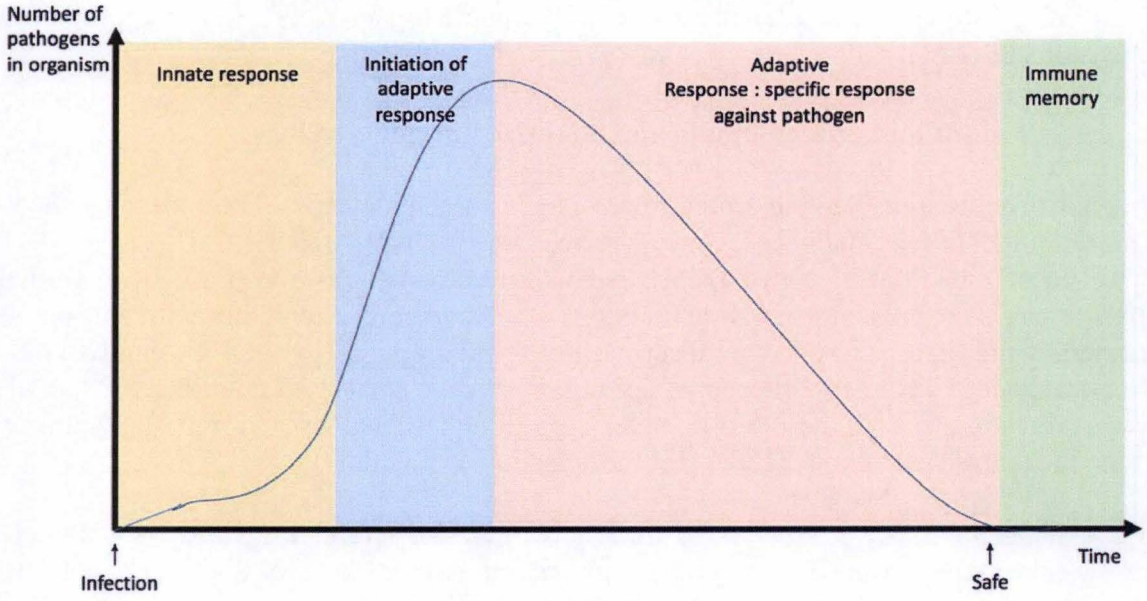


Figure 7: Evolution of immune response with time

After the infection by a pathogen, the innate response is directly active against this pathogen. This response is non-specific and is therefore independent of the pathogenic species. After the detection of pathogen antigens, the adaptive response is initiated, which is specifically efficient against the pathogen and leads to its elimination. Some of lymphocytes are able to become memory cells, which will be directly efficient in the case of a second infection by this same pathogen.

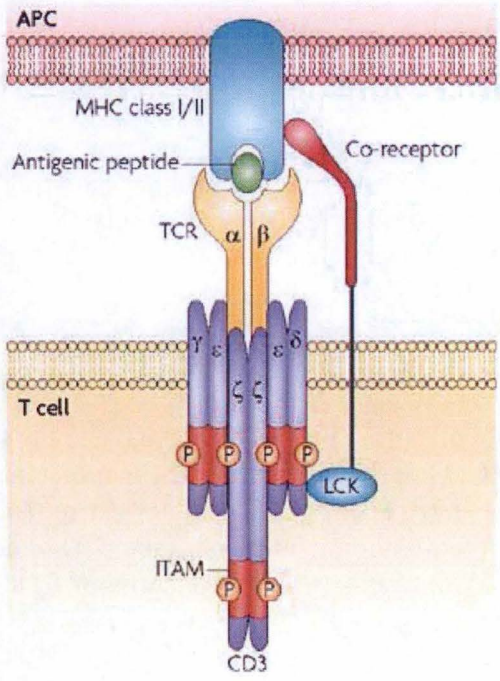


Figure 8: T cells receptor (TCR)

The TCR possesses one site of recognition and has only a function of detection. It is composed of CD3 molecule and a TCR and ζ/ζ chains. The alpha and beta chains (or gamma and delta) form the TCR and CD3 is composed of γ/ε chains, ε/δ chains. The co- receptor is CD4 or CD8 and has a role of stabilization in the interaction. The ITAM (immunoreceptor tyrosine-based activation) will allow the signalling after the detection of a pathogen via the presentation of antigenic peptide by the MHCI/II (N. Gascoigne,2008).

TCR: T cells receptor, CD: cluster of differentiation, ITAM: immunoreceptor tyrosine-based activation motif, MHC: major histocompatibility complex.

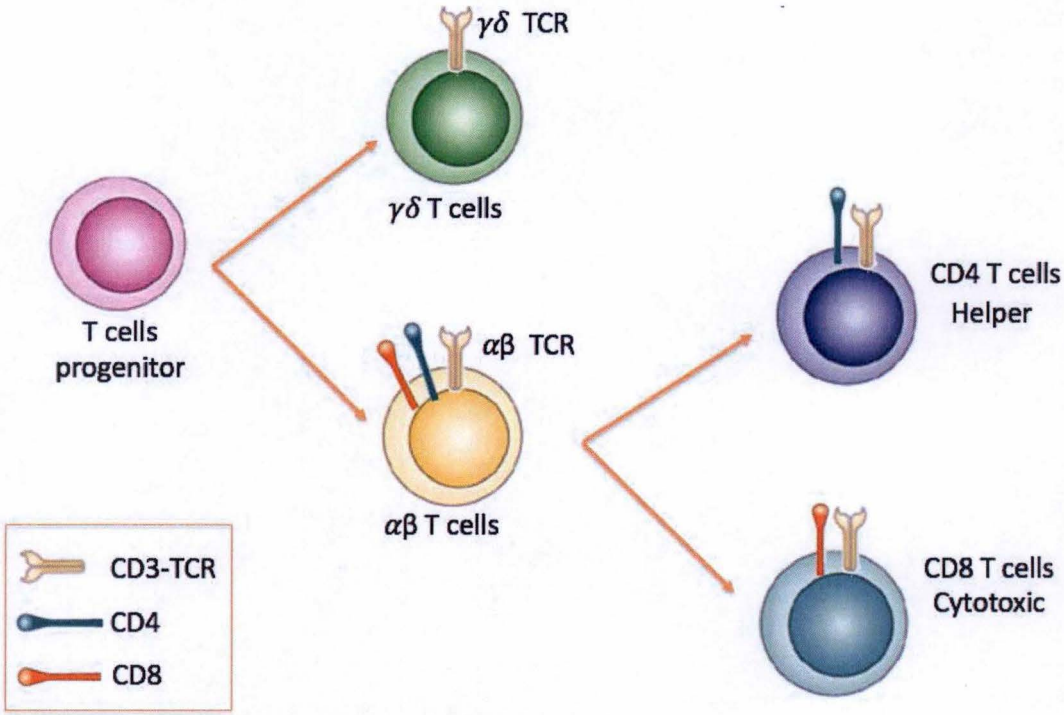


Figure 9: Different subsets of T cells

The T cells come from the T cells progenitors. T cells have at the surface a T cells receptor (TCR). This TCR is composed of a CD3 molecule and of a TCR molecule composed of alpha/beta chains or gamma/delta chains (see **figure 8**). The T cells with alpha/beta chains, that represent the majority of T cells, have two co-receptors at the surface: CD4 and CD8 molecules. Among these T cells, after selection, the CD4 T cells (=Helper T cells) or CD8 T cells (=cytotoxic T cells) are selected.
TCR: T cells receptor, CD: cluster of differentiation.

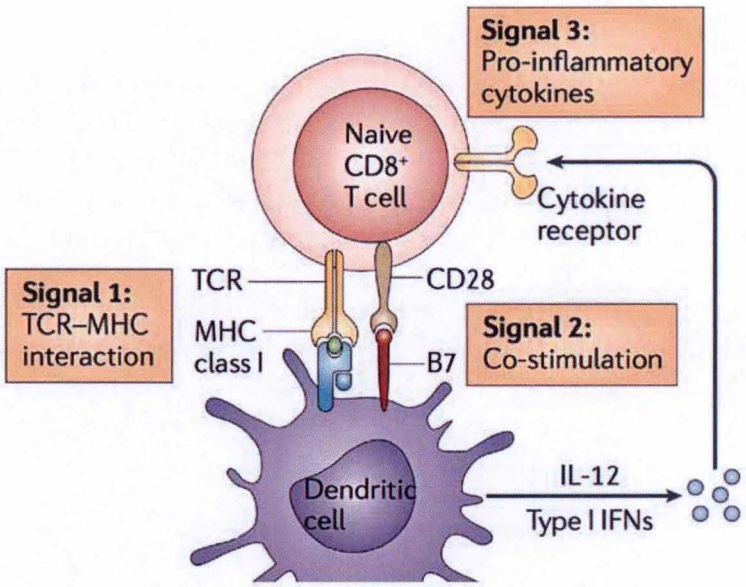


Figure 10: The activation of T cells in the lymph node by DCs requires three signals

The activation of T cells requires three signals: **signal 1**: the interaction between the MHC of a DC and the TCR of a T cell, **signal 2**: a co-stimulatory signal (B7 and CD28 for example) and the **signal 3**: cytokines allowing the orientation of the differentiation of T cells (Adapted from Sun and Lanier, 2011).

ε/δ chains (N. Gascoigne, 2008). The ITAM[6] (Immunoreceptor Tyrosine-based Activation Motif) allows the signal transduction until the nucleus. In 95% of T cells, the TCR is composed of an alpha (α) and a beta (β) chains (**figure 8**), whereas in 5% of T cells this consists of a gamma (γ) and a delta (δ) chains. When the TCR is composed of alpha and beta chains, the activation of the T cells requires an antigen processing and the MHC presentation of antigenic peptides on an APC. A co-receptor is present at the surface of αβ T cells. It can be the CD4 or the CD8 glycoprotein. The lymphocytes possessing the CD4 protein at their surface are the helper T cells ($CD4^+$ $\alpha\beta TCR^+$ T cells; specific for MHC class II) and the lymphocytes possessing the CD8 protein at their surface are the cytotoxic T cells ($CD8^+$ $\alpha\beta TCR^+$ T cells, specific for MHC class I) (K. Wucherpfennig *et al.*, 2010). The **figure 9** represents the different subsets of T cells.

In the thymus, the T cells are selected depending on their self-antigen tolerance as explain before. Next, the T cells migrate towards the lymphoid organs where they will be activated and differentiated through the contact with the DCs (APC).
In the lymphoid organs, the activated T cells are able to induce the differentiation of the B cells. These T lymphocytes are thus the "helper T" because they are involved in the activation of other lymphocytes.

The activation of T cells is depending on (i) the antigenic signal (generated by the recognition of antigenic peptides presented by the MHC to the TCR), (ii) the co-stimulatory signals between the DCs and T cells, and (iii) the soluble signals such as cytokines that allow the differentiation of T cells based on the nature of the pathogen (**figure 10**) (J.C. Sun and L. Lanier, 2011).

The activation of $CD4^+$ T cells is dependent on the antigen presentation by APC. $CD4^+$ T cells are divided in different subsets and secrete cytokines that allow to initiate and amplify the activation of others immune cells such as $CD8^+$ T cells, B cells or innate immune cells.
When the pathogen is extracellular, it is phagocytized by a macrophage or a DC. The pathogen is thus in an endocytic vesicle where the pH is acidic, allowing the degradation of the pathogen through activated proteases. The vesicle containing peptides fuse with a vesicle containing the MHCII molecules. This latter vesicle originates from the endoplasmic reticulum (ER). To avoid the binding of the peptides of MHCI to MHCII, an invariant chain (Ii) prevents the fixation of peptides on the MHCII. Once in the endosome, Ii is cleaved and CLIP (class II-associated invariant chain peptide) stays on the MHCII. CLIP is next removed, allowing the binding of peptides on MHCII. The peptides can be presented to the TCR of $CD4^+$ T cell (**figure 11**) (T. M. Holling *et al.*, 2004 ; K. S. Kobayashi and J. van den Elsen, 2012).

Depending on the signal 3 that are transmitted to the T cells via the phagocytic cells, T cells can differentiate to various subsets of T_H (T Helper) cells (**figure 12**). The nature of pathogens and signals such as cytokines are involved in the polarization of the T_H response. The secreted interleukins (IL) by innate immune cells will be different in function of pathogens, that allows a differentiation of T lymphocytes towards a specialized adaptive response. Here, only the T_H1 and the T_H17 will be detailed[7].

---

[6] ITAM is a conserved sequence of four amino acids (Tyrosine – X – X – Leucine).

[7] *T_H2 response*: IL-4 will be adapted to differentiate T cells into T_H2 responses to fight helminthic infections.

T_H22 response: Another response, less known, is the T_H22 response which is specific to the skin. The function of these cells are not completely understood.

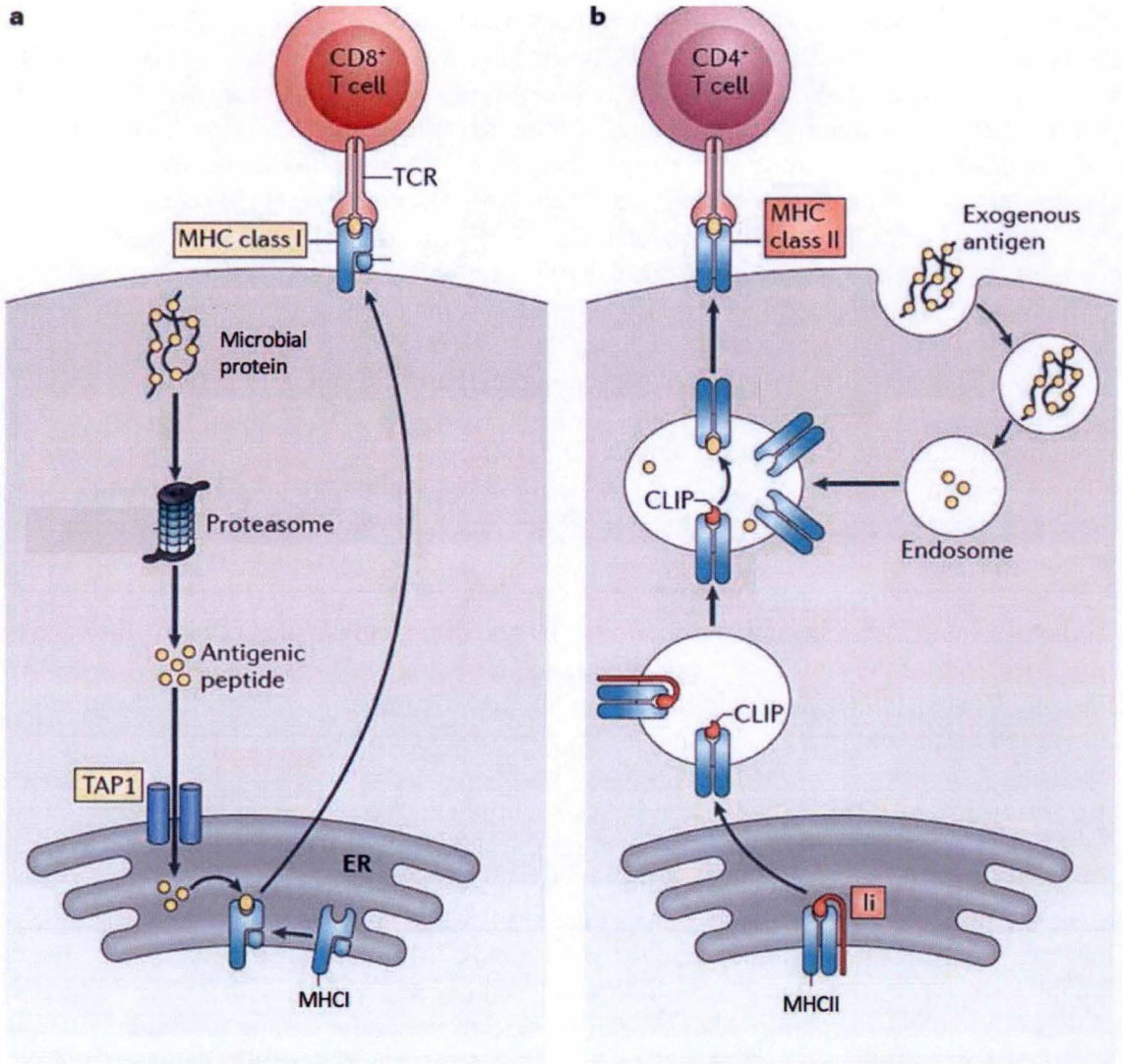


Figure 11: Antigenic presentation for CD4 and CD8 T cells

(a) An intracellular pathogen is presented by MHCI to $CD8^{\pm}$ T cells: the proteins of the pathogen are degraded into peptides by the proteasome. Peptides enter in the ER via TAP1 and bind MHCI. They are presented to $CD8^{+}$ T cells

(b) An extracellular pathogen is presented by MHCII to $CD4^{\pm}$ T cells: the proteins of the pathogen are degraded by proteases in the endocytic vesicle. This vesicle fuses with a vesicle that contains the MHCII. Peptides bind the MHCII and are presented to $CD4^{+}$ T cells. Li and CLIP bind MHCII and next release the MHCII allowing the binding of extracellular peptides to MHCII. Then, it will be presented to $CD4^{+}$ T cells (Adapted from K. S. Kobayashi and J. van den Elsen, 2012).

MHC: major histocompatibility complex, CD: cluster of differentiation, ER: endoplasmic reticulum, TAP: antigen peptide transporter, li: invariant chain, CLIP: Class II-associated invariant chain peptide.

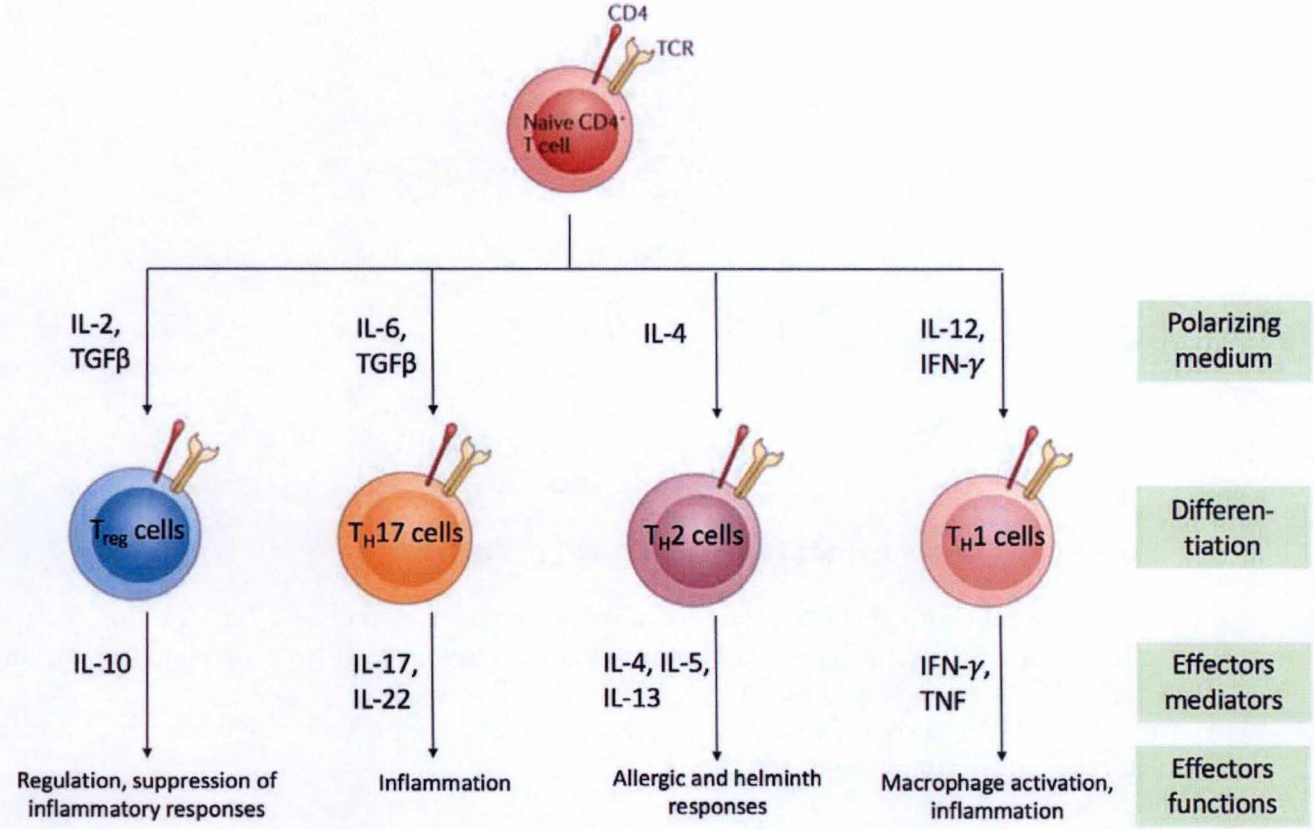


Figure 12: Differentiation of naive T cells to different subsets and associated responses

Depending on the cytokinic environment, the naive $CD4^+$ T cells differentiate into a specific type of T Helper effector cells. A specific function is associated to the specific T cells. The polarization is possible thanks to different cytokines (Adapted from Swain *et al.*, 2012).
CD: cluster of differentiation, IL: interleukin.

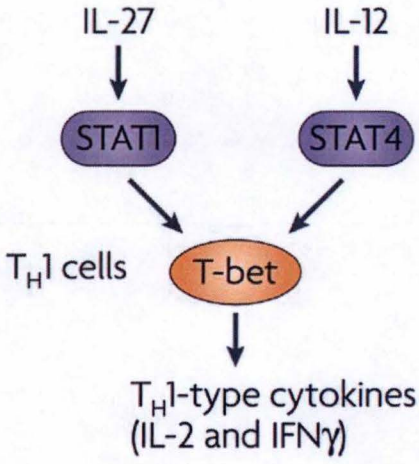


Figure 13: Two distinct pathways to induce the T_H1 response

The transcription factor T-bet can be activated by two pathways: via IL-27 / STAT-1 or via IL- 12 / STAT-4. Once activated, T-bet can control the expression of IFN-γ, standing for the main cytokine of T_H1 immune response (Adapted from P. J. Barnes, 2008).
T_H: T helper, T-bet: T-box expressed T cells, IL: interleukin, STAT: Signal Transducers and Activators of Transcription, IFN: interferon.

T_H1 response: IL-12 allows a differentiation of naive T cells into a T_H1 subset, specific to intracellular pathogen. It is the case for *Brucella* infection, but the specific *Brucella* response will be detailed later.

The IL-12 is the first inducer of T_H1 response as described above. The main cytokine of this response is IFN-γ. IFN-γ is induced by the T-box expressed in T cells (T-bet), a transcription factor that controls the expression of IFN-γ. T-bet expression results in a specific transactivation of IFN-γ gene. T-bet can be activated by different pathways: STAT-1 (induced by IL-27) and STAT-4 (induced by IL-12) (**figure 13**) (P. J. Barnes, 2008).

IL-12 acts via STAT-4 signalling pathway. The molecular basis of differentiation of T_H1 is not very clear but it is known that in absence of STAT-4, the T_H1 response is reduced. T cells can also produce IFN-γ in the absence of STAT-4, suggesting that IL-12-driven STAT-4 activation is not sufficient for the production of IFN-γ by T cells. Indeed, it is known that $CD8^+$ T cells can produce the cytokine of an IL-12-independent manner (S. Szabo *et al.*, 2000 ; A. O'Garra and N. Arai, 2000).

It has been recently reported that IL-27 was a novel IL-12 family member and that it can induce T-bet expression via the JAK1/STAT-1 pathway. STAT-1 appears to be more important in the induction of T-bet compared to STAT-4, but the pathways are not completely understood (S. Kamiya *et al.*, 2004).

T_H17 response: The T_H17 lymphocytes act at the epithelial surfaces and assure the elimination of extracellular bacteria. These T cells notably produce IL-17. This cytokine induces a high recruitment of neutrophils towards the site of infection. The differentiation of T cells in T_H17 is induced by IL-6 and the transforming growth factor-beta (TGF-β). The T_H17 induces inflammatory responses.

The *regulatory T cells* constitute a particular subset of T cells that have a role in the suppression of inflammatory responses and the maintain of self-tolerance. They interact with DC and prevent a too high activation of lymphocytes, which can be deleterious of the host (Swain *et al.*, 2012).

The $CD8^+$ T lymphocytes, expressing the CD8 co-receptor, are cytotoxic cells. They recognize the infected cells and destruct them by releasing perforins, forming a pore in the membrane of infected cells, and granzymes, passing through this canal to trigger the mechanism of cell death. The $CD8^+$ T cells are activated by cytosolic antigen presented by the MHCI of DCs. The unfolded proteins of intracellular pathogen are degraded by the proteasome in peptides that pass in the ER via TAP1 (transporters associated with antigen processing). In the ER, the MHCI is formed. The peptides bind the MHCI and are presented at the receptor and co-receptor of $CD8^+$ T cells (**figure 11**) (K. S. Kobayashi and J. van den Elsen, 2012).

3.4.2 The non-conventional T cells

Among the T cells, it exists other cells called « the non-conventional » T cells. These cells present a TCR at their surface but do not possess a CD4 or CD8 co-receptor. Unlike the conventional T cells, the TCR does not seem to require the presence of a classical MHCI or MHCII to be activated. These cells correspond for example to the NKT (Natural Killer T) cells and the $\gamma\delta TCR^+$ T cells.

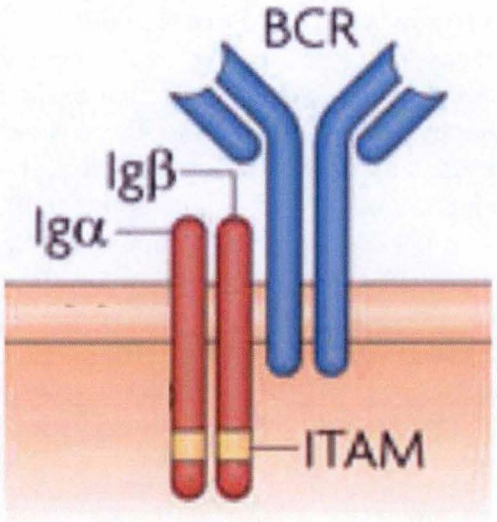


Figure 14: BCR structure

The BCR is composed of two heavy and two light chains, generating two sites of detection. The heterodimer Ig alpha/beta is associated with ITAM, allowing the intracellular signalling (Adapted from S.K. Pierce and W. Liu, 2010). ITAM: immunoreceptor tyrosine-based activation motif, Ig: immunoglobulin, BCRs: B cells receptors.

The **NKT cells** express an alpha/beta receptor and recognize mainly glycolipid antigens presented by CD1 on the cell surface of APCs. CD1 is structurally similar to MHCI but does not present peptide. The role of NKT is not really defined, but if these cells are absent, auto-immune diseases are induced. A hypothesis is that NKT could have a role of regulation by production of pro- and anti-inflammatory cytokines such as IFN-γ and IL-10 respectively (Nestle *et al.*, 2009). However, these cells can also participate to immune defence (SM. Behar and SA Porcelli, 2007).

The **γδTCR$^+$ T cells** express a receptor composed of a gamma/delta chains. These cells do not seem to require antigen processing and MHC presentation of peptidic epitopes, although some of them recognize MHC class Ib molecules. By contrast with αβTCR$^+$ T cells, the γδTCR$^+$ T cells do not express a co-receptor or co-stimulatory molecules at their surfaces. Their ligands are today unidentified but seem to vary and to be of diverse natures. The γδTCR$^+$ T cells are mainly present in specialized compartments of the body such as the skin and mucosa. The main function of these cells are the maintenance of epithelial homeostasis and tissue repair. These cells provide a crucial first line of defence at the interface between the innate and the adaptive immune response (D. A. Witherden *et al.*, 2014).

3.4.3 The B lymphocytes or B cells

The B lymphocytes express antigenic receptors to their surface, the BCRs. These receptors are able to recognize antigens with a native form (whatever its chemical nature). BCRs are receptors in membrane (role of pathogen detection, like the TCRs) or can be secreted as a monomer (IgE, IgG) or a polymer (IgA, IgM) (and play an effector function). In this case, we talk of immunoglobulins or antibodies.

The BCR is composed of a membrane and a signalling subunits. The first one is composed of two heavy and two light chains. This first structure confers to the BCR two sites of detection. The second one is composed of a heterodimer protein (Igα and Igβ). ITAMs are found in the tails of this last subunit and will allow the intracellular signalling after the detection of a pathogen (**figure 14**) (L. Matsuuchi and M. Gold, 2001).

The activation of B cells will be less detailed than T cells because this master thesis focuses mainly on the T cells. B cells can be activated on T cells-dependent or -independent way. The **thymo-dependent activation** of B cells requires two signals: the specific antigenic signal from BCR and the co-stimulatory signal from activated CD4$^+$ T cells. The role of these signals is the limitation of the risk of an auto-immune reaction. The **thymo-independent activation** of B cells does not require the CD4$^+$ T cells. Some PAMPs or specific structure of antigens can directly induce the proliferation and the differentiation of B cells (C. Janeway *et al.*, 2001).

Class	Properties
IgA	Found in gastrointestinal, respiratory and genital tract mucosa. Prevents the colonization by pathogens. Also present in saliva, tears and milk.
IgD	Membrane immunoglobulin. It is part of the membrane receptor of naive B lymphocytes (BCR).
IgE	Involved in allergic and parasitic processes. Its interaction with basophils and mastocytes causes histamine release.
IgG	Main immunoglobulin of adaptive immunity. It has the capacity to cross the placental barrier in certain animals such as carnivores, rodents and primates.
IgM	It is part of the membrane receptor of naive B lymphocytes (BCR). Form found in the serum, secreted early in adaptive immune response.

Table 5: Different classes of immunoglobulins and their main properties

The 5 classes of immunoglobulin (Ig) (IgA, D, E, G and M) are found in specific location and present different properties. This table presents a brief description of each class.

B cells derive from bone marrow, where the BCRs are generated and where the selection of B cells based on their self-tolerance takes place. After this selection, B cells continue their maturation in secondary lymphoid organs. After that, a part of B cells secretes IgM antibodies of low affinity. Other part of B cells is activated by T cells and undergo a clonal expansion and a maturation of affinity of their BCR[8]. The cytokines produced by T cells and DCs lead to the expression of new classes of Ig. This process is called the isotypic switch and consists of a change of the heavy chain of antibody and allows a better adaptation of the Ig. The other classes of antibodies are thus produced: IgG, IgA or IgE. The **table 5** shows the different classes of Ig and their properties (C. Janeway *et al.*, 2001).

The effector mechanisms of antibodies are the neutralization, the opsonization and the activation of complement. Some class of antibodies can be preferentially produced on a T-independent manner or on a T-dependent manner. IgG1 or IgG2a are mainly produced following T cell dependent-activation of B cells. Although IgG3 constitutes a minor fraction of IgG produced on a T-cell-dependent manner, it is the major IgG subclass in response to bacterial polysaccharides (LJ Rubinstein and KE Stein, 1988), and seems to be important in the defence against bacterial and fungal infections (J. McLay *et al.*, 2002).

3.5 Immune memory

After an infection, to reduce the risk of autoimmune reaction, the majority of T and B cells are eliminated by apoptosis. However, a small fraction of these lymphocytes persists in host and constitutes the immune memory. Their frequency is dependent on the persistence of the pathogen. Indeed, if it is an acute infection, the memory cells will be progressively eliminated in function of their half-life time. However, in a chronic infection, the memory cells will be present during all life of the host because a chronic infection will stimulate the amplification of the memory cells pool. The memory cells could receive a survival signal that would allow them to survive, but the mechanism is not still very clear (O. Boyman *et al.*, 2009).

After the immune response, a part of T cells constitutes a pool of memory T cells, specific to the encountered antigens. Some of memory cells reside in peripheral tissues such as the skin and constitute the **peripheral memory**. During a second infection, these T cells can rapidly initiate a cytotoxic or inflammatory response. Other memory T cells are in the lymph nodes and participate at the **central memory**. This reserve of memory T cells can rapidly differentiate in effector memory T cells and migrates at the site of infection during a second contact with the pathogen (C. Janeway *et al.*, 2001).
The memory T cells memorize the antigenic determinant, the nature of the pathogen and thus the differentiation of T cells adapted to the pathogen, and the location of the pathogen. This latter information is crucial for the development of an effective vaccine.

[8] That takes place in the germinative center. This process is called hypermutations.

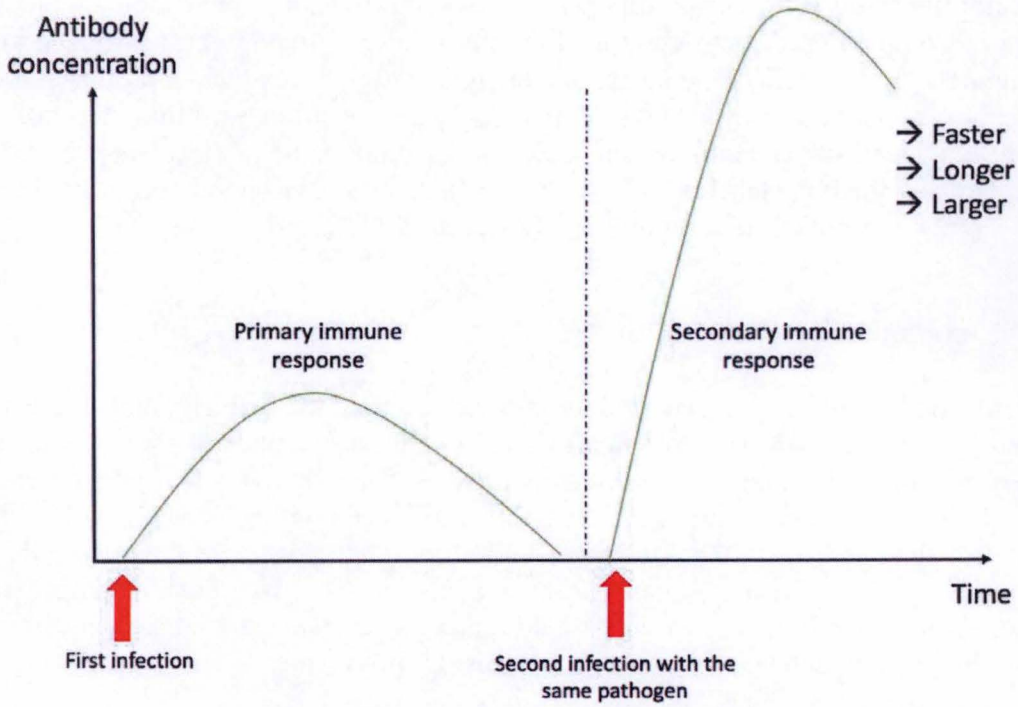


Figure 15: Concentration of antibodies during a second infection

During the first infection, the primary response takes place. After that, an immune memory is created. During the second infection with the same pathogen, the concentration of antibodies will be higher and the response will be faster and longer.

Concerning the B cells, the primary and secondary responses are very different. Indeed, in the secondary response (the memory) the number of clones of a B cell is weaker than in a primary response and each clone has a higher affinity. The secondary antibodies have a better affinity because only the B cells with a high affinity are stimulated in the second response. The **memory B cells** reside in the secondary lymphoid organs. These cells express a BCR of a high affinity. During a second infection, the B cells differentiate in plasmocytes, secreting antibodies. The **memory plasmocytes** reside mainly in bone marrow. These cells express only a few BCRs, but permanently secrete antibodies in blood (Kalia *et al.*, 2006).
Thanks to the memory lymphocytes, during a second contact with the same pathogens, the response will be more effective and faster (**figure 15**). The vaccination involves the injection of an antigen preparation to induce a specific immune response against the pathogen and therefore protects against natural infection or mitigate its effects. It relies on the ability of the adaptive immunity to develop an immunological memory.

3.6 Skin immunity

The immunity is specific to the concerned compartment. In this master thesis, mice were infected with *Brucella melitensis* in intra-dermal (ID). It is thus interesting to know the structure, the components and the immune cells of a skin. This is a brief description of the skin (D. Gawkrodger and M. Arden-Jones, 2012 ; A. Haake *et al.*, 2001).
One of the functions of the skin is to ensure a physical barrier to protect the host against injuries and in this case, against pathogen invasion. The objective is to keep the internal systems intact.

3.6.1 Structure of the skin

The skin is composed of three layers: **epidermis, dermis and hypodermis (figure 16 A.).**

The **epidermis** is the most outer layer, directly in contact with the environment. It is a stratified epithelium of about 0.1 mm thick and is continually renewed. Its main function is to act as a protective barrier. The cells the most representative of this layer are the keratinocytes, cells producing the keratin, a fibrous protein playing a role of protection and support. The other types of cells in epidermis are the melanocytes, Langerhans cells (see Skin immunity) and Merkel cells[9].

The epidermis is composed of four layers:

The stratum basale is mainly composed of keratinocytes, attached to the basal membrane by hemidesmosomes (**figure 16 B.**). 5-10 % of cells are melanocytes, inserted between the keratinocytes. These cells synthesize the melanin that pigmented the skin. The basal keratinocytes produce antimicrobial peptides, playing an important role in the defence against bacterial invasion.

The stratum spinosum is composed of cells derived from the basal cells. The cells are inter-connected by desmosomes (**figure 16 B.**). Differentiating keratinocytes synthesize keratins, which aggregate to form tonofilaments, supportive mesh of these cells. Finally, Langerhans cells are often present in this layer. These cells are the resident dendritic cells of skin.

[9] Merkel cells have a function in the dispersed neuroendocrine system.

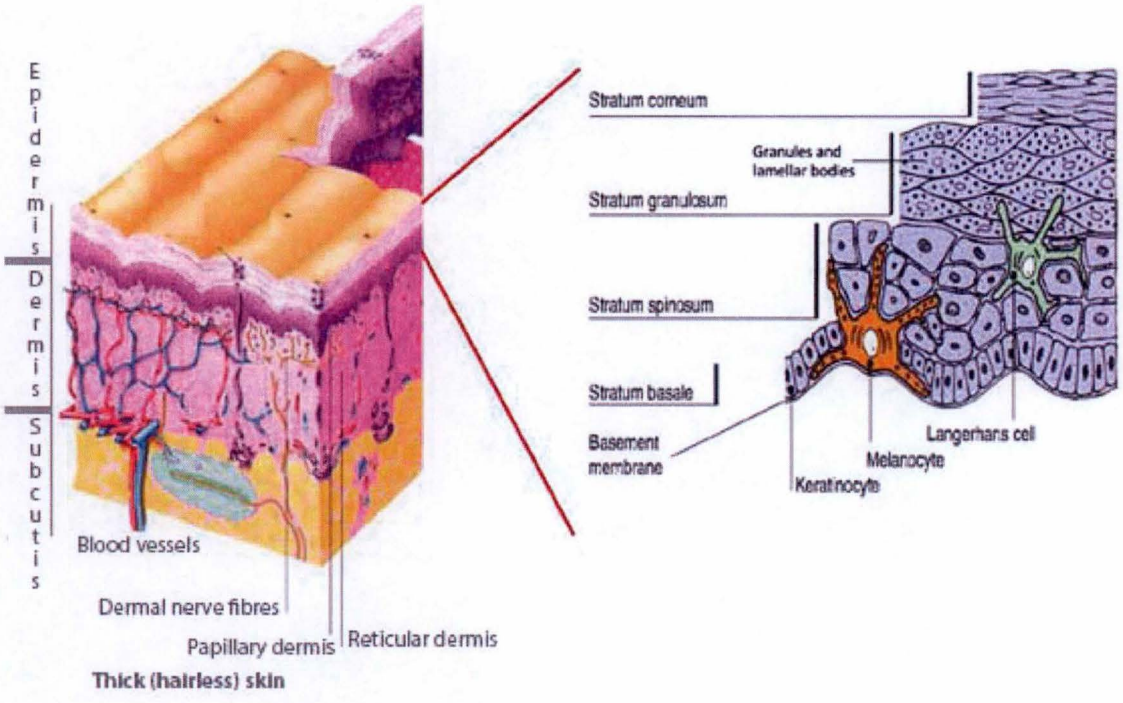


Figure 16 A.: Composition of the skin

The skin is composed of the epidermis, dermis and hypodermis. The epidermis is constituted of 4 layers; the stratum corneum, the stratum granulosum, the stratum spinosum and the deepest one, the stratum basale. Keratinocytes are the main cells of the epidermis. Melanocytes are present in the stratum basale and pigmented the skin. Langerhans cells are present in the stratum spinosum and are the resident dendritic cells. The cells of the stratum granulosum possess keratin granules and lamellar bodies that will allow the impermeability of the skin. Stratum corneum is composed of dead cells, the corneocytes. In the dermis (papillary and reticular dermis), blood vessels and nerve are present in the conjunctive tissue (Adapted from Gawkrodger D. and Arden-Jones M., 2012).

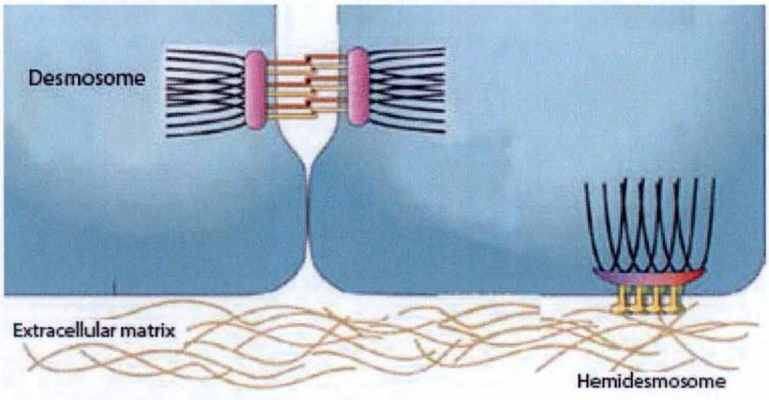


Figure 16 B.: Hemidesmosomes and desmosomes

Adhesive proteins maintain the contact between cells (for example desmosomes) or between the cells and the basal lamina (hemidesmosomes). Desmosomes are stronger connections that join the intermediate filaments of neighboring cells.
Hemidesmosomes bind the intermediate filaments of a cell to the basal lamina (Adapted from JJ. Jefferson *et al.*, 2004).

The stratum granulosum is composed of flattened cells, losing their nuclei. The keratohyalin granules[10] and the lamellar bodies[11] are in the cytoplasm of cells. These bodies contain lipids and proteins and they lead to the formation of hydrophobic envelope, conferring to the skin its protective barrier function.

The stratum corneum is the layer containing the keratinocytes at the end of their maturation. This layer is composed of sheets of cells without nuclei (called corneocytes). The cells are stuck together via a lipid glue derived from lamellar bodies.

The **dermis** is a supportive connective tissue, containing structures directly connected with the epidermis. The thick of this layer is approximately of 0.6 mm. It is divided in 2 layers: the papillary dermis, the thin upper layer of the dermis and the reticular dermis, the deeper and thicker layer of the dermis. Dermis is composed of 70 % of collagen, imparting strength to the structure. The elastin fibres provide elasticity of the skin. Nervous fibres and blood vessels are present in this layer and assure the innervation and vascularization of the skin. The cells present are the fibroblasts (synthesizing notably collagen and elastin), dermal dendritic cells, mast cells, macrophages and lymphocytes.

The **hypodermis** is the deepest layer of the skin and is composed of adipocytes and connective tissue. Its thick can be up to 3 cm on the abdomen. Nerves, blood vessels and lymphatic vessels are present.

3.6.2 Immunity of the skin

Thanks to its structure and its components, the skin constitutes an important physical barrier. The epidermal barrier plays a role in the innate immunity to not be invaded by pathogens. The role of blood vessels is to allow the migration of immune cells to the site of infection and the role of lymphatic vessels is to allow the migration of infected cells from the site of infection to the lymphoid organs.

In the human epidermis, the layer in contact with the environment, some of immune cells are always present and are the sentinels of the cellular immune system. These cells are the professional APCs (dendritic cells) which are the **Langerhans cells**.
The **keratinocytes** play also a role in the immunity by synthesizing antimicrobial peptides, producing pro-inflammatory cytokines such as IL-1 and expressing MHC on their surface during inflammation. Keratinocytes are able to signal to dendritic cells.

In the dermis, the dendritic cells are the **dermal DCs**. The T lymphocytes circulate in a safe skin for immuno-surveillance. When epithelial danger signals are detected, the influx of lymphocytes into the site of action is increased. The **lymphocytes** present in the skin are the $CD4^+$ T cells and $CD8^+$ T cells. The $CD4^+$ T cells produce cytokines that determine the switching of B cells to IgG (T_H1) or to IgE (T_H2). The $CD8^+$ T cells target the cells to kill with perforin (to create a pore) and granzyme B (to induce apoptosis of target cell). These cells are mainly present in the dermis, but sometimes $CD8^+$ T cells are found in the stratum spinosum (M. Pasparakis et al., 2014).

---

[10] Keratohyalin is a structural protein present in a granule formed in the cytoplasm of stratum granulosum cells.
[11] Lamellar bodies are secretory organelles secreted from keratinocytes, containing lipids. Their secretory function results in the formation of an impermeable membrane.

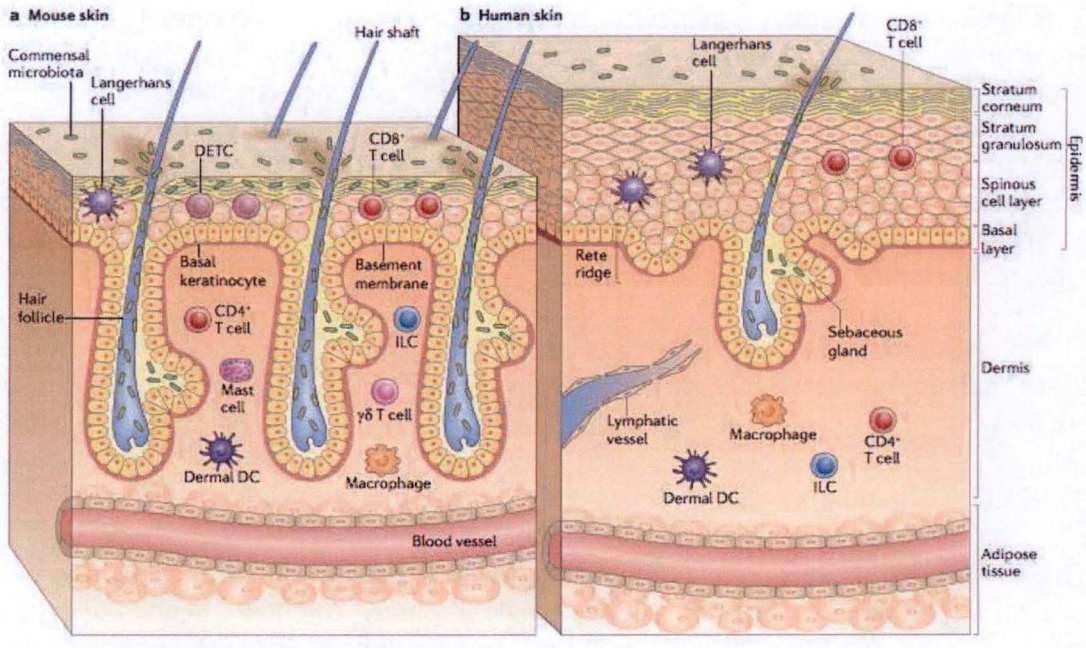


Figure 17: Immune cells present in the skin

Differential composition between murine and human skin. Murine skin: in the epidermis, dendritic epidermal T cells (DETC), Langerhans cells (LC) and CD8 T cells are present and ensure the first protection against skin injuries. In the dermis, CD4 T cells, mast cells, dermal dendritic cells (DCs), γδTCR T cells and macrophages are the cells the most present. In the human skin: DETC are absent in the epidermis. In the dermis, macrophages, dermal DC, CD4 T cells are present. The epidermis of human is proportionally larger than mice epidermis (M. Pasparakis *et al.*, 2014).
DETC: dendritic epidermal T cells, LC: Langerhans cells, CD: cluster of differentiation, DC: dendritic cells.

In addition to the T cells and the dermal DCs, the cells playing an immune role in the dermis are the **mast cells**, the **macrophages** and the **innate lymphoid cells** (ILCs). The mast cells have the ability to degranulate and to release histamine[12]. They are normal residents and their number increases during inflammatory reaction. The ILCs belong to the lymphoid lineage but lack of a B- or T-CR. The ILCs secrete cytokines to contribute to the early immune response against infection.

The populations of immune cells are a little bit different between the mouse skin and human skin (**figure 17**). First, the density of hair follicles is higher and the epidermis is less thick in the mouse skin. Next, in the mouse epidermis, there is a predominance of **Dendritic Epidermal T Cells** (DETCs), expressing a $\gamma\delta TCR^+$ T cells (Sumaria N. *et al.*, 2011), that are absent in the human skin.

4 Experimental models to study *Brucellae* infection

To study a pathogen, models of infection are developed in laboratory: the *in vitro* and the *in vivo* models. *In vitro,* it has been reported that *Brucellae* are able to invade phagocytic and non-phagocytic cells (Ko and Splitter, 2003). *In vivo*, when *Brucellae* penetrate host, bacteria are rapidly translocated across the mucosal epithelium and are able to infect myeloid cells such as macrophages and dendritic cells (DCs) (Copin *et al.,* 2012), but also placental trophoblasts (P. de Figueiredo *et al.*, 2015).

4.1 Discovery from *in vitro* models: the trafficking

The trafficking of *Brucellae* inside host cells has been analyzed *in vitro*, mainly in Hela epithelial and RAW264.7 macrophage cell lines. In these cells (**figure 18**), *Brucellae* are immediately integrate in a *Brucellae*-containing vacuole (BCV), its intracellular compartment. This BCV interacts with components of the early endosomal (EE) and late endosomal (LE) pathways and next partially fuses with lysosomes (Lys), that allows to BCV to become an endosomal BCV (eBCV). The interactions with late endosomes and lysosomes are associated with the acquisition of endosomal markers such as lysosomal-associated membrane protein 1 (LAMP1) and the acidification of the vacuole (J. Celli, 2015 ; T. Starr *et al.*, 2008). This acidification induces the expression of the VirB type 4 secretion system (T4SS). VirB is able to release effectors that control the interactions with the ER exit sites (ERES) and to mature the eBCV into replicative BCV (rBCV) via the fusion of eBCV with ER-derived membranes and elimination of endosomal membranes. The ER seems to be the replication niche of *Brucellae* (J. H. Brumell, 2012). This niche allows to escape the destruction performed by the phagolysosome.

How bacteria are able to disseminate from one cell to another is not very clear, but the rBCVs would be converted into an autophagic BCV (aBCV) via an autophagy process. *Brucellae* could manipulate the autophagy pathway of the host to disseminate in other cells (J. Celli, 2015, R. M. Roop *et al.*, 2004).

[12] Histamine is a vasoactive molecule allowing the passage of white blood cells to the infected site.

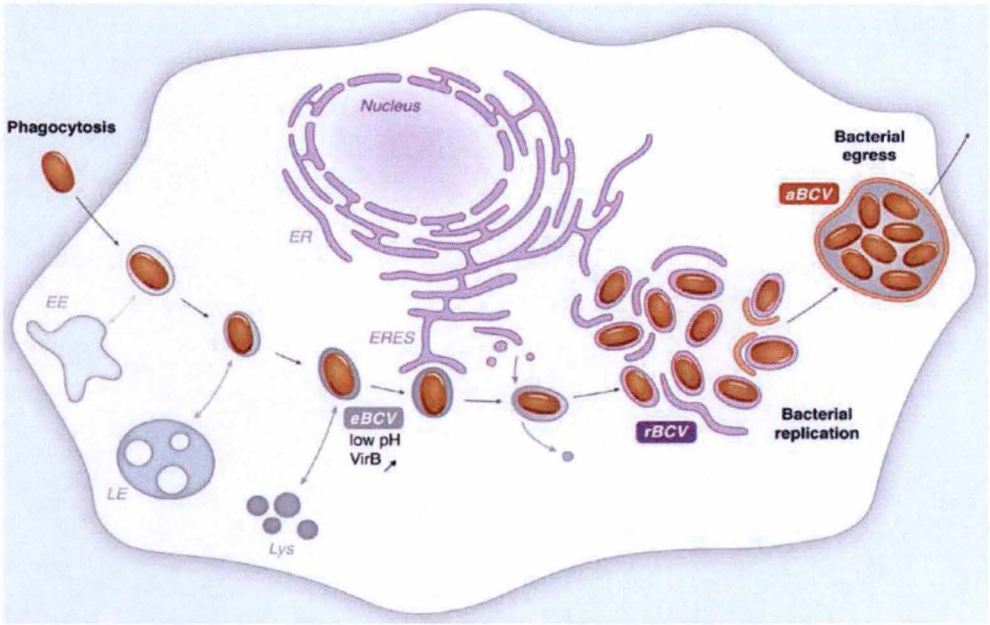


Figure 18: Representation of intracellular trafficking of *Brucellae* in phagocytic cells

Brucellae are phagocyted and reside in BCV (*Brucella*e-containing vacuole). This BCV interacts with EE (early endosomes), LE (late endosomes) and Lys (lysosomes). The BCV fuses partially with lysosomes to become an eBCV. In this eBCV, there is an acidification of pH that causes the induction of VirB. This VirB type 4 secretion system (T4SS) releases effectors that prevent its degradation. eBCV fuses with ER-derived membranes to become the rBCV. *Brucellae* replicate in the ER and are integrated in an autophagic aBCV, that facilitates the bacterial egress (adapted from J. Celli, 2015).

BCV: *Brucellae*-containing vacuole, EE: early endosome, LE: late endosome, Lys: lysosome, eBCV: endosomal *Brucellae*-containing vacuole, pH: potential hydrogen, T4SS: Type 4 secretion system, ER: endoplasmic reticulum, rBCV: replicative *Brucellae*-containing vacuole, aBCV: autophagy *Brucellae*-containing vacuole.

4.2 *In vivo* study models: *Mus musculus*

After the *in vitro* studies, to characterize a pathogen and its relation with the immune system, it is important to move to the *in vivo* models. The study of brucellosis in humans, ruminants or primates has been banned for financial, practical and ethical reasons. Small animals of laboratories are frequently employed as models in the researches about *Brucella*. The chicken embryo and the rabbit models have been put aside for different reasons such as costs, size and management. The guinea pig is an animal that seems to be the most physiological and susceptible to the infection with *Brucella*, but the reproduction and the realization of deficient guinea pigs are not easy. Although this model is the best for the vaccine studies, it is more and more replaced by other laboratory animals (M.-J. Grillo *et al.*, 2012).

Now, the *in vivo* model in the study of immune system after infection with a pathogen is classically the mouse. The mice model possesses several characteristics among which an easy reproduction and the ability to create mice genetically deficient for key element of immune system.

4.2.1 Intra-peritoneal (IP) infection model

The intra-peritoneal model of infection is the most frequently used experimental model to study *Brucellae* infection in mice. This model has allowed to know the information about the detection escape: the modifications of surface components allow to *Brucellae* to be weakly recognized by the PRRs of the host cells. For example, the lipopolysaccharide (LPS) Lipid A of *Brucellae* is modified to not be recognized by TLR4 and to trigger an immune response. The flagellin lacks of an essential domain for the detection by TLR5 (M. Terwagne *et al.*, 2014 ; Conde-Alvarez *et al.*, 2012 ; Alturi *et al.*, 2011). The protein BtpB is a translocated effector that blocks the signalling of TLR2 and TLR4, receptors involved in the recognition of LPS and lipoprotein respectively (Salcedo *et al.*, 2013). Once in the cell, there is the T4SS that allows to bacteria to modify the intracellular trafficking to prevent the degradation by lysosomes and to control the fusion with ER to catch nutrients. Other strategies known are the inhibition of apoptosis of infected cells, the prevention of DCs maturation, the reduction of antigen presentation by MHCII via the unconventional structure of LPS that forms an inactive complex with MHCII, resulting in a decrease of activation of T cells (Forestier *et al.*, 1999 ; P. de Figueiredo *et al.*, 2015 ; Alturi *et al.*, 2011). Despite its strategies, *Brucellae* are finally recognized by the innate immune system. Bacteria are detected through their unmethylated CpG by the TLR9. The induction of cells producing iNOS and IFN-γ required TLR4 and TLR9 stimulation, coupled to the pathways dependent of Myeloid differentiation primary response (MyD) 88. MyD88 is an adaptor molecule and is involved in the regulation of the downstream signalling of TLRs (R. Copin *et al.*, 2007).

The IP model has allowed to generate a lot of information about the immune response of mice in spleen after an infection with *Brucellae*. In this model, *Brucellae* are found in blood of mice from 10 minutes post-infection (p.i.) and persist until around 20 days p.i. (R. Copin *et al.*, 2012, M.-A. Vitry *et al.* 2014). *Brucellae* are found in spleen only 10 minutes after IP infection and are able to persist in this organ at least 50 days.
The spleen cells infected by *Brucellae* have been characterized: resident macrophages (red pulp macrophages and marginal zone macrophages), recruited monocytes and inflammatory DCs (Copin *et al.*, 2012). Following activation, DCs secrete IL-12 and TNF-α in small amount and present *Brucellae* antigens to naive $CD4^+$ T cells via MHCII molecule, in the lymph node to

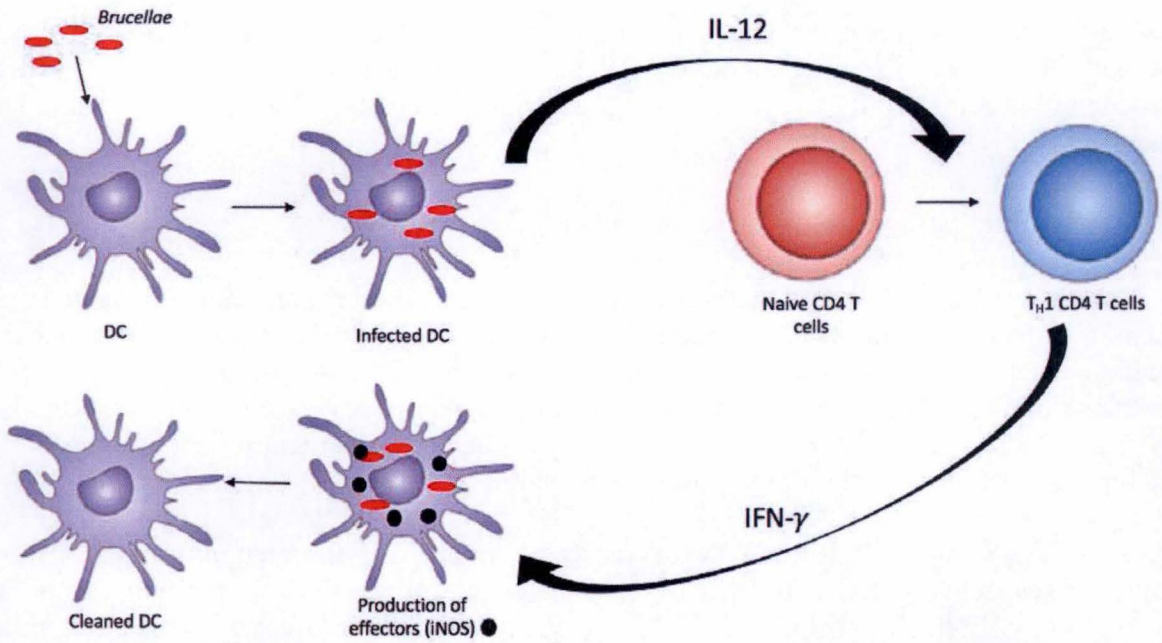


Figure 19: T_H1 immune response developed by host after *Brucellae* infection

Once infected, macrophages or DCs produce IL-12, allowing the differentiation of naive T cells into T_H1 cells. These cells are able to produce IFN-γ, that induces the production of effectors such as iNOS to clear the infected cells. Other non-infected cells can also produce IL-12 to amplify the response.

T_H: T helper, DC: dendritic cells, IL: interleukin, IFN: interferon, iNOS: inducible nitric oxide synthase.

differentiate naive cells into T_H1-mediated cells. TNF-α allows the activation of macrophages and increases their ability to fight *Brucellae*. The secretion of IL-12 results in the production of IFN-γ by activated $CD4^+$ T cells. (Y. Zhan and C. Cheers, 1993; V. Weynants et al., 1998; C. Baldwin and M. Parent, 2002; E. A. Murphy *et al.*, 2001; V. Suraud *et al.*, 2008). IFN-γ is the main cytokine produced in a T_H1 response and is important for the control of *Brucellae*. IFN-γ is known to induce the activation of effectors mechanisms – *e.g.* iNOS – in the infected cells, leading to the elimination of bacteria (**figure 19**) (R. Copin *et al.*, 2007 ; R. Copin *et al.*, 2012). Note that $CD4^+$ T cells are not the only cells producing IFN-γ during *Brucellae* infection. Indeed, this cytokine can be secreted by both innate (by $\gamma\delta TCR^+$ T cells and NK cells) and adaptive ($CD4^+$ and $CD8^+$ T lymphocytes) immune systems. IFN-γ also induces the granuloma formation in liver and spleen at 6 days p.i. (Copin *et al.*, 2012). The granuloma is composed of infected macrophages and inflammatory DCs surrounded by T cells. The granuloma seems to be the main bacterial contention mechanism in several model of intracellular bacterial infections such as *Mycobacterium tuberculosis* and *Brucellae* (T.D. Bold and J.D Ernst, 2009) (**figure 20**). As expected, mice deficient for IL-12 or IFN-γ displayed high susceptibility to *Brucellae* infection.

Despite their activation during infection, $CD8^+$ T cells and B cells do not seem to play an indispensable role to control *Brucellae* growth in spleen (M.-A. Vitry *et al.*, 2012) during primary infection. The course of infection appears similar in wild type mice and mice deficient for $CD8^+$ T cells ($TAP1^{-/-}$ mice) or B cells ($MuMT^{-/-}$ mice). At 28 days p.i., the IgG2a and IgG3 are the dominant antibodies that are detected. The role of antibodies against *Brucellae* is probably the opsonization (Ko and Splitter, 2003).

The difficulty to develop an efficient vaccine against brucellosis comes from the lack of understanding of protective memory against *Brucellae*. In mice infection model, the protective immune memory can be evaluated via a second infection, called the challenge (immunization). In the intra- peritoneal (IP) infection model, both the humoral and the cellular immune responses are indispensable to control *Brucellae* dissemination and growth. Indeed, memory mice deficient for B cells, $MuMT^{-/-}$ mice, have more colony forming units (CFU) in blood compared to wild- type (WT) mice, suggesting a role of B cells in the immune memory. Specific antibodies of immunized mice are able to neutralize *Brucellae* before the erythrocyte invasion and thus reduce the dissemination of bacteria into organs. Only the IgM seems to be sufficient in the control of bacteria. Memory mice deficient for $CD4^+$ T cells ($MHCII^{-/-}$ mice), or for T_H1 response ($IL\text{-}12p35^{-/-}$ mice) are not able to control the secondary infection, suggesting that IFN-γ-producing $CD4^+$ T cells are key elements of cellular memory immunity. In contrast, memory mice deficient for $CD8^+$ T cells or $\gamma\delta TCR^+$ T cells appear to be able to control the secondary infection (M.-A. Vitry *et al.*, 2014).

Despite the important information generated by this experimental model, the IP mode of infection is not natural and bypasses numerous immune defences of host organism such as mucosal defences. Following an IP infection, bacteria disseminate immediately in all compartments via the blood where there are rapidly found.

4.2.2 Intra-nasal (IN) infection model

As said above, *Brucellae* can be transmitted by aerosols. In order to analyze the role of mucosal immunity in the control of *Brucellae* infection, an intra-nasal (IN) model has been developed by our group (D. Hanot Mambres *et al.*, in review) (**table 6**). In striking contrast with the IP model, no bacteria are found in the blood following IN infection (**figure 21**). The infection

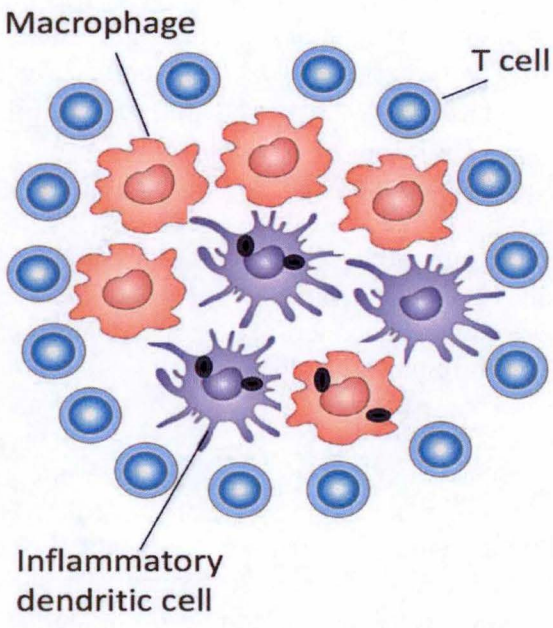


Figure 20: Granuloma during chronic brucellosis

The granuloma is a structure that allows the contention of bacteria and limits the progressive infection. It is composed of inflammatory DCs and macrophages in the center, around of T cells. Bacteria therefore undergo privation of oxygen and nutrients starvation, but it is insufficient to kill the bacteria.
The black circles represent *Brucella*. DC: dendritic cells.

	Intra-peritoneal	Intra-nasal
Primary immune response	T_H1 (role of $CD4^+$ T cells with IL- 12 and IFN-γ) B cells not involved	T_H17 (role of IL-17 and $\gamma\delta TCR^+$ - 5 days p.i.) and then T_H1 (role of $CD4^+$ T cells with IL-12 and IFN-γ) B cells not involved
Blood infection?	Yes, from 10 minutes	No detected
Secondary immune response	$CD4^+$ T cells and B cells	$\alpha\beta TCR^+$ T cells ($CD4^+$ and $CD8^+$ T cells) Compensation of T_H1 and T_H17 responses

Table 6: Comparison of intra-peritoneal and intra-nasal models

Comparison of the intra-peritoneal and intra-dermal models. The primary immune response, the infection of the blood and the secondary immune response are comparated.

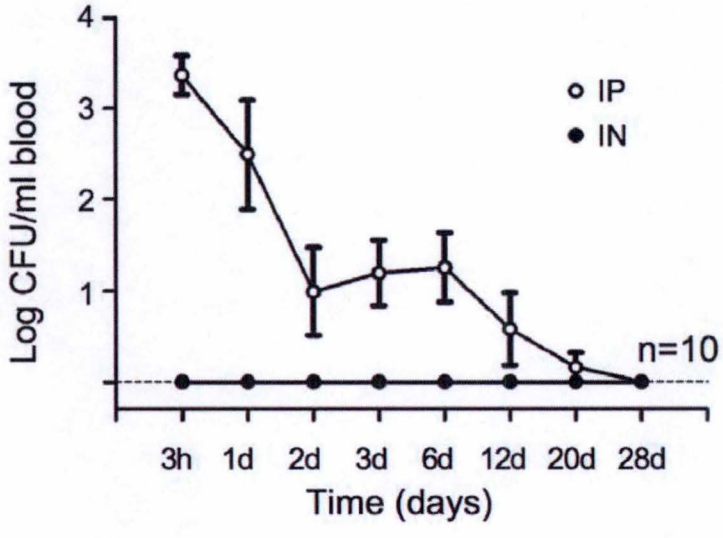


Figure 21: CFU in blood of mice after IP and IN mode of infection

After IP mode of infection, bacteria are found in the blood of mice. The high rate of CFU in blood after only 3 hours can explain why the spleen is rapidly infected in this model. By contrast, no bacteria are found in blood of mice after an IN mode of infection.
IP: intra-peritoneal, IN: intra-nasal.

disseminates slowly from lung to spleen and liver. The lung has been shown to be involved in the control of bacterial growth and dissemination through different mechanisms: an early (5 days p.i.) IL-17-mediated response (T_H17) associated to $\gamma\delta TCR^+$ T cells, and a late (12 days p.i.) IL-12/IFN-γ-mediated immune response (T_H1) associated to $CD4^+$ T cells. The control of *Brucellae* in spleen and liver (12 - 28 days p.i.) seems mainly dependent on IFN-γ producing $CD4^+$ T cells. In this model, B cells seem to do not play the role in the control of *Brucellae*, because B cells deficient mice do not appear to be more susceptible to infection.
On the whole, these results suggest that the cellular immunity is crucial to control intra-nasal primary infection by *Brucellae* and that the effector mechanisms depend on organs and timing of the infection.

When mice are challenged with *Brucellae* to study the secondary immune response, these mice efficiently control *Brucellae* growth and dissemination at lung level. Using genetically deficient mice, it has been showed that T cells, but not B cells, are crucial to control secondary intra-nasal infection. $CD3^+$ and $\alpha\beta TCR^+$ T cells deficient mice do not display a protective memory response. In contrast, B cells, $\gamma\delta TCR^+$ T cells, $CD4^+$ T cells and $CD8^+$ T cells deficient mice control secondary infection with the same efficiency of wild type mice. These results suggest that $\alpha\beta TCR^+$ T cells are indispensable for the protective memory response and that memory $CD8^+$ T cells are able to compensate for the deficiency of memory $CD4^+$ T cells. Surprisingly, the deficiencies in IL-12p35 or IL-17RA do not affect the control of secondary infection, suggesting that the absence of T_H1 may be compensated by the T_H17 response and conversely.

The absence of B cells does not impact the protective memory, suggesting that *Brucellae* disseminate from lung to spleen and liver inside phagocytic cells, allowing to escape to the neutralization by the antibodies.

The comparison between IP and IN infection models suggests that the immune mechanisms implicated in the control of bacterial growth and dissemination are strongly dependent on the entry route and legitimate the study of other natural routes of *Brucellae* transmission.

4.2.3 Intra-dermal infection (ID) model

Another frequent reported natural pathway of *Brucellae* transmission is the direct cutaneous infection, for example by the contact with infected fluid as amniotic fluid or tissues from infected animals allowing an hematogenous spread. The risk of an infection by *Brucellae* through a skin lesion is higher for practitioners such as cattle dealers, butchers, vets, farmers or scientists working with this pathogen (E. M. Galinska and J. Zagorki, 2013). In this context, our research group has recently started the development of an intra-dermal (ID) infection model in mice.

In this model, the infection of mice with *Brucellae* is realized at the footpad. This mode of infection has been already established for an infection of *Leishmania major* protozoa in mice. The fact to use a syringe to inject the pathogen into the footpad could create itself a lesion and an inflammatory environment. However, the syringe inducing lesion can imitate the skin lesion induced by cutting instruments used by a vets or a butcher.

Preliminary data on this model are available from Aurore Lison's Master thesis (2014-2015). It has been showed that monocyte recruitment at lesion site is crucial to the control of primary infection.

The recruitment of monocytes is partially dependent on C-C chemokine receptor type 2 (CCR2) and their activation is dependent of IFN-γ. In CCR2 or IFN-γ-receptor deficient mice, there is a delayed or absence of monocytes recruitment and an important neutrophils recruitment. The infection is not controlled, and the neutrophils induce tissue damage. Flow cytometric analysis shows that the main producers of IFN-γ seem to be the NK and $CD4^+$/ $CD8^+$ T cells in the draining lymph node.

OBJECTIVES

The main objectives of this master thesis are (i) the characterization of the intra-dermal (ID) infection with *Brucella melitensis* in wild type C57BL/6 mice. This first section notably consists of the study of the infection kinetic in lesion, draining lymph node and spleen. The bacterial load is also studied in blood. (ii) The identification of infected cells in the lesion and in the draining lymph node is tested through different markers specific of monocytes, dendritic cells or neutrophils. (iii) Because we know that the immune response is depending on the route of infection, we want identify the subclasses of immune response and the lymphoid cell populations involved in the control of *Brucella melitensis* after a primary and a secondary ID infection through the use of mice deficient for key elements of the immune system. The results will be compared to the intra-peritoneal (IP) and intra-nasal (IN)models.

Results

A.



Figure 22 A.: Intra-dermal infection of mice

A. The day of infection, the infectious dose is prepared to obtain a suspension of $2x10^6$ *Brucella melitensis*/mL of RPMI. Around 20 µL of this suspension are injected into the footpad of C57BL/6 mice. The swelling confirms the injection.

RESULTS

In all experiments, C57BL/6 mice were infected at the footpad with a suspension containing $2x10^6$ bacteria/mL. A volume of approximately 20 µL was injected, that means that each mouse receives approximately $4x10^4$ bacteria (**figure 22 A.**). The immediate swelling of the footpad confirms the intradermal (ID) injection and the evaluation of the CFU in footpad at early times (2h) p.i. allows to estimate that approximately $5x10^3$ CFU have been injected. The inflammatory swelling can be estimated at selected times post-infection via a tool called « Vernier ». In the following sections of this master thesis, the footpad, the primary site of infection, will be called the « lesion ».

1 Characterization of WT C57BL/6 mice after intra-dermal infection

The objective of the first experiment is to characterize the course of intra-dermal infection in WT C57BL/6 mice. For this, six mice have been used and the right footpad of each mice has been infected, while the left footpad, non-infected, was used as control (**figure 22 B.**). In the A. Lison's master thesis (2014), the RPMI injection of footpad had been realized as a second control to assess the swelling only due to the injection. However, no swelling was observed, suggesting that it was not induced by the injection itself (data not shown). The measure of the lesion has been realized before the injection and at 3, 7 and 12 days p.i.. The size of the control footpad (uninfected; in green) is approximately stable around 2.2-2.3 mm at all time points. Concerning the infected footpad (red), the size reaches its peak of swelling at 3 days p.i. infection with a size of 2.6 mm, and next decreases to reach again a normal size around 2.2 mm at 12 days p.i. (**figure 22 C.**). This swelling could be due to the recruitment of inflammatory cells at the site of pathogen infection and due to the inflammatory edema.

The bacterial load in the lesion, draining lymph node (popliteal lymph node) and spleen has been determined by counting the colony forming units (CFU) at selected times p.i. (**figure 23 A.**). The CFU count allows to evaluate the number of a live bacteria at specific times in each organ. The peak of bacterial load is reached at 3 days p.i. in the three organs. In the lesion, this peak corresponds to the peak of swelling of the footpad. At this time, there is approximately $5x10^4$ CFU in the lesion. This number then decreases approximately of three orders of magnitude to reach a mean of less than 10^2 CFU at 50 days p.i.. In the dLN, a mean of 27 CFU can be recovered at 2 hours p.i.. The bacterial load then shows a three-log increase to reach the peak of infection (at 3 d. p.i.). After this time, the bacterial load decreases to be under the threshold of detection at 50 days p.i.. This threshold is estimated at 10 bacteria preventing therefore an absolute confidence about the complete elimination of *B. melitensis*. In the spleen, the peak of infection at 3 days correspond to 10^4 CFU. The CFU number is relatively stable during the rest of the kinetic with around 10^3 detectable CFU. Importantly, in contrast to lesion and draining lymph node, *B. melitensis* appears to be able to persist at high level in the spleen for a period as long as 50 days p.i..

The dissemination of *Brucella* is dependent on the infection route. In the intra-peritoneal model (IP), it has been shown that bacteria quickly infect both spleen and liver and are able to persist in blood for several weeks (R. Copin *et al.*, 2012, M.-A. Vitry *et al.* 2014). In contrast, following intra-nasal infection (IN), *Brucella* disseminates slowly into the spleen and the liver and is not detected in the blood (D. Hanot Mambres *et al.*, in reviewing). After intra-dermal infection (ID), more than 10^3 CFU are already detected in the spleen at 2 hours p.i.. This result suggests that bacteria pass through the blood to disseminate. To test this hypothesis, the bacterial load

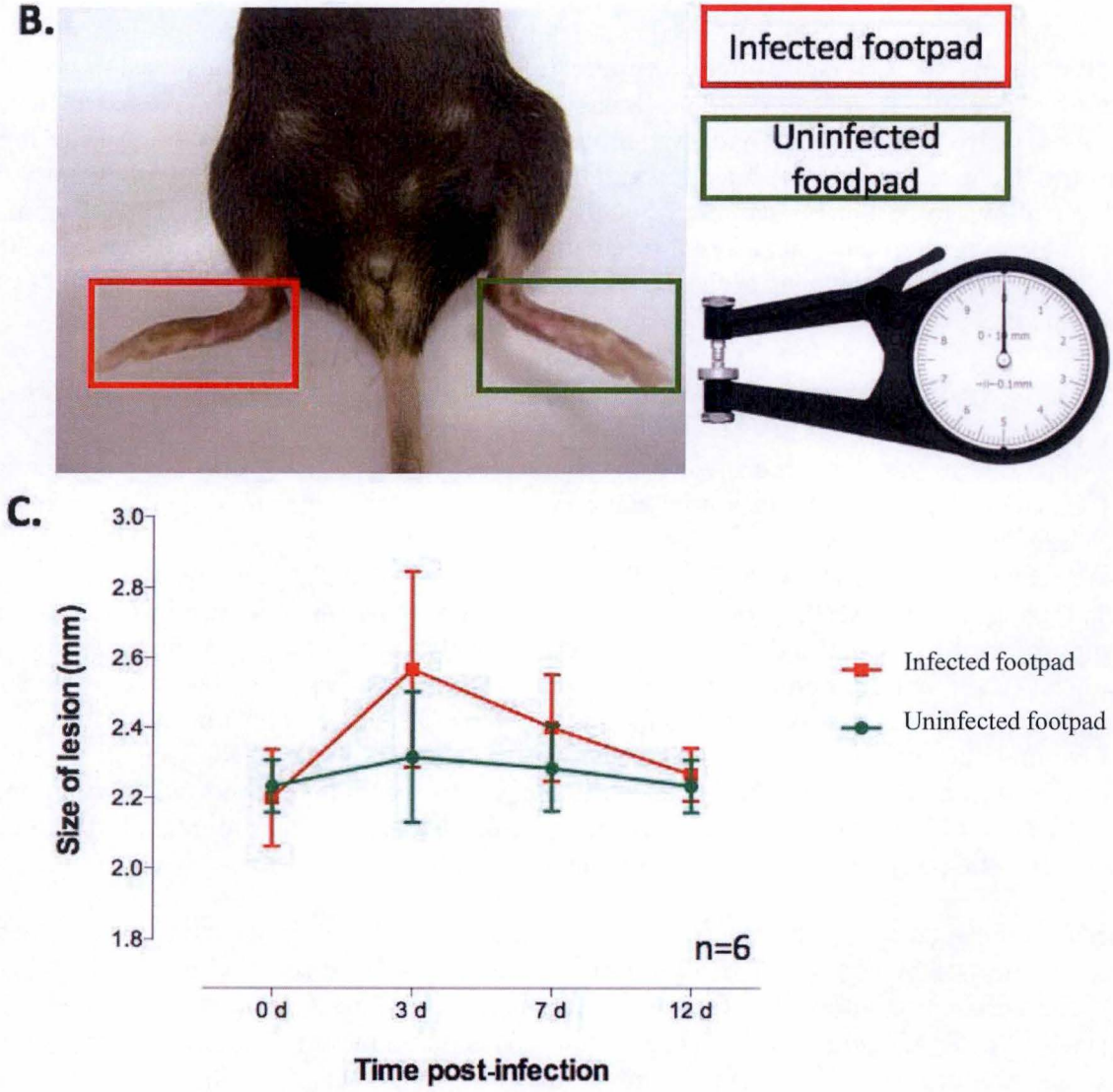


Figure 22 B. and C.: Comparison of infected and uninfected footpad of WT C57BL/6 mice (B.) and variation of the size of the lesion (mm) of infected WT C57BL/6 mice and uninfected WT C57BL/6 mice (C.)

WT C56BL/6 mice have been infected with 20 µL of a suspension containing $2x10^6$ bacteria/mL. Six
mice have been used and only one footpad by mouse was infected. The infected footpad is called "infected footpad" (red). The footpad called "Uninfected footpad" (green) has not been infected. At selected times post-infection, the footpads have been measured with a tool called "Vernier" (see **figure 22 B.**) as described in Materials and Methods. d (days), n (number of organs), WT(wild-type).

B. Picture of mice footpads (12 days post-infection), one infected (red) and the other uninfected (green). The « Vernier » is the tool allowing the measure of the footpad swelling. **C.** The size of lesion has been measured at selected times post-infection.
These data are representative of at least two independent experiments.

A.

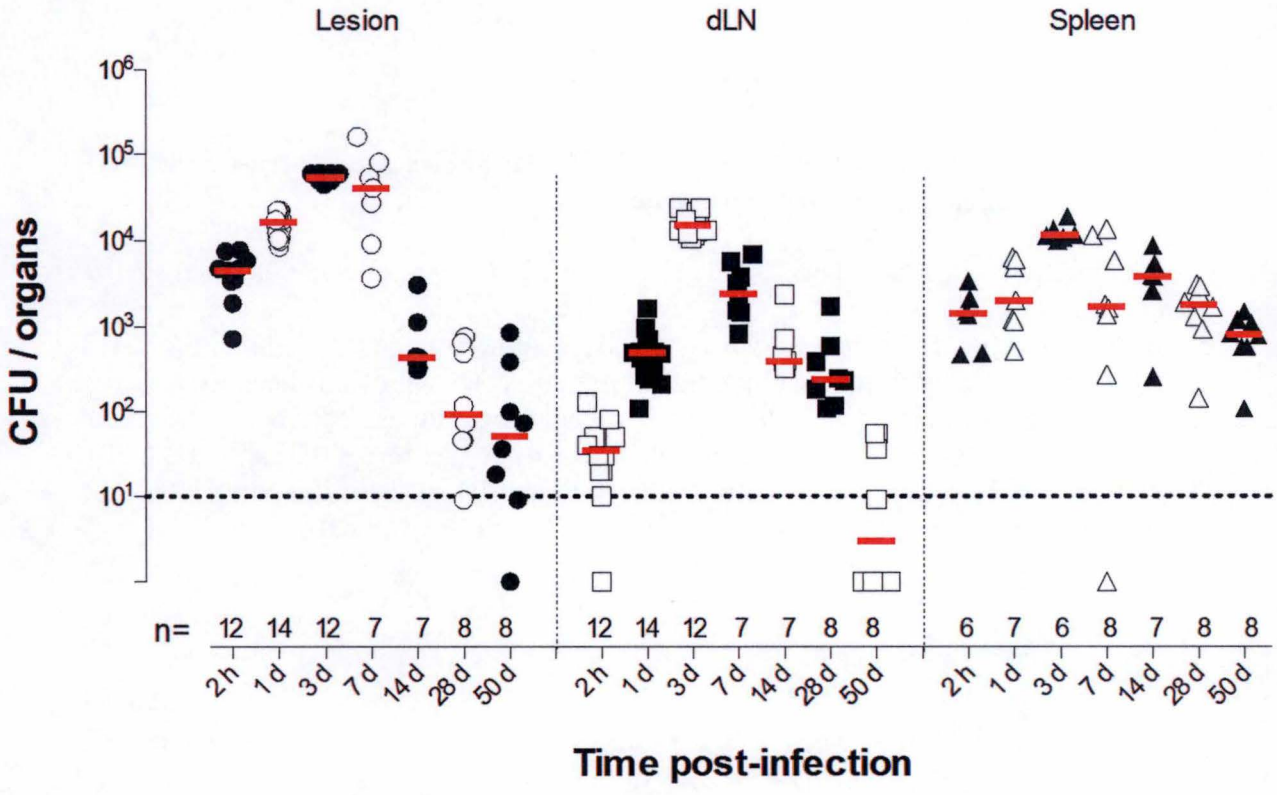


Figure 23 A.: Kinetic of bacterial load in lesion, draining lymph node and spleen in WT C57BL/6 mice after intra-dermal infection

WT C57BL/6 mice have been infected with 20 µL of a suspension containing $2x10^6$ bacteria/mL. At selected times post-infection, the footpads, draining lymph nodes and spleens have been harvested and plated on 2 YT agar medium to assess the bacterial load (CFU) as described in Materials and Methods. The data are representative of at least two independent experiments. h (hours), d (days), n (number of organs), dLN (draining lymph node), red bar: median, dotted line: threshold of detection of bacteria. In this case, white and black colors have no specific signification.

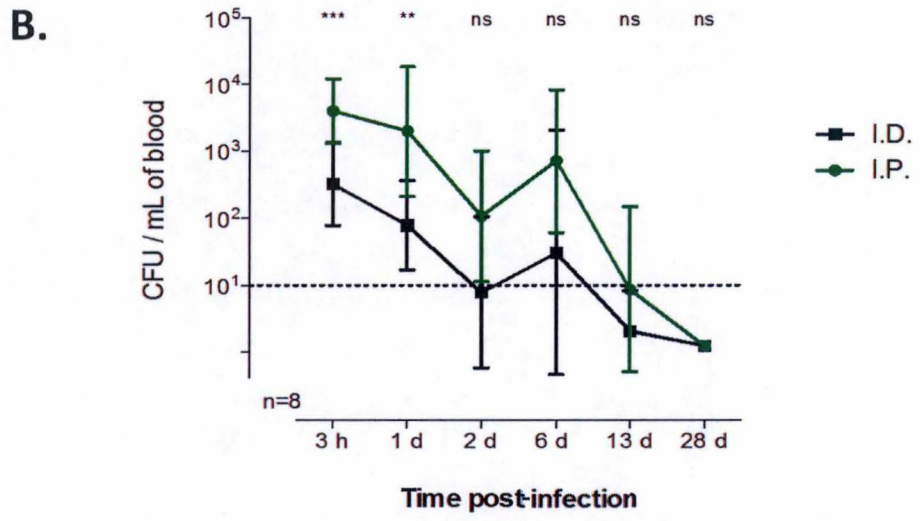


Figure 23 B.: Bacterial load in blood of WT C57BL/6 mice after intra-dermal (ID) and intra-peritoneal (IP) modes of infection

For ID infection, mice have been infected with 20 µL of a suspension containing $2x10^6$ bacteria/mL. For
IP infection, $4x10^4$ CFU of *B. melitensis*/500 µL have been injected by mice. Eight WT C57BL/6 mice have been infected by mode of infection. The blood has been harvested at selected time post-infection and plated on 2 YT agar medium as described in Materials and Methods. Significant differences are denoted by asterisks: ** $p < 0.01$, *** $p < 0.001$. The statistical differences are compared between IP and ID mode of infection. h (hours), d (days), n (number of mice), ns (non-significant), IP (intra-peritoneal),
ID (intra-dermal), dotted line: threshold of detection of bacteria.

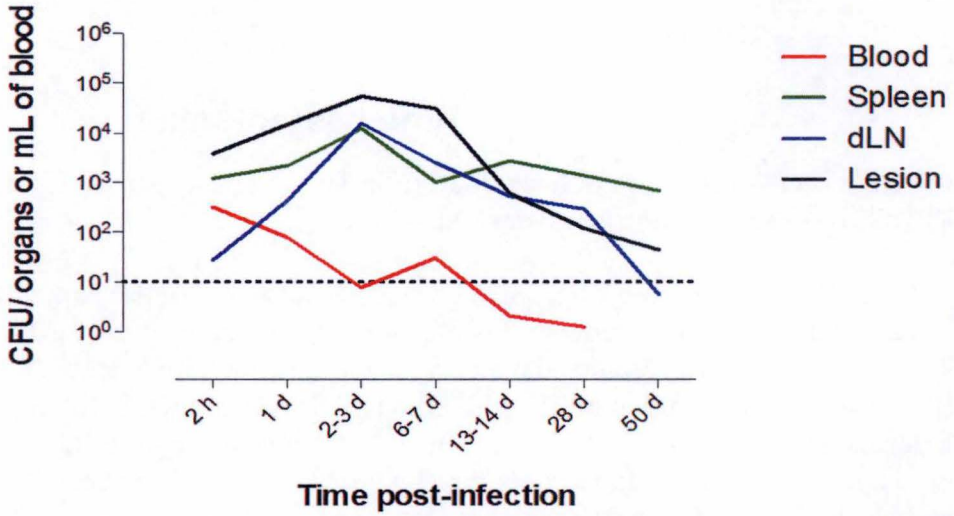


Figure 24: Summary graph of the bacterial load in the lesions, the draining lymph nodes, the spleens and the blood (Figure 23) after intra-dermal infection

Mice have been infected with 20 µL of a suspension containing $2x10^6$ bacteria/mL. At different times post-infection, the lesions, the draining lymph nodes, the spleens and the blood have been harvested and plated on 2 YT agar medium as described in Materials and Methods. The figure shows the means of CFU/organs or mL of blood at each selected times post-infection. d (day), dotted line: threshold of detection of bacteria.

presents in the blood of mice following an ID infection was measured. Eight mice have been infected with $4x10^4$ bacteria/500 µL in IP and eight mice have been infected with approximately $5x10^3$ CFU in ID. The blood of ID and IP infected mice was harvested at different times p.i. (3 h, 1 d, 2 d, 13 d and 28 d) and plated on 2 YT agar medium (**figure 23 B.**). In the blood of IP infected mice, approximately $7x10^3$ CFU/mL are detected at 3 h p.i.. This bacterial load decreases at 1 d and 2 d p.i., then surprisingly increases at 6 d p.i., then decreases again to finally be under the detection threshold (10 CFU/ml) at 28 days p.i.. The kinetic of bacteria after ID infection appears similar but the ID bacterial load is approximately one log lower, presumably due to the difference of the infectious dose. These results suggest that following ID injection, some bacteria pass directly into the blood and are able to directly disseminate from blood to spleen.

To summarize these first results, the **figure 24** shows the bacterial load par organs or mL of blood after ID infection. From 13 days p.i., the number of CFU per mL of blood or per organs decreases, suggesting a control of *Brucella melitensis* by the immune system of WT mice.

As described in the introduction section, the skin of the footpad is divided into three distinct layers (epidermis, dermis, hypodermis). The **figure 25** represents a transverse section of a footpad of a naive wild type C57BL/6 mouse. The following stainings have been realized: DAPI (to mark the DNA in blue) and phalloidin (to mark the actin in green).

Mice were ID infected and the lesions harvested at 2 hours and at 72 hours p.i.. The mCherry fluorescent tracer expressed by *Brucella* allows to visualize the bacteria present in infected cells and to count them (**figure 26**). At 2 hours p.i., only one bacterium is generally detected per cell. However, at 72 hours p.i., the number of bacteria per cell increases and is difficult to quantify. These results suggest that *Brucella* actively divides between 2 and 72 hours p.i.. This correlates with the CFU count measured in the lesion during the course of infection (**figure 23 A.**).

2 Phenotype of infected cells

Specific immunostainings have been performed on lesion and draining lymph node from control and infected mice. The **figure 27** shows a representative image of MHCII and Ly-6G staining, respectively, on lesion from naive and a 3 days-infected lesion of mice. The standard DAPI (blue) and phalloidin (green) stainings have been performed and *mCherry-Brucella* is in white. The MHCII antibody (red) (**A.**) has been used to mark myeloid cells. In the uninfected lesion, MHCII-expressing cells are detected mainly in the epidermis. These cells correspond presumably to Langerhans cells, the resident dendritic cells of the skin. In the lesion at 3 days p.i., the myeloid cells in the epidermis are always present and a recruitment of $MHCII^+$ cells is observable in the dermis. Ly-6G staining (red) (**B.**) is considered as specific to the neutrophils. In the naive footpad, no neutrophil has been detected. In contrast, in the lesion at 3 days p.i., a massive recruitment of neutrophils is observable in the dermis. Note that the thickness of the dermis increases at 3 days post-infection compared to the naive lesion, correlating with the swelling observed at 3 days (**figure 22 C.**).

After the generation of a large collection of images from stained lesions, a counting has been performed to have an overview of the percentage of infected cells for each staining. The infected cells are classified as « isolated cells » for infected ($mCherry^+$) cells that are positive for the specific staining and that are isolated, « aggregated cells » for the infected cells positive for the specific staining and forming aggregates, and finally, « negative cells » for the infected cells

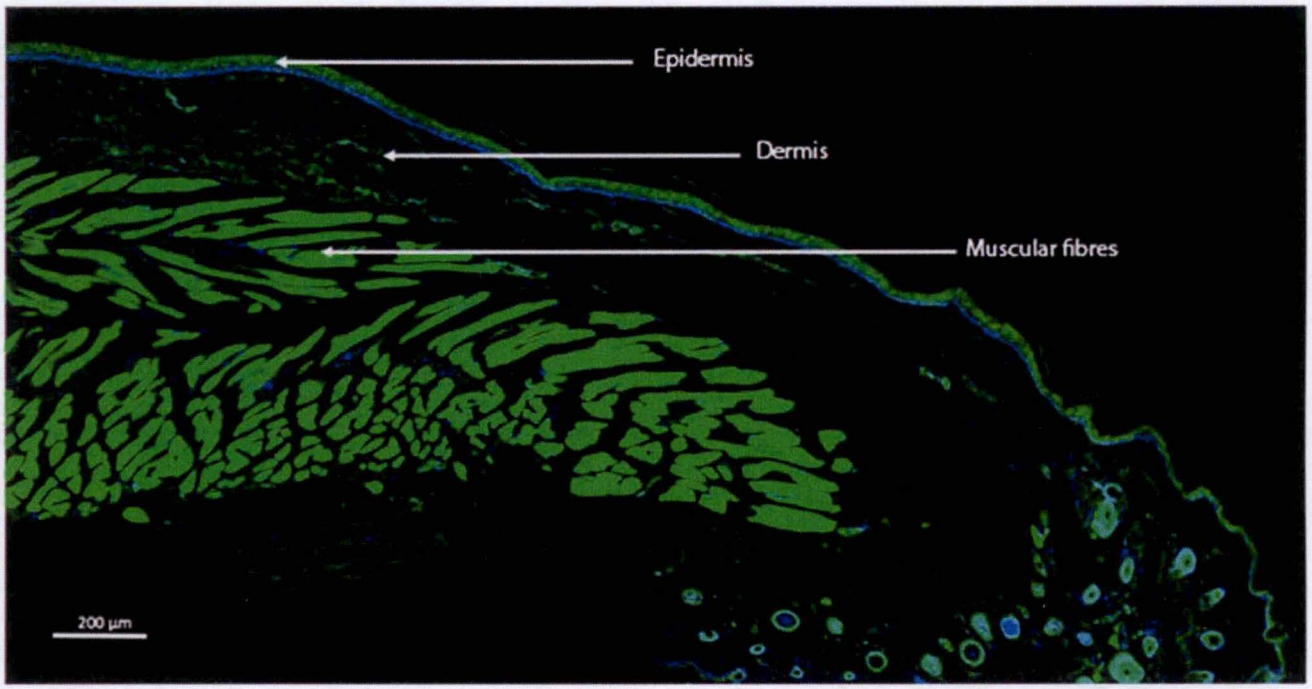


Figure 25: Histofluorescence analysis of a lesion from a naive WT C57BL/6 mouse

The lesion of a naive mouse has been harvested and the following stainings have been used: DAPI (DNA; blue) and Phalloidin (actin; green). Epidermis, dermis and muscular fibres are observable and are indicated with white arrows. Bar scale: 200 µm.

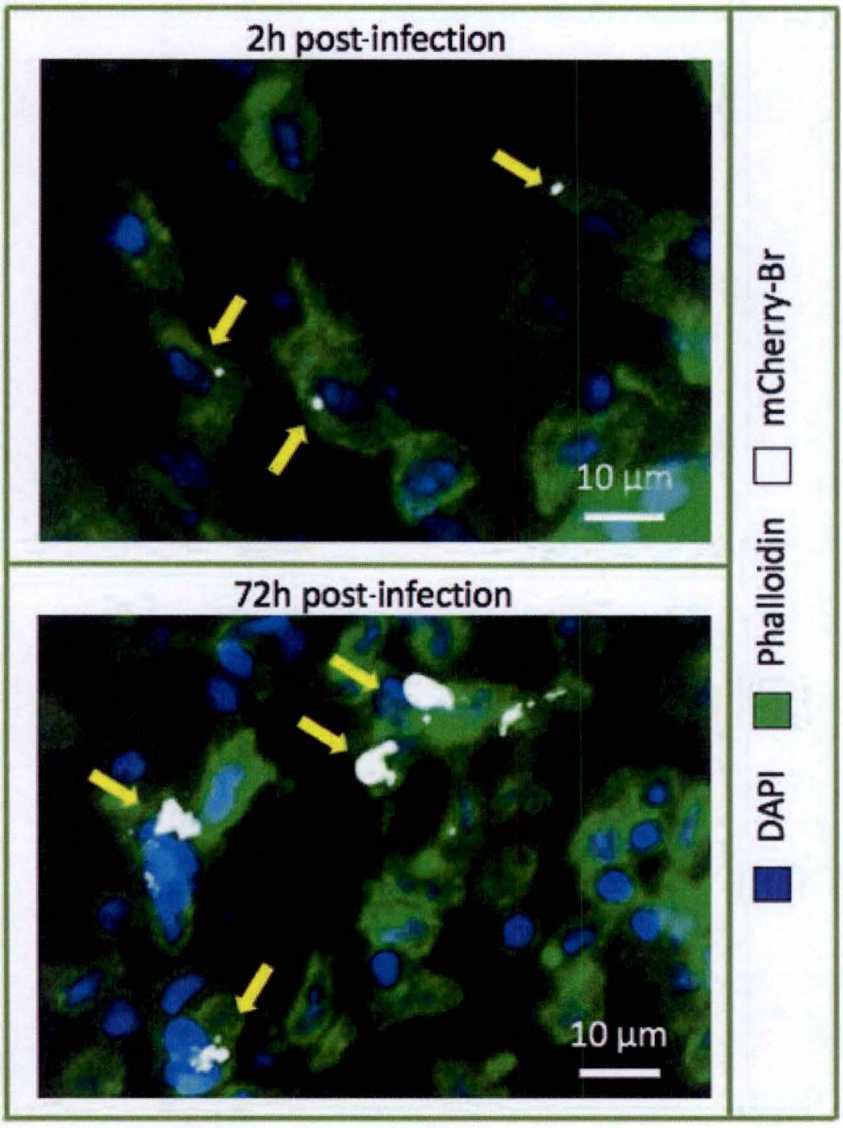


Figure 26: Immunohistofluorscence analysis of lesion after intra-dermal infection of WT C57BL/6 mice

Mice have been infected with 20 µL of a suspension containing $2x10^6$ bacteria/mL. At 2 hours and 72 hours post-infection, the footpads have been harvested to perform immunohistofluorescence stainings as described in Materials and Methods. The following stainings have been used: DAPI (DNA) and phalloidin (actin). Scale bars: 10 µm. Yellow arrows show the infected cells representative of the number of bacteria by cell.

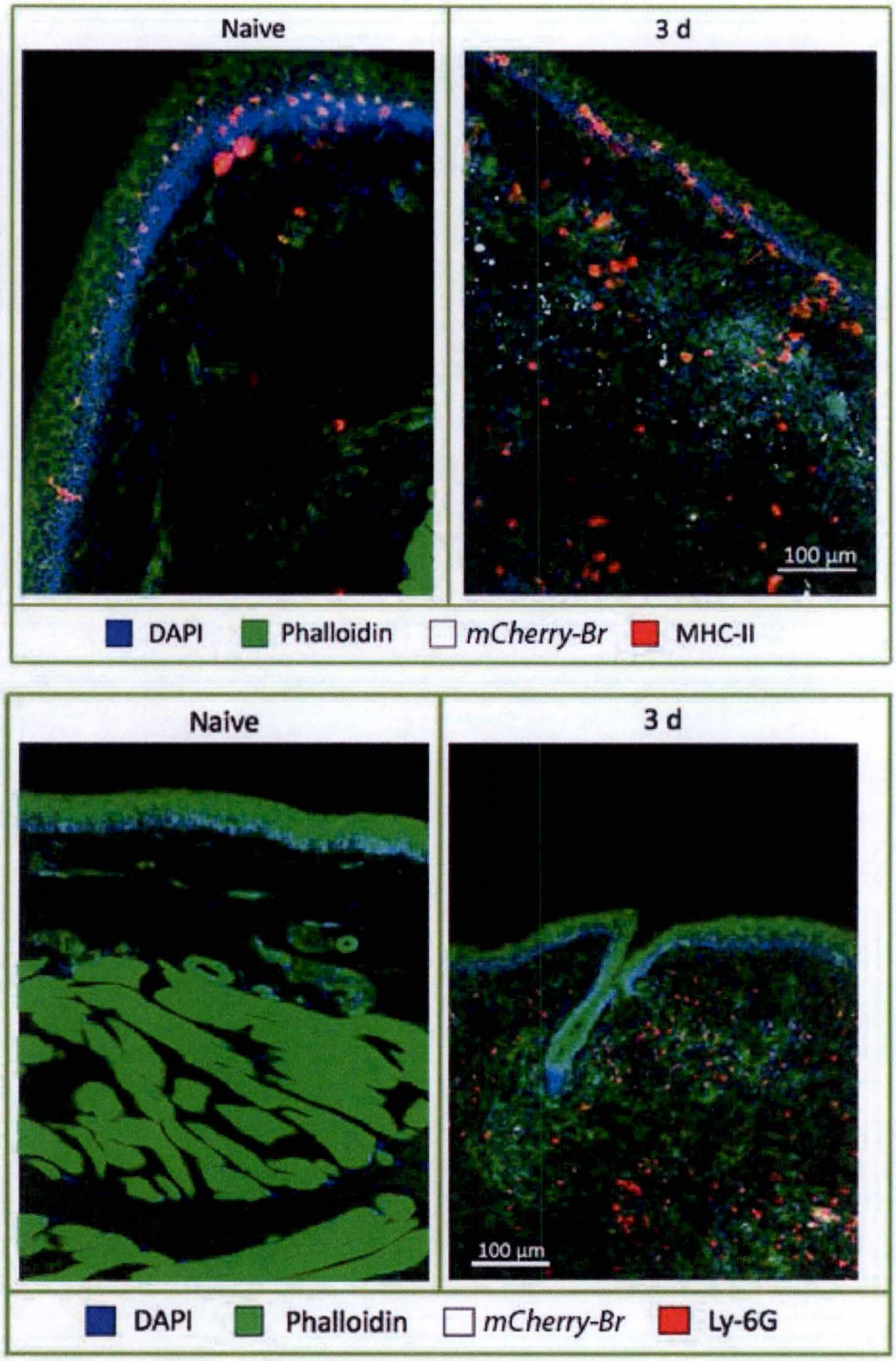


Figure 27: Immunohistofluorscence analysis of lesion after ID infection of C57BL/6 WT mice

Mice have been infected with 20 µL of a suspension containing $2x10^6$ bacteria/mL. At 3 days post-infection, the footpads have been harvested to perform immunohistofluorescence stainings as described in Materials and Methods. Lesion of naive mice has undergone the same treatment. The following stainings have been used: DAPI (DNA), phalloidin (actin) and MHCII (MHCII expressing-myeloid cells) (**A.**) or Ly-6G (neutrophils) (**B.**) Scale bars: 100 µm . Each image that is shown here is representative of the whole observation.

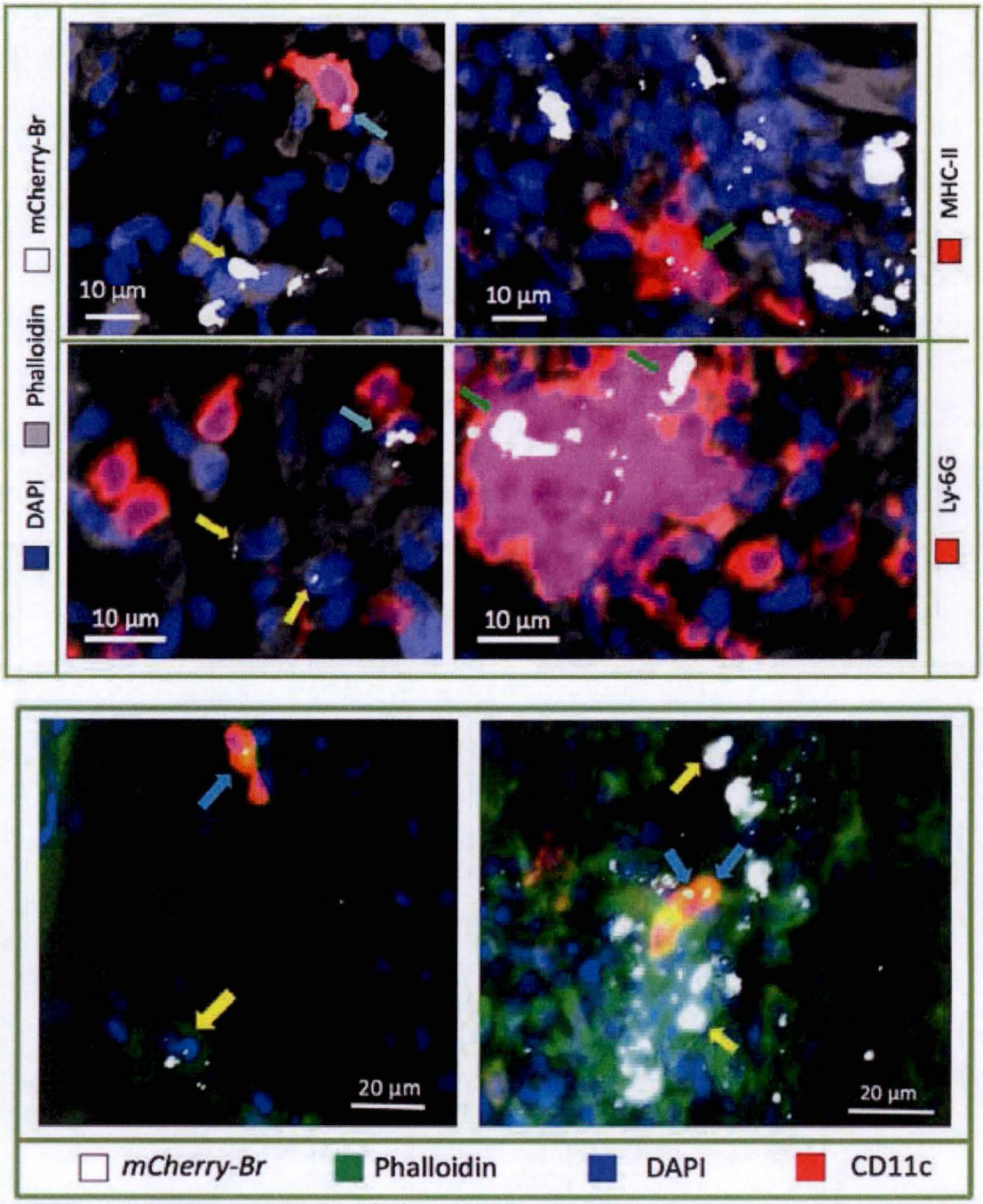


Figure 28: Characterization of infected cells expressing MHCII, Ly-6G or CD11c in the lesion of WT C57BL/6 mice

Mice have been infected with 20 µL of a suspension containing $2x10^6$ bacteria/mL. At selected times post-infection, the footpads have been harvested to realize immunohistofluorescence stainings as described in Materials and Methods. The following stainings have been used: DAPI (DNA), phalloidin (actin), MHCII (MHCII expressing-myeloid cells) or L6-6G (neutrophils) or CD11c (dendritic cells). Scale bar: 10 µm. The data represent what means in this case « negative » (yellow arrows), « isolated » (blue arrows), or « aggregated » (green arrows) infected cells. Each image that is shown here is representative of the whole observation.

negative for the specific staining. The **figure 28** shows representative images of each category. Although the aggregates formed between Ly-6G$^+$ cells frequently contain a great number of cells, the aggregates formed by MHCII$^+$ cells are generally composed of only 2 or 3 cells. It should be noticed that a positive is considered as a merged image between the antibody staining and *mCherry-Brucella*. A confocal microscopic analysis could be used for the confirmation of the location of *Brucella* and to be sure that it is indeed inside of the cell.

For the **Ly-6G-specific staining (figure 29) of neutrophils**, 490 (2 hours), 955 (24 hours) and 3,018 (72 hours) infected cells have been observed. These numbers represent 100 % of counted cells at each specific time. Among these cells, at 2 hours and 1 day p.i., more than 96 % of infected cells appear « negative ». However, at 3 days p.i., the percentage of the positive (isolated and mostly aggregated) infected cells increases to reach 8.5 % and 25.6 % respectively. Concerning the **MHCII staining (figure 29)**, the counting has been realized on 504 (2 hours), 239 (24 hours) and 1,774 (72 hours) infected cells. During the kinetic, the percentage of MHCII$^+$ isolated cells stays stable and corresponds to a mean of 9 % of infected cells.
Finally, for the **CD11c staining (figure 29)** specific of DCs, 62 (2 hours), 352 (24 hours) and 1,560 (72 hours) infected cells have been counted. The results show that more than 92 % of infected cells are negative for the staining.
These results suggest that in a lesion, 25.6 % of infected cells seems to be neutrophils (expressing Ly-6G) at 3 days p.i.. However, at 2 hours, 1 day and 3 days p.i. the infected cells are neither predominantly activated mature monocytes (expressing high level of MHCII) nor DCs (expressing CD11c) nor neutrophils (at 2 hours and 1 day p.i.). At this stage, we cannot conclude about the identity of the infected cells at early times post-infection in the lesion.

The same stainings (DAPI, Phalloidin, Ly-6G, MHCII, CD11c) have been realized on cryo-sections from infected popliteal lymph nodes (**figure 30**). At 2 hours and 1 day p.i., the number of bacteria appears insufficient to allow a statistical analysis of the phenotype. As a consequence, we have limited our analysis to the 3 d infected-draining lymph node (**figure 31**). For the Ly-6G staining, on 201 infected cells, only 6.5 % are positive. We observed that, in contrast to lesion, approximately half of infected cells are positive for MHCII and CD11c markers, suggesting that infected cells in popliteal lymph nodes are mainly mature DCs (CD11c$^+$ MHCII$^+$).

Preliminary data from the Aurore Lison'master thesis (2014) have suggested the involvement of recruited monocytes in the control of *Brucella* growth in the lesion. Indeed, a flow cytometric analysis of recruited cells in lesion has shown that the major recruited population at 3 days p.i. is CD11b$^+$ (myeloid marker) F4/80$^+$ (monocytes/macrophages marker) and Ly- 6G$^-$ (neutrophils marker) (**figure 32**). This phenotype is correlated to the monocytes. Monocytes recruitment correlates with the size reduction of the lesion. To test the implication of these cells in the control of infection, CCR2$^{-/-}$ C57BL/6 mice (partially deficient for the recruitment of monocytes) and WT mice were infected. The CFU count has been measured at 3 days, 7 days and 28 days p.i. (**figure 33**). CCR2 deficiency significantly affects the ability of mice to control *Brucella* growth at 7 days and 14 days p.i. in lesion and draining lymph node but not in spleen. This experiment has been performed only one time, but confirms the previous experiments realized by A. Lison during her master thesis. They confirm a key role of monocytes in the early control of *Brucella* in the ID infection and the involvement of the CCR2 chemokine receptor in the recruitment of monocytes.

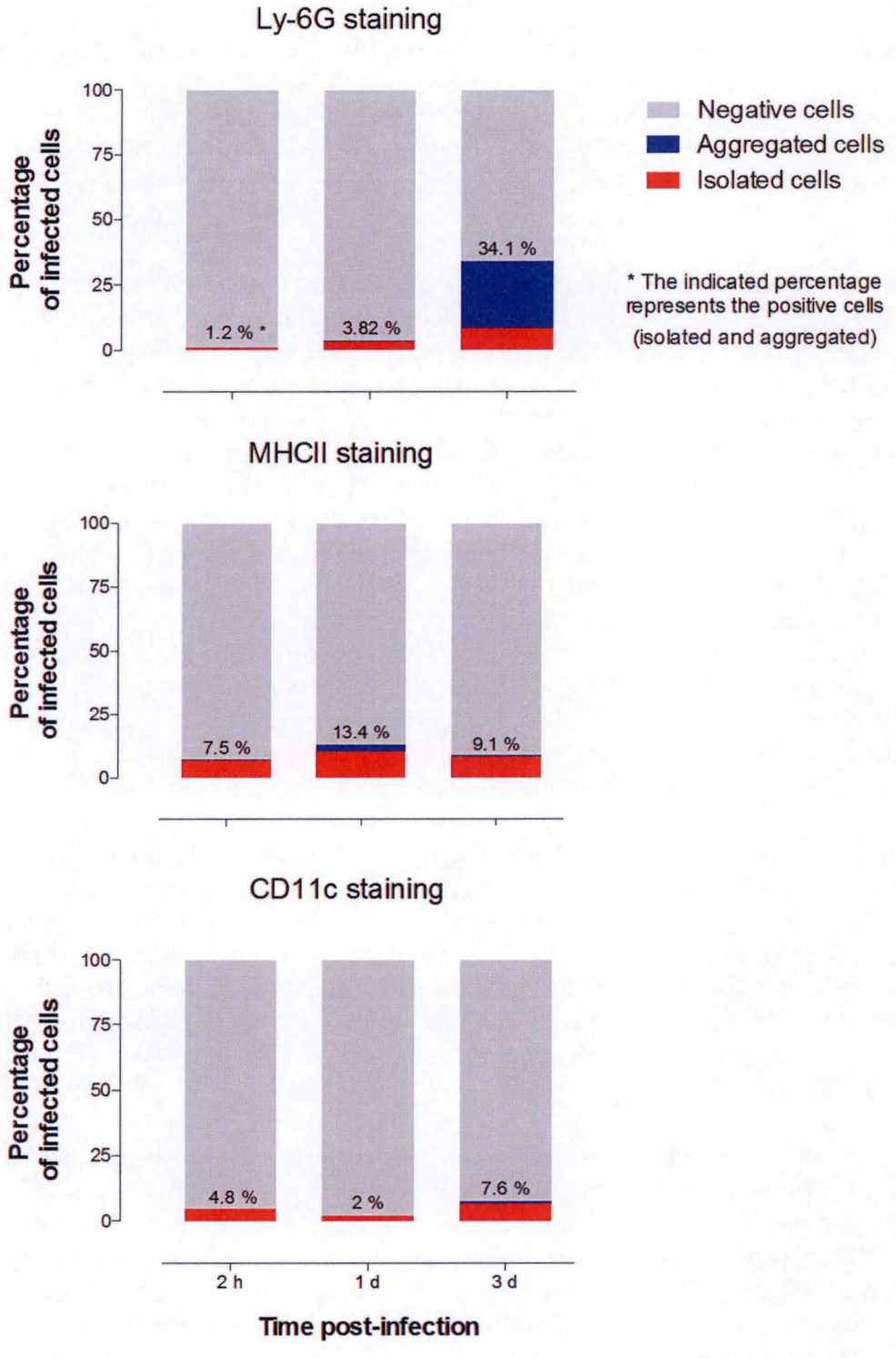


Figure 29: Comparison of the phenotype of infected cells in the lesion of WT C57BL/6 mice

Mice have been infected with 20 µL of a suspension containing $2x10^6$ bacteria/mL. At selected times post- infection, the footpads have been harvested to perform immunohistofluorescence stainings as described in Materials and Methods. The following stainings have been used: DAPI (DNA), phalloidin (actin), MHCII (MHCII expressing-myeloid cells) or Ly-6G (neutrophils) or CD11c (dendritic cells). 100 % represents 490 ; 955 and 2,018 infected cells counted at 2 hours, 1 and 3 days post-infection for the Ly-6G staining – 504 ; 239 ; 1,774 infected cells counted at 2 hours, 1 and 3 days post-infection for the MHCII staining – 62 ; 352 ; 1,560 infected cells counted at 2 hours, 1 and 3 days post-infection for the CD11c staining.

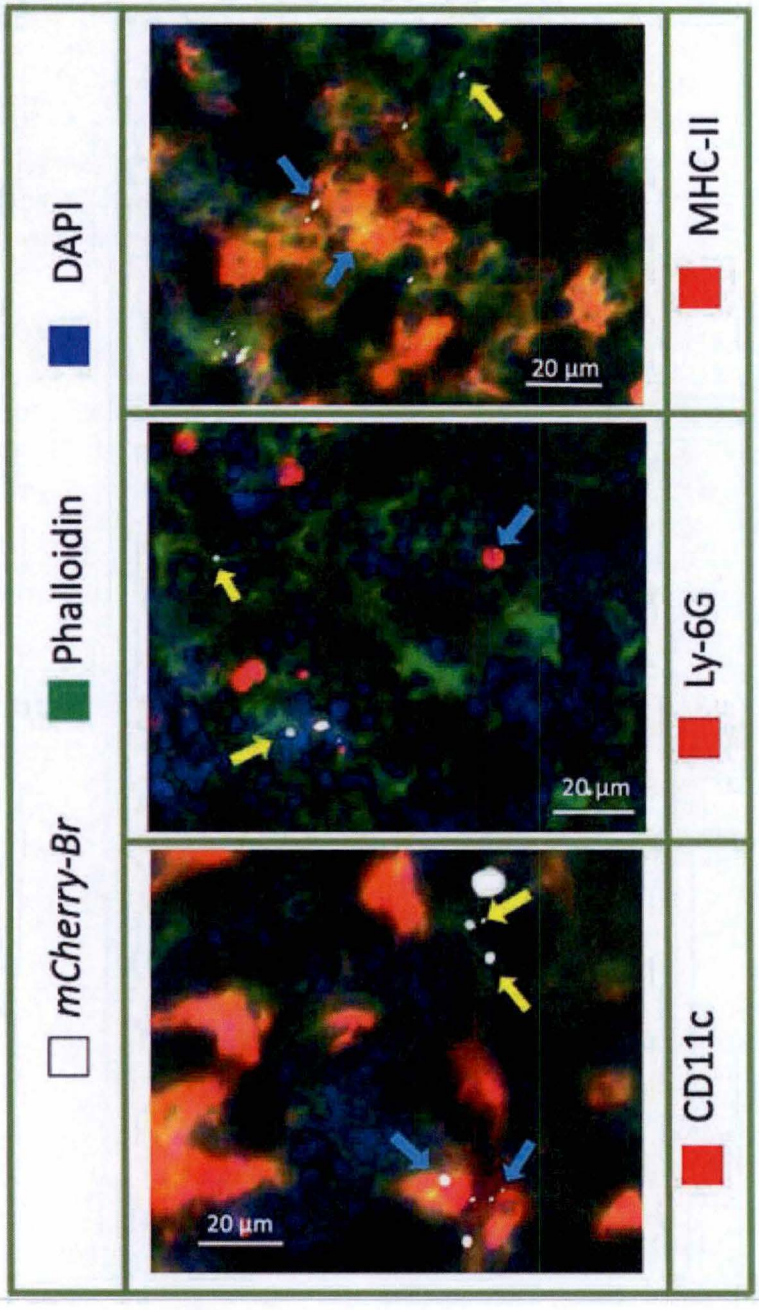


Figure 30: Characterization of infected cells expressing MHCII or Ly-6G or CD11c in the dLN of WT C57BL/6 mice

Mice have been infected with 20 µL of a suspension containing $2x10^6$ bacteria/mL. At selected times post-infection, the draining lymph nodes have been harvested to perform immunohistofluorescence stainings as described in Materials and Methods. The following stainings have been used: DAPI (DNA), phalloidin (actin), MHCII (MHCII expressing-myeloid cells) or Ly-6G (neutrophils) or CD11c (dendritic cells). Scale bars: 20 µm. The data represent what means in this case « negative » (yellow arrows) or « positive isolated » (blue arrows) infected cells. Each image that is shown here is representative of the whole observation.

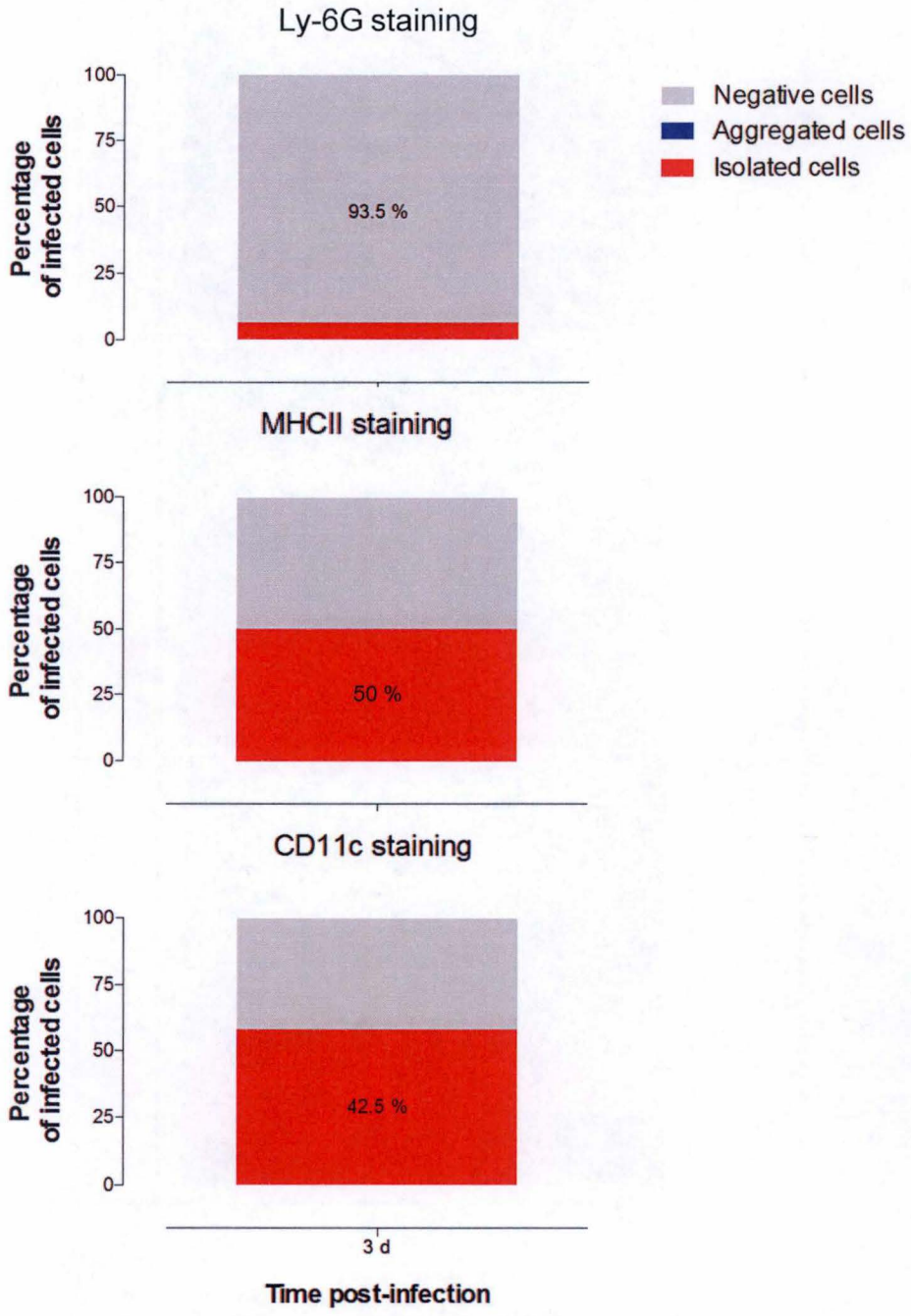


Figure 31: Comparison of the phenotype of infected cells in the popliteal lymph node of WT C57BL/6 mice

Mice have been infected with 20 µL of a suspension containing $2x10^6$ bacteria/mL. At selected times post-infection, the draining lymph nodes have been harvested to realize immunohistofluorescence stainings as described in Materials and Methods. The following stainings have been used: DAPI (DNA), phalloidin (actin), MHCII (MHCII expressing-myeloid cells) or Ly-6G (neutrophils) or CD11c (dendritic cells). 100 % represents 201 infected cells counted at 3 days post-infection for the Ly-6G staining – 96 infected cells counted at 3 days post-infection for the MHCII staining – 181 infected cells counted at 3 days post-infection for the CD11c staining. Data must be reproduced.

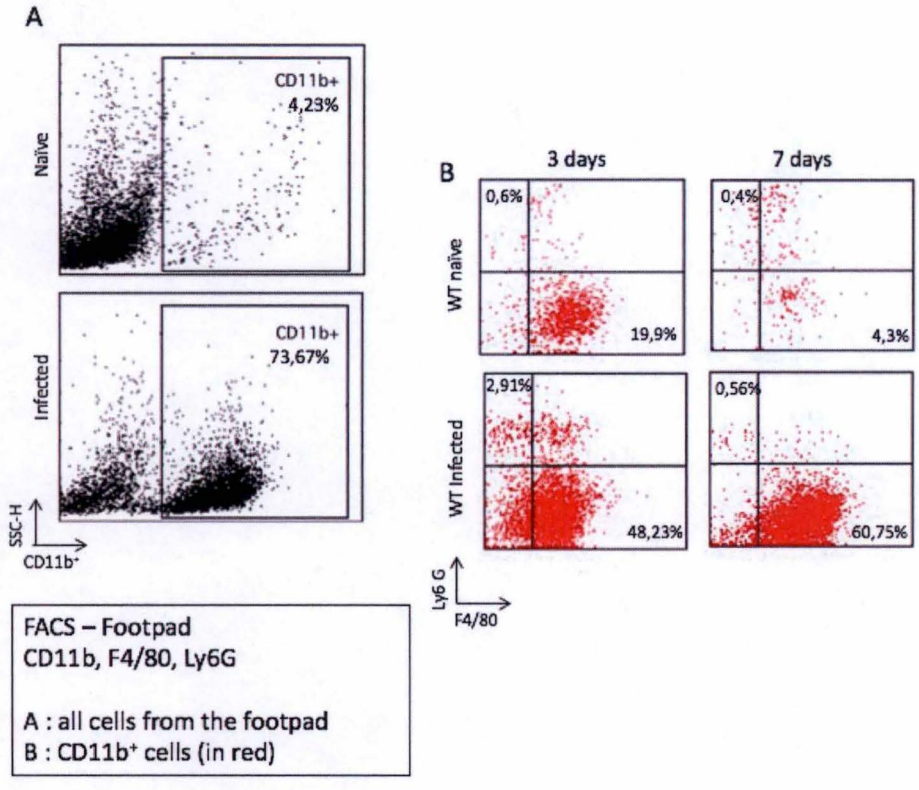


Figure 32: Flow cytometric analysis of an infected lesion of WT C57BL/6 mice

Mice have been infected with 20 µL of a suspension containing $2x10^6$ bacteria/mL. At 3 and 7 days post-infection, lesions have been harvested to perform cytofluorometric analysis. (**A.**) First, CD11b staining has been used (to mark the myeloid cells). Next, from these $CD11b^+$ cells (73.67 % in an infected foodpad), (**B.**) Ly-6G (neutrophils) and F4/80 (monocytes/macrophages) stainings have been used. Data from A. Lison's master thesis(2014-2015).

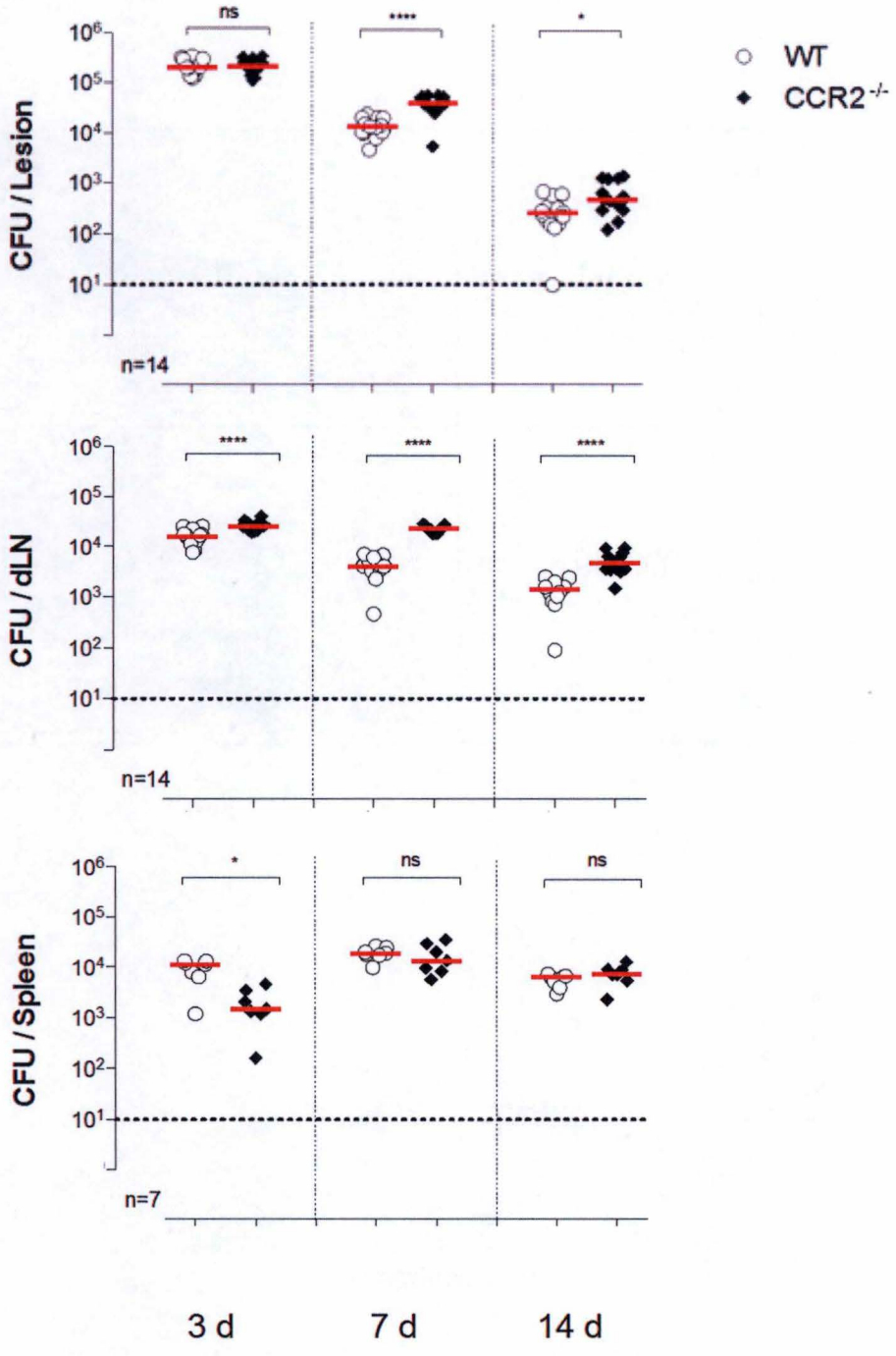


Figure 33: Variation in time of the bacterial load in lesion, draining lymph node and spleen in WT and CCR2-deficient C57BL/6 mice after intra-dermal infection

Mice have been infected with 20 µL of a suspension containing $2x10^6$ bacteria/mL. At selected times post-infection, the footpads, draining lymph nodes and spleens have been harvested and plated on 2YT agar medium to assess the bacterial load (CFU) as described in Materials and Methods. Significant differences are denoted by asterisks: * $p < 0.05$, **** $p < 0.0001$. n (number of organs), ns (non-significant), red bar: median, dotted line: threshold of detection of bacteria.

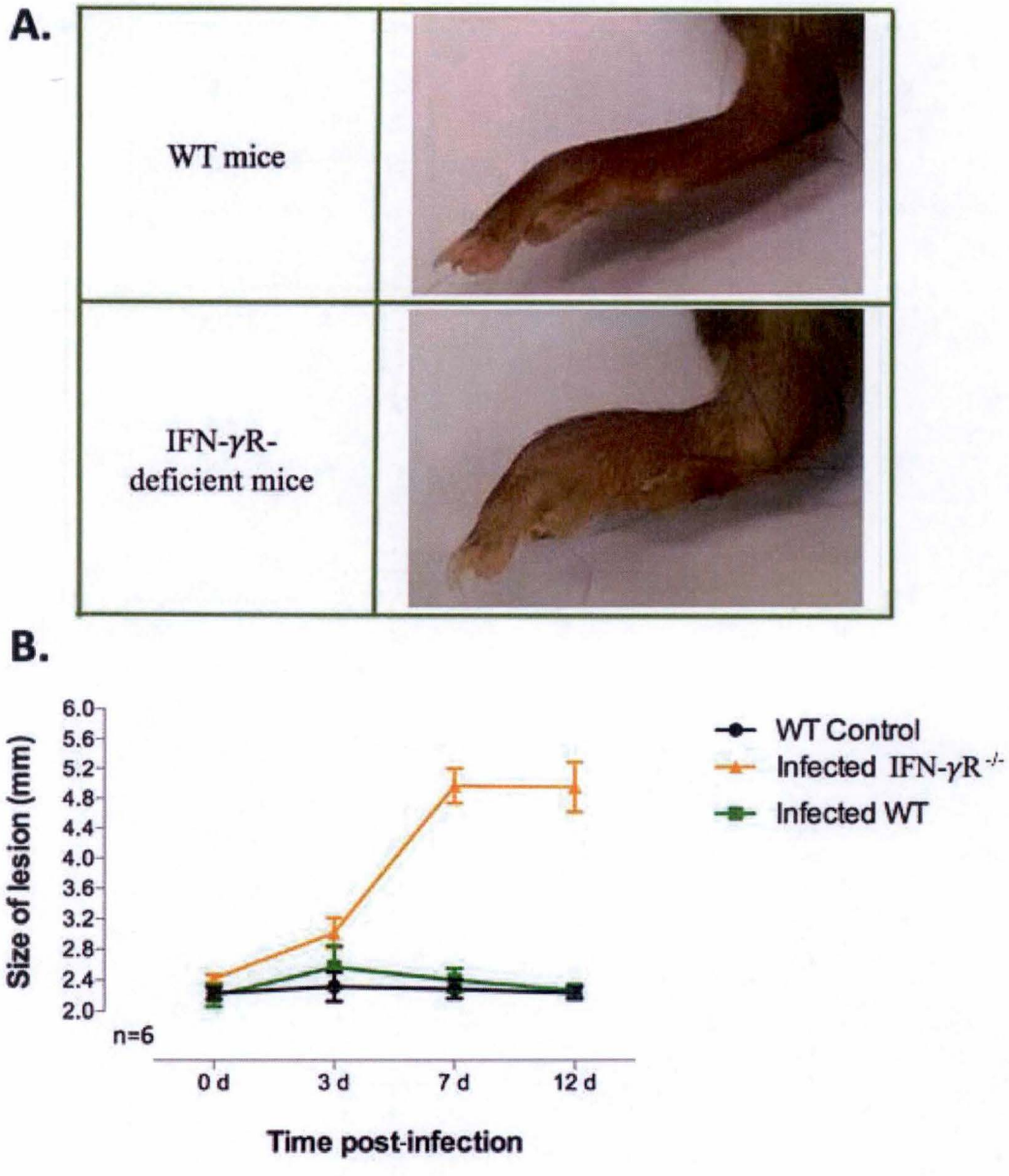


Figure 34: Comparison of infected footpad of WT and IFN-γ deficient C57BL/6 mice

Mice have been infected with 20 µL of a suspension containing $2x10^6$ bacteria/mL. The pictures (**A.**) have been taken at 14 days post-infection. The size of the lesion (**B.**) has been measured at selected times post-infection with the Vernier tool. Six mice by group have been used to measure the lesion at each time. d (day), n (number of footpad measured).

3 Characterization of immune response following primary ID infection

To characterize the type of T helper immune response involved in the control of primary infection, WT, IFN-γR$^{-/-}$ and IL-17RA$^{-/-}$ C57BL/6 mice have been ID infected. At 14 days post-infection, IFN-γR$^{-/-}$ mice display a strong swelling and a necrotic aspect (**figure 34 A.**). In contrast, footpad from WT and IL-17RA$^{-/-}$ (not shown) mice appear small and non necrotic. The size of the lesion has been measured for infected WT mice, control WT mice (uninfected) and IFN-γR$^{-/-}$ mice before the infection (0 day), 3 days, 7 days and 12 days p.i. (**figure 34 B.**). The peak of infection of WT mice is reached at 3 days, as already demonstrated. The size of the lesion of IFN-γR-deficient mice increases from the day of the infection to 7 days p.i. and is then stable around 4.9 mm.
To evaluate the bacterial load in the different organs, lesions, draining lymph nodes and spleens have been harvested at 3 days, 7 days and 14 days p.i. (**figure 35**). In the lesion, although the bacterial load of the WT and IL-17RA$^{-/-}$ mice decreases with the time, the bacterial load of IFN-γR$^{-/-}$ mice remains high and stable, with a bacterial load between 10^5 and 10^6 CFU/lesion. In the draining lymph node, the bacterial load of WT, IFN-γR$^{-/-}$ and IL-17RA$^{-/-}$ mice is the same at 3 days p.i.. At 7 and 14 days p.i., WT and IL-17RA$^{-/-}$ mice present approximately the same number of CFU, but the CFU of IFN-γR-deficient mice increase of around one log. Finally, in the spleen, the number of detected bacteria is approximately the same between the three groups of mice during all the kinetic.
Collectively, these results suggest that the IFN-γ-mediated T_H1 response, but not IL-17-mediated T_H17 response, plays an important role in the control of the ID infection with *Brucella.*

A possible pathway for the production of IFN-γ is through the regulator T-bet, itself regulated by two possible routes: STAT-1 (via IL-27) and STAT-4 (via IL-12). To identify the pathway involved in IFN-γ production in our model, WT mice and mice genetically deficient for STAT-1, IL-12p35 (one of the two subunits of IL-12 cytokine) and T-bet have been infected. As previously, the representative images of lesions are showed (**figure 36 A.**) and the evolution of swelling of the infected footpad has been monitored (**figure 36 B.**).
Following ID infection, IL-12p35$^{-/-}$ and T-bet$^{-/-}$ mice display a lesion close to WT mice. The size of lesion of T-bet$^{-/-}$ mice follows the lesion size of the WT mice until 3 days p.i., but does not decrease after this time as observed in WT mice. In striking contrast, infected STAT-1$^{-/-}$ mice present a high swelling (> 5 mm) and necrosis. Note that the size of the lesion of STAT-1$^{-/-}$ mice has been measured for only two mice at later time because the other mice were dead during the experiment (see survival curve figure 38). Before dying, other mice presented the same lesion at the macroscopic level.

To evaluate the ability of each group of mice to control *Brucella* infection, a CFU count has been realized at 14 days p.i. (**figure 37**) on lesion, draining lymph node and spleen. At this time, STAT-1$^{-/-}$ mice appear unable to control bacterial growth in all tissues that were analyzed. Indeed, in lesion and the lymph node, the bacterial load is 3 log-higher than in WT mice. Note that the bacterial load has been evaluated with only the two survival mice for STAT-1$^{-/-}$ mice. Mice deficient for IL-12p35 have a number of CFU significantly higher than the WT mice in the lesion (*), draining lymph node (****) and the spleen (****). However, the significant difference between WT and IL-12p35$^{-/-}$ mice increases less than 1 log in three organs. Concerning T-bet, its deficiency does not seem to impact the control of bacteria. These results suggest that the production of IFN-γ could be dependent of STAT-1 pathway, but independent

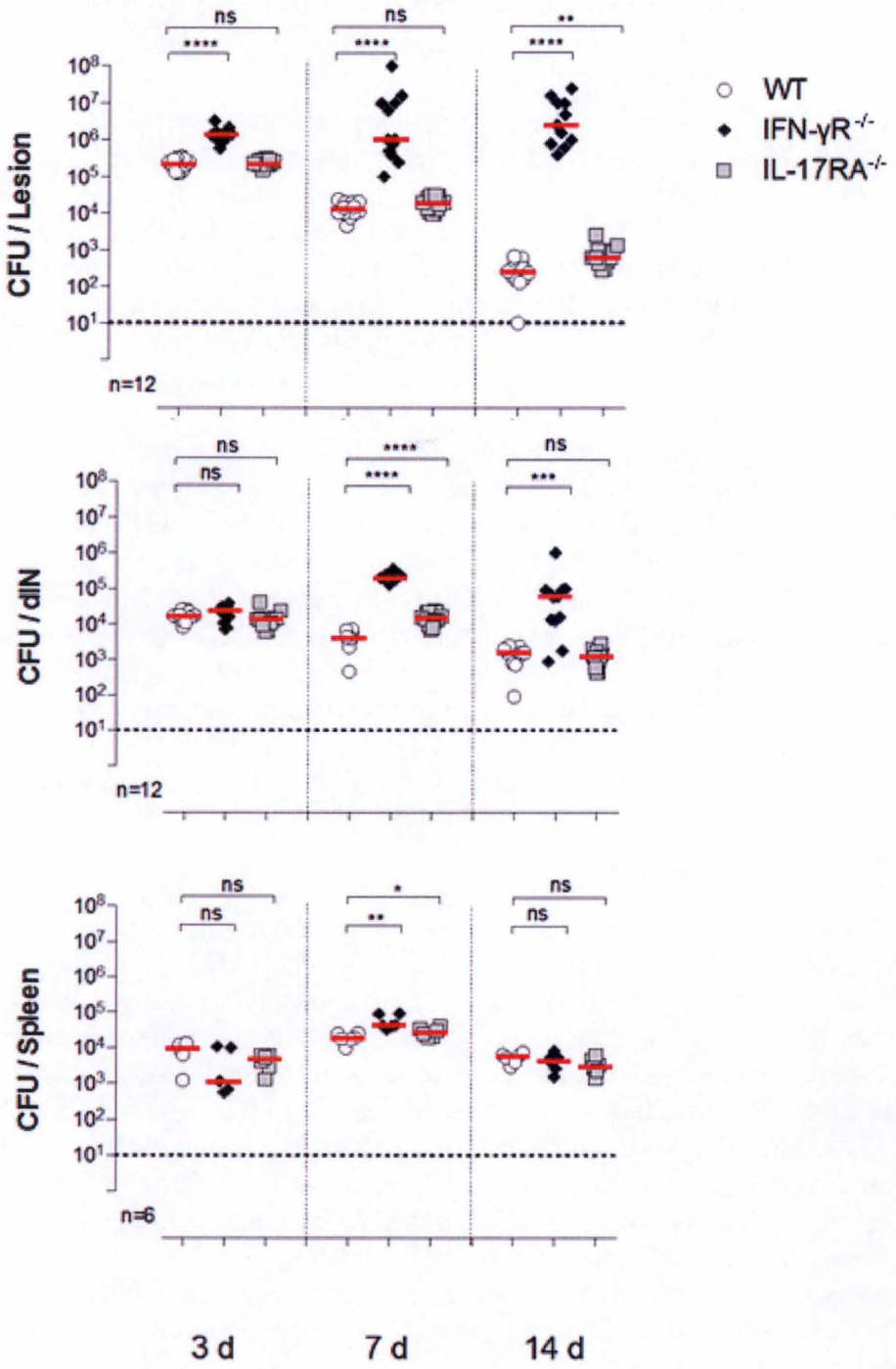


Figure 35: Kinetic of bacterial load in lesion, draining lymph node and spleen in WT, IFN-γR- and IL-17RA- deficient C57BL/6 mice after intra-dermal infection

Mice have been infected with 20 µL of a suspension containing $2x10^6$ bacteria/mL. At selected times post-infection, the footpads, draining lymph nodes and spleens have been harvested and plated on 2 YT agar medium to assess the bacterial load (CFU) as described in Materials and Methods. Significant differences are denoted by asterisks: * $p < 0.05$, ** $p < 0,01$, *** $p < 0,001$, **** $p < 0.0001$. n (number of organs), ns (non-significant), red bar: median, dotted line: threshold of detection ofbacteria.

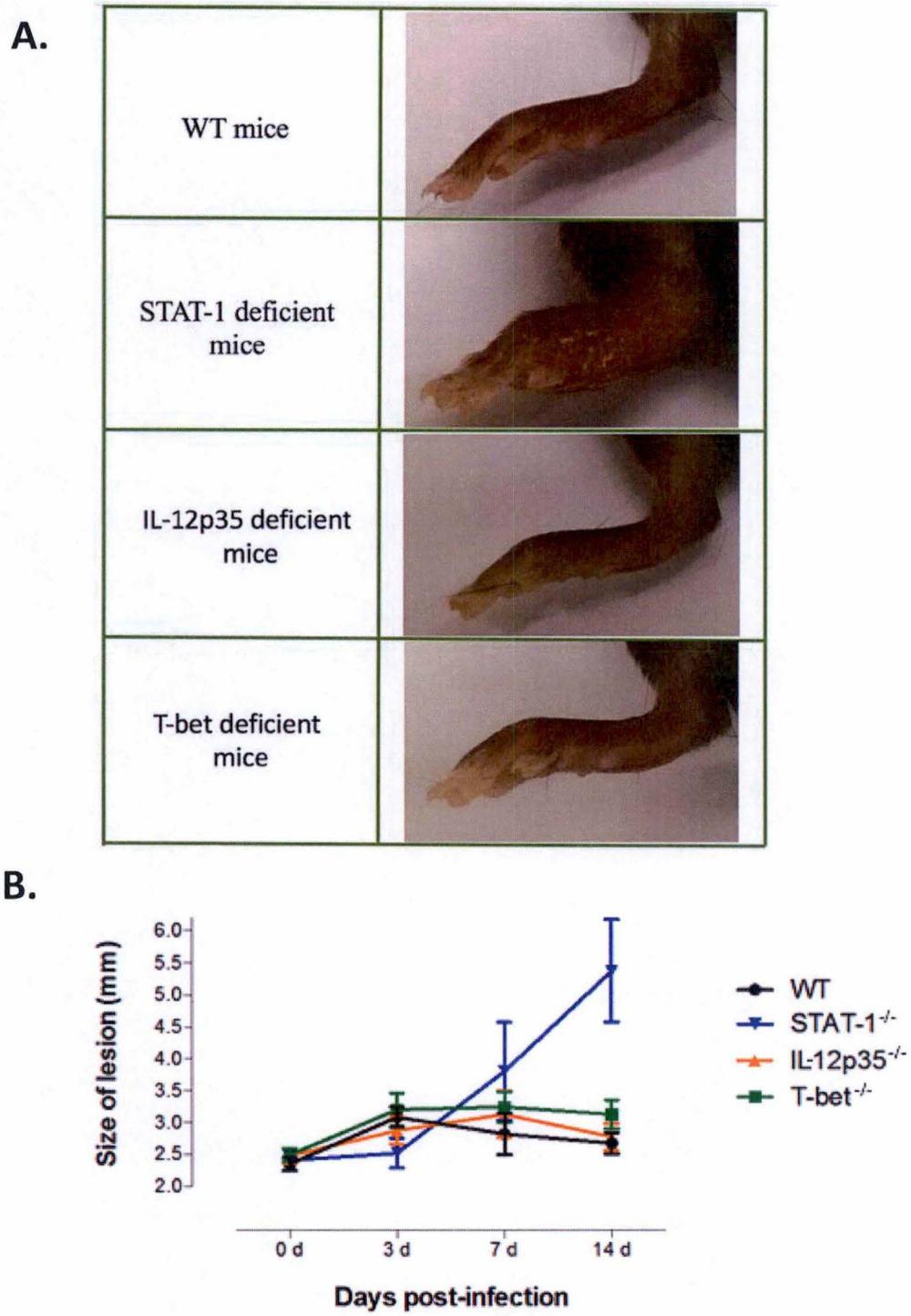


Figure 36: Comparison of infected footpad of WT, IFN-γR- and STAT-1-deficient C57BL/6 mice

Mice have been infected with 20 µL of a suspension containing $2x10^6$ bacteria/mL. The pictures (**A.**) have been taken at 14 days post-infection. The size of the lesion (**B.**) has been measured at selected times post-infection with the Vernier tool. 11 WT, 9 T-bet-, 9 IL-12p35-deficient mice have been used to measure the lesion at each time. For the STAT-1 deficient mice, 12 mice have been used at the early times (0 and 3 days), 10 mice at 7 days and 2 mice at 14 days post-infection because mice died during the experiment (see **figure38**).

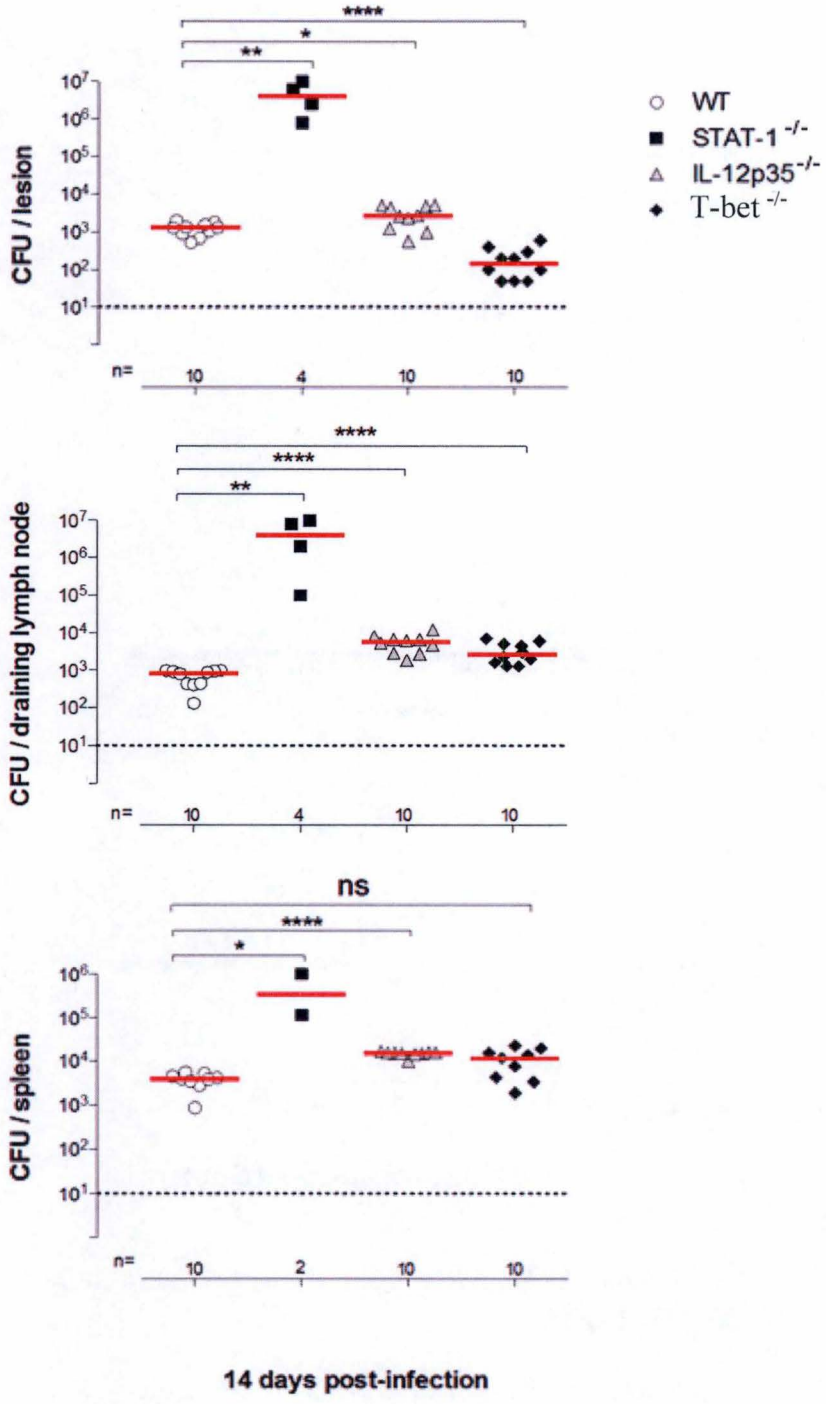


Figure 37: Variation of bacterial load at 14 days post-infection in lesions, draining lymph nodes and spleens in WT, STAT-1-, IL-12p35- and T-bet-deficient C57BL/6 mice after intra-dermal infection

Mice have been infected with 20 µL of a suspension containing $2x10^6$ bacteria/mL. At 14 days post- infection, the footpads, draining lymph nodes and spleens have been harvested and plated on 2 YT agar medium to assess the bacterial load (CFU) as described in Materials and Methods. Significant differences are denoted by asterisks: * $p < 0.05$, ** $p < 0.01$, **** $p < 0.0001$.

n (number of organ), ns (non-significant), red bar: median, dotted line: threshold of detection of bacteria.

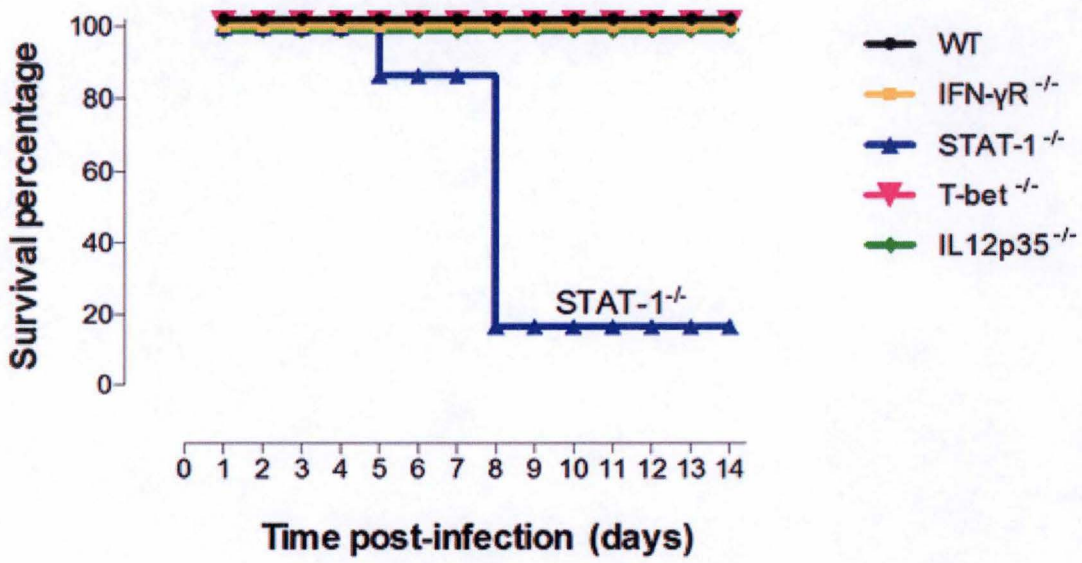


Figure 37: Survival curve of WT C57BL/6 mice and C57BL/6 deficient mice for IFN-γ, STAT-1, T-bet and IL-12p35

Mice have been infected with 20 µL of a suspension containing $2x10^6$ bacteria/mL. The survival of mice has been observed every day during 14 days. 100 % represents 11 mice for WT, 6 mice for IFN-$\gamma^{-/-}$ mice, 9 mice for T-bet$^{-/-}$, 9 mice for IL-12p35$^{-/-}$ and 12 mice in the case of STAT-1 deficient mice.

of T-bet. STAT-1-deficient mice have been tested in other experiments at other times and the same bacterial load at present every time.

As highlighted above, some STAT-1$^{-/-}$ mice died during this experiment. As a consequence, we have performed a survival curve with these groups of mice (**figure 38**). All WT or deficient mice survived during the 14 days, except the STAT-1$^{-/-}$ mice. Indeed, at 5 days p.i., 2 mice were dead. Six mice died after 8 days of infection and two other mice which were about to die have been sacrificed. To determine whether these mice died because of the infection with *Brucella melitensis*, or because they were more susceptible to the environmental conditions (humidity, other environmental pathogens, etc.), the survival can be tested by placing mice in two different cages, in the same environmental conditions and by infecting mice of only one cage. We do not have performed this experiment yet because STAT-1$^{-/-}$ mice are quite difficult to obtain.

4 Identification of lymphocyte cells critically involved in the control of primary and secondary *Brucella* infection

4.1 Primary immune response following ID infection

In order to identify the T lymphocyte populations involved in the control of primary *Brucella* infection, WT and mice deficient for T cells subsets (CD3, γδTCR, αβTCR, MHCII and TAP1) have been infected and the organs harvested at 3, 7, 14 and 28 days p.i. (**figure 39**). In the lesion, draining lymph node and spleen at 3 days p.i., there was no significant increase of deficient mice bacterial load compared to the WT mice. At later times in lesion and draining lymph node, CD3$^{-/-}$, αβTCR$^{-/-}$ and MHCII$^{-/-}$ mice showed a statistically higher CFU count when compared to WT mice, suggesting that CD4^{+} T cells are important to control *Brucella* growth. Finally, in the spleen, no particular T cells population seems indispensable at early times p.i. (3 and 7 days) as WT and deficient mice displayed similar CFU levels. However, at later time (14 and 28 days p.i.), the αβTCR T cells seemed as important as CD3$^{-/-}$. Indeed, the CFU of these deficient mice were more than 1 log higher than CFU of WT mice. The bacterial load in WT, TAP1$^{-/-}$ and MHCII$^{-/-}$ mice appear similar, suggesting that in the spleen, αβTCR T cells are indispensable but that CD4^{+} and CD8^{+} T cells can compensate the absence of each other.

Concerning the role of B cells in primary infection, ELISA tests to detect circulating antibodies specific to *Brucella* have been performed on sera from infected WT mice at different times p.i. (6, 13, 28 and 50 days) (**figure 40**). Mice have been infected via intra- peritoneal or intra-dermal mode. Each time has been tested to detect the presence of the following isotypes: IgG1, IgG2a, IgG3 and IgM. A first general observation is that the antibodies kinetic for ID and IP infection are very similar for each isotype. IgM antibodies are detected from 6 days p.i. and their amount increases to finally decreases at 28 days p.i.. IgG1, IgG2a[13] and IgG3 are not detected before 13 days p.i. but then are present in blood at least until 50 days p.i.. These experiments have been realized only once and must be thus reproduced but it suggests that IgM could be the antibody present at early times post-infection and could be replaced later by IgG1, IgG2a and IgG3. These results show that antibodies are produced and thus that the B cells are activated, but at this stage, we do not know if these antibodies are used to fight *Brucella.* A preliminary experiment (data not shown) demonstrated that MuMT$^{-/-}$ mice (deficient for B cells) display the

[13] In C57BL/6 mice, the IgG2a isotype is replace by IgG2c isotype, but "IgG2a" is often the term used.

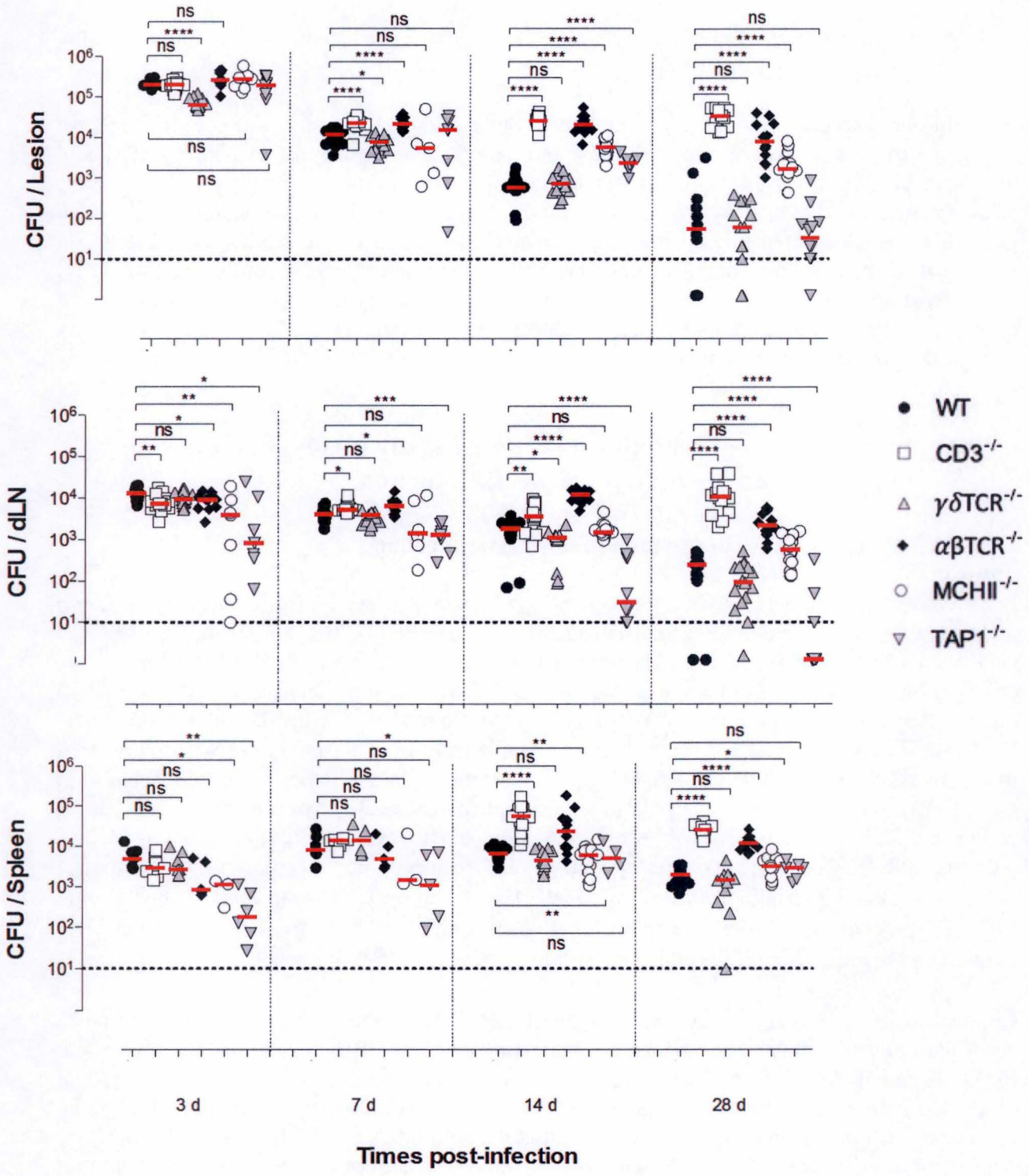


Figure 39: Variation of bacterial load with time in lesions, draining lymph nodes and spleens in WT, CD3-, αβTCR-, γδTCR-, MHCII-, TAP1-deficient C57BL/6 mice after intra-dermal infection

Mice have been infected with 20 µL of a suspension containing $2x10^6$ bacteria/mL. At selected times post-infection (3, 7, 14, 28 days p.i.), the footpads, draining lymph nodes and spleens have been harvested and plated on 2 YT agar medium to assess the bacterial load (CFU) as described in Materials and Methods. Significant differences are denoted by asterisks: * $p < 0.05$, ** $p < 0.01$, **** $p < 0.0001$. n (number of organ), ns (non-significant), red bar: median, dotted line: threshold of detection of bacteria.

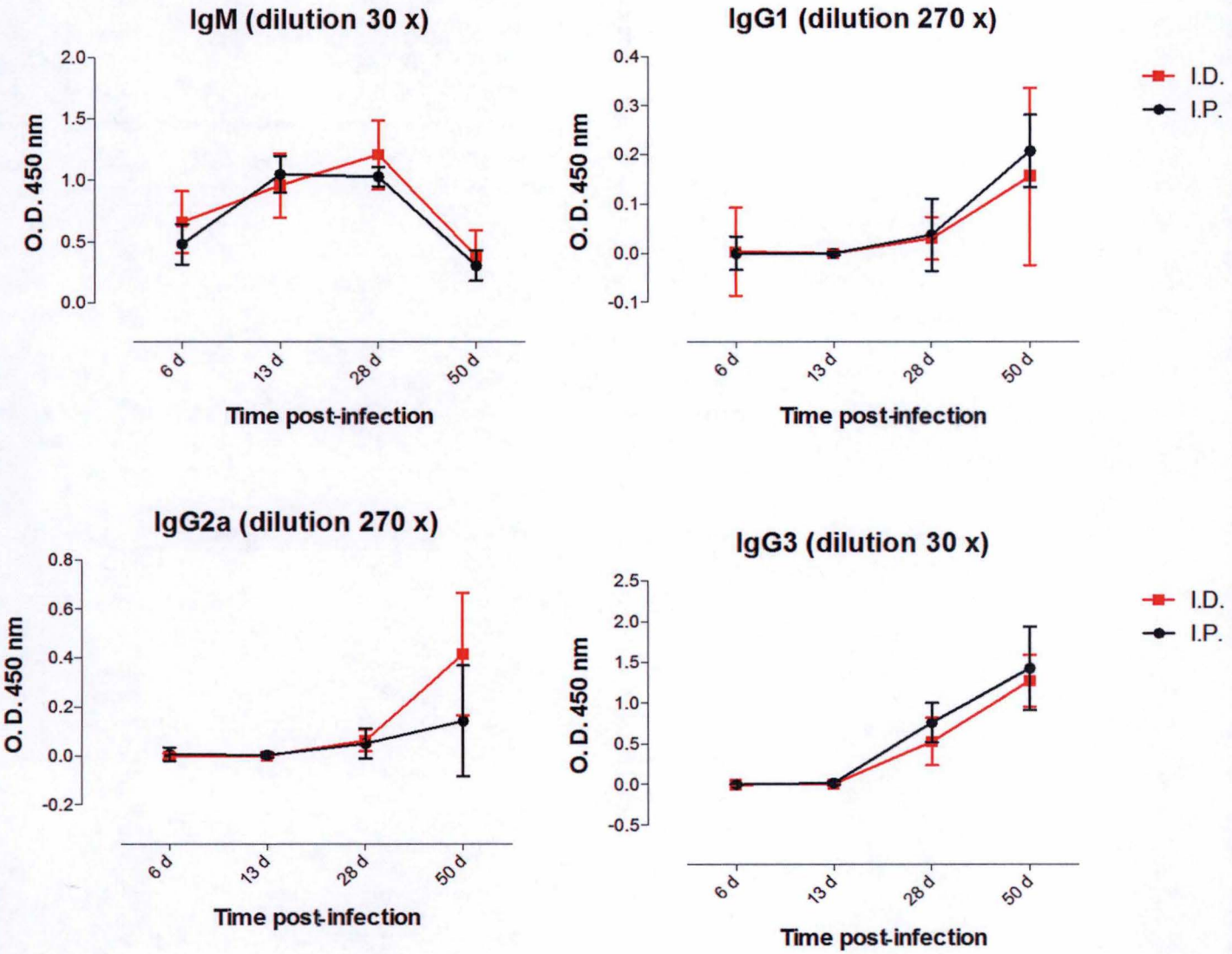


Figure 40: ELISA test on serum of WT C57BL/6 mice after intra-dermal or intra-peritoneal mode of infection

Six WT C57BL/6 mice have been ID infected with 20 µL of a suspension containing $2x10^6$ bacteria/mL. Six other WT C57BL/6 mice have been IP infected with $4x10^4$ CFU of *B. melitensis*/500 µL. At selected times post-infection, sera have been collected and ELISA have been performed to detect isotype distribution of *Brucella*-specific antibodies. The data represent the O.D. (optical density) in function of time post-infection for the indicated antibody dilution.

I.D. (intra-dermal), I.P. (intra-peritoneal), d (day).

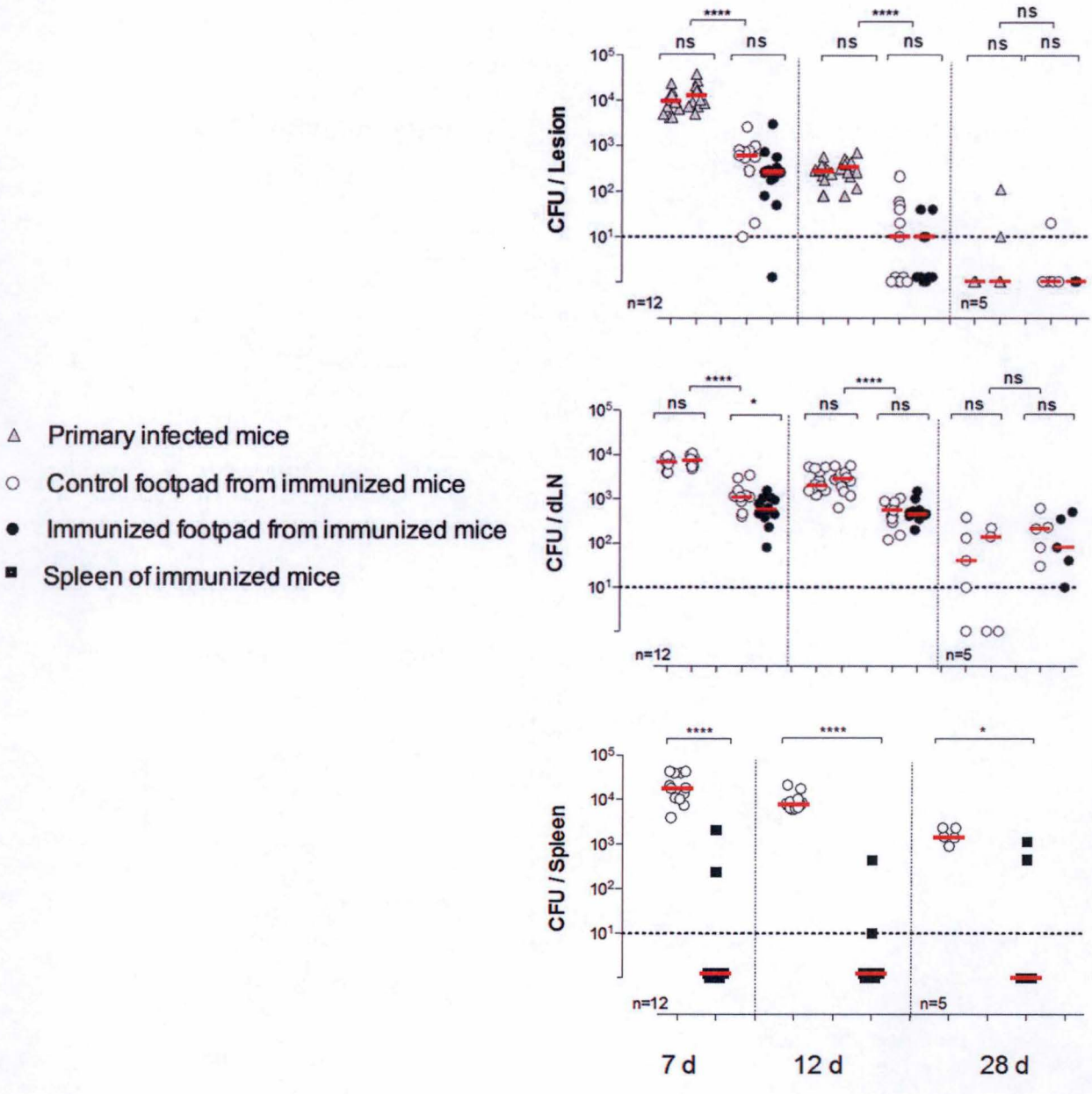


Figure 41: Comparison of protective immunity in WT C57BL/6 mice immunized previously with live *B. melitensis*

An infectious dose of $2x10^6$ *B. melitensis* 16M/mL for intra-dermal infection was used in this experiment. Approximately 20 µL of this suspension have been injected in the right footpad WT C57BL/6 mice. All mice were treated with antibiotics as described in the Materials and Methods and then challenged with 20 µL of an infectious dose ($2x10^6$ bacteria/mL) of *mCherry-Brucellae melitensis* 16M at both footpads. Mice have been sacrificed for lesion, draining lymph node and spleen harvesting at the selected times. The organs have been plated on 2 YT agar medium to assess the bacterial load (CFU) as described in Materials and Methods. Significant differences are denoted by asterisks. * $p < 0.05$, **** $p < 0{,}0001$.

These results are representative of two independent experiments. d (days), n (number of organ), ns (non significant), dLN (draining lymph node), red bar: median, dotted line: threshold of detection of bacteria.

same bacterial load than WT mice, suggesting that B cells may not be involved in the control of the bacteria.

4.2 Secondary immune response following ID infection

Previous results demonstrated that cellular immunity (T cells), mainly $CD4^+$ T lymphocytes, but not humoral immunity (via B cells), plays a crucial role in the control of primary *B. melitensis* infection.

In order to analyze the course of a secondary ID *B. melitensis* infection, WT mice were infected a first time (*Brucella melitensis* 16 M) at the right footpad, treated with antibiotics 28 days p.i. to eliminate bacteria (see Material and Methods). These mice were finally infected a second time (*mCherry-Brucella melitensis* 16 M) at both footpads, and are therefore called "immunized mice". In parallel, naive mice, called "primary infected mice", have been infected only one time with *mCherry-Brucella melitensis* 16 M at both footpads. At 7, 12 and 28 days p.i., lesions, draining lymph nodes and spleens from primary infected and immunized mice have been harvested (**figure 41**). No statistically difference is observed between the immunized (right) footpad and the control (left) footpad from immunized mice, suggesting that the peripheral memory plays a negligible role in the control of infection. However, we can observe that there is a significant difference of 1 log between the footpad and dLN of primary infected mice and the footpad and dLN of immunized mice. Concerning the spleen, at 7 and 12 days p.i., more than 83 % of spleens from immunized mice do not display detectable bacteria compared to spleen from primary infected mice that all display approximately 10^4 bacteria/spleen (7 and 12 d. p.i.). Collectively, these results could suggest that infected WT mice develop a protective memory immunity to efficiently control secondary infection. These results are representative of two independent experiments.

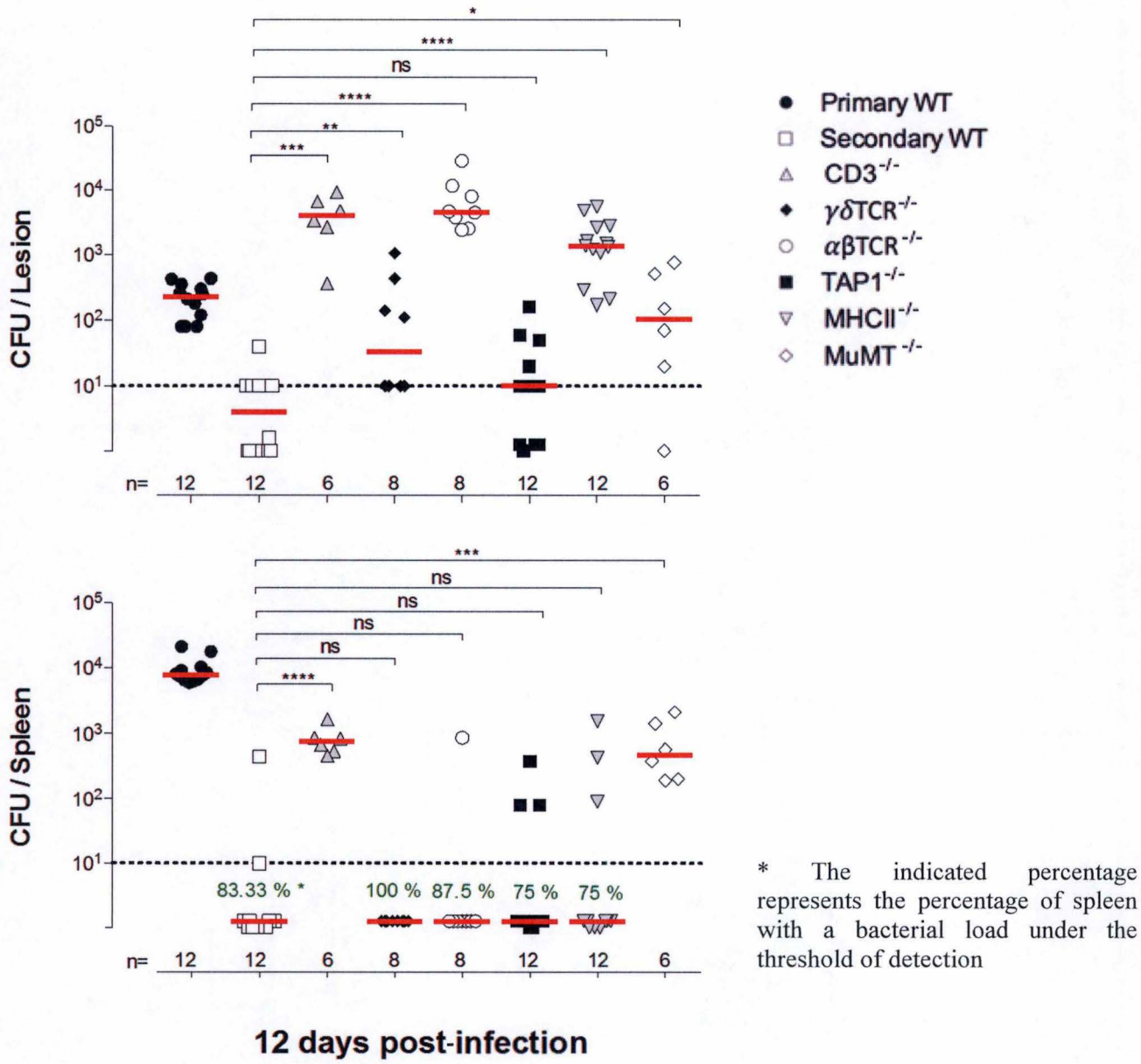
In order to characterize the memory lymphoid cells involved in the control of *Brucella* during a second infection, a similar experiment has been performed with WT mice and mice genetically deficient for CD3, γδTCR, αβTCR, TAP1, MHCII and MuMT. All groups of mice have received the same treatment. As previously, a group of primary infected WT mice has been used as an internal control. On the **figure 42**, only the immunized footpad[14] are shown. As expected, immunized WT mice control the infection better than primary infected WT. At the lesion level, immunized $MuMT^{-/-}$, $CD3^{-/-}$, $\alpha\beta TCR^{-/-}$ and $MHCII^{-/-}$ mice, but not $TAP1^{-/-}$ and $\gamma\delta TCR^{-/-}$ mice, display reduced ability to control infection when compared to immunized WT mice. These results suggest that protective immunity at lesion is mainly dependent of $CD4^+$ T cells and B cells. In striking contrast, in the spleen, all deficient mice at the exception of $CD3^{-/-}$ and $MuMT^{-/-}$ mice appear able to control secondary infection like WT mice, suggesting that T cells and B cells are indispensable to control secondary infection but that $\gamma\delta TCR^+$ T cells and $\alpha\beta TCR^+$ T cells have an equal ability to control infection.

Because we know that following an IP infection (but not after IN infection), circulating antibodies play a key role in the control of secondary *Brucella* infection, ELISA tests have been performed on sera from ID infected WT, $\alpha\beta TCR^{-/-}$, $CD3^{-/-}$ and $MHCII^{-/-}$ mice at 67 days post-infection (just before the challenge[15]) to detect the presence of *Brucella* specific antibodies (**figure 43**).

---

[14] Have undergone two injections.

[15] As a reminder, the protective immune memory can be evaluated via a second infection, called the challenge.



* The indicated percentage represents the percentage of spleen with a bacterial load under the threshold of detection

Figure 42: Comparison of protective immunity in C57BL/6 WT and deficient mice immunized previously with live *B. melitensis*

An infectious dose of $2x10^6$ *B. melitensis* 16M/mL for intra-dermal infection was used in this experiment. Approximately 20 µL of this suspension have been injected in the right footpad WT and deficient C57BL/6 mice. All mice were treated with antibiotics as described in the Materials and Methods and then challenged with an infectious dose ($2x10^6$ bacteria/mL) of *mCherry-Brucella melitensis* 16M at both footpads. Mice have been sacrificed for lesion and spleen harvesting at 12 days post-infection. The organs have been plated on 2 YT agar medium to assess the bacterial load (CFU) as described in Materials and Methods. The primary WT mice have received only the first injection.
Significant differences are denoted by asterisks. * $p < 0.05$, ** $p < 0.01$, *** $p < 0.001$, **** $p < 0,0001$. These results are representative of two independent experiments.
n (number of organ), ns (non significant), red bar: median, dotted line: threshold of detection of bacteria, green percentage: percentage of spleen having no bacteria detected.

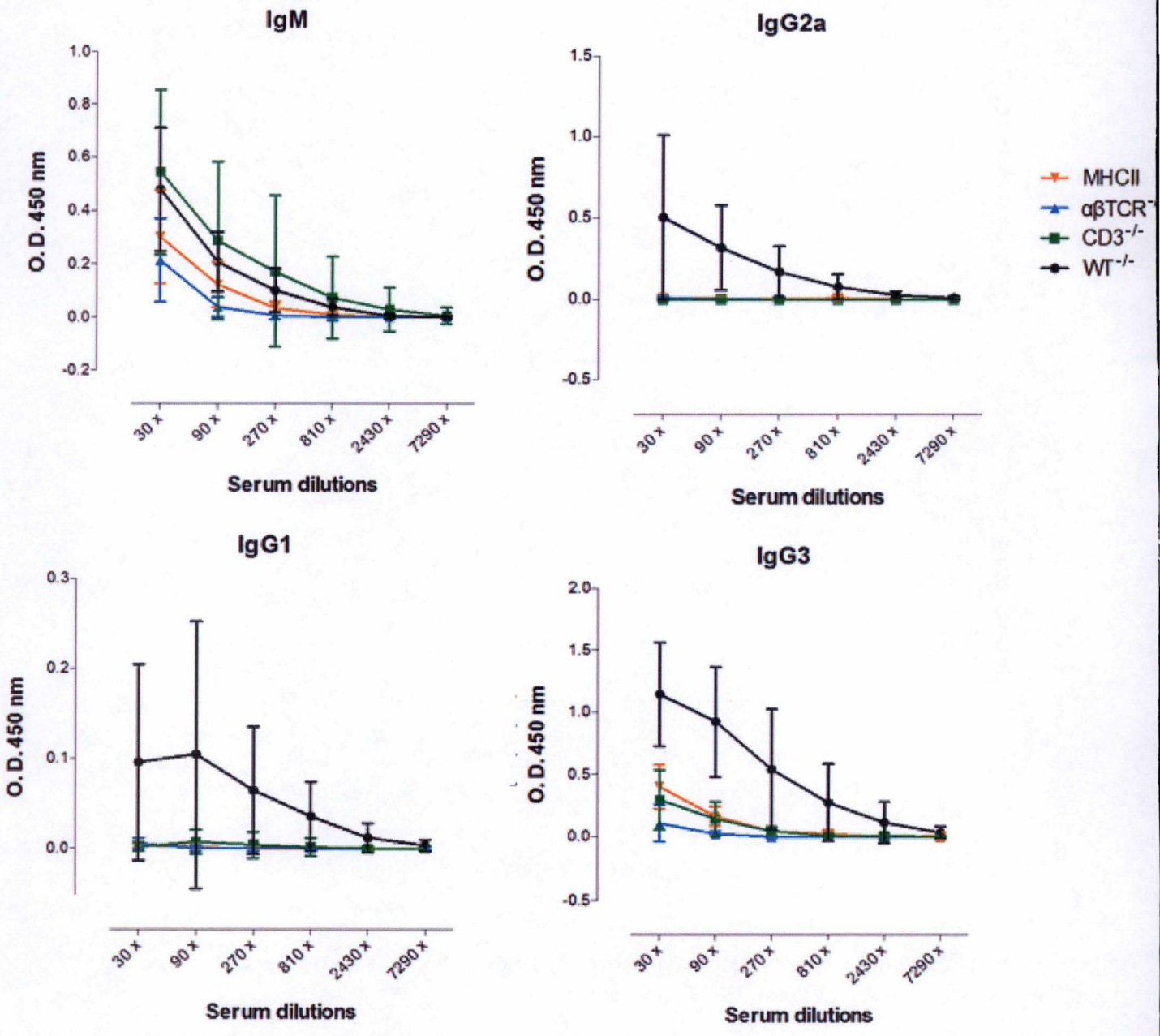


Figure 43: ELISA test on serum of C57BL/6 WT and deficient mice before the challenge

An infectious dose of $2x10^6$ *B. melitensis*/mL for intra-dermal infection was used in this experiment. Approximately 20 µL of this suspension have been injected in the footpad of WT and CD3-, αβTCR-, MHCII-deficient C57BL/6 mice. Six mice of each group have been used. Three days before the challenge, sera have been collected and ELISA have been performed to detect isotype distribution of *Brucella*-specific antibodies. The data represent the O.D. (optical density) in function of serial dilutions for the indicated antibody (IgM, IgG1, IgG2a,IgG3).

Each group of mice has been tested for the presence of IgM, IgG1, IgG2a and IgG3. The optical density is represented in function of serum dilutions. We observed that all mice deficient for T cells (CD3, αβTCR or MHCII) display a strong reduction of IgG2a and IgG1 titer. Concerning IgM and IgG3, these isotypes seem still present in mice deficient for CD3, αβTCR and MHCII, but in reduced amount compared to WT mice.

Discussion

DISCUSSION

In order to mimic the natural *Brucella* infection by direct contact between a skin lesion and infected tissue or fluid, we have developed an intra-dermal infectious model in C57BL/6 mice. We have analyzed the footpad - the primary skin lesion where *B. melitensis* is injected -, the popliteal draining lymph node, and finally the spleen. In this model, mice are infected with around 20 µL of a suspension containing $2x10^6$ bacteria/mL, equivalent to approximately $4x10^4$ CFU/mice. However, based on CFU detected at early time p.i. in lesion, the infectious dose seems closer to $5x10^3$ CFU/mice. This difference could be due to the drop that just comes out after the infection, the direct entry of some bacteria in the blood, or due to the fact that all bacteria are not released after the grinding of the lesion. The main objectives of this master thesis were (i) the characterization of the course of the intra-dermal (ID) infection in WT C57BL/6, (ii) the identification of the infected cells in the lesion and in the draining lymph node, (iii) the identification of the immune response after intra-dermal infection and (iv) the identification of cells involved in the control of *Brucella melitensis* after a primary and a secondary ID infection.

1 Characterization of WT C57BL/6 mice after intra-dermal infection

We have first tried to characterize the course of bacteria in wild type mice. After an ID infection in the footpad, the bacterial load between 2 hours and 72 days p.i. increases more than 1 log to finally reach a peak of around $5x10^4$ bacteria in the lesion. This result suggests a high rate of division of bacteria at early times p.i., which is not observed in pulmonary tissue after intra-nasal (IN) infection. Indeed, the bacterial load in lung between 2 hours and 72 hours p.i. reaches a plateau phase corresponding to the infectious dose. However, microscopy observations of infected lung showed that the number of bacteria by cell increases between 2 hours and 72 hours p.i.. That could suggest that a large fraction of infected cells controls the infection or are eliminated. This phenomenon leads to the conclusion that the lung develops an efficient immune response quite early after the infection. In the footpad lesion, the number of bacteria by cells between 2 and 72 hours p.i. increases and the growing number of CFU detected suggests that the skin presents a less efficient response in the early days of infection.

Previous studies have demonstrated that in the IP and IN models, the infected cells are mainly myeloid phagocytic cells. Indeed, after IP infection, the first infected cells in the spleen are likely the red pulp and marginal zone macrophages (R. Copin *et al.*, 2007). In the IN model, the alveolar macrophages are the main infected cells at 24 hours p.i. (Archambaux, 2010), but it could be possible that neutrophils are also infected later in the lung. In the footpad lesion, an important recruitment of neutrophils (detected by Ly-6G staining) is observable at 3 days p.i., and a weak frequency of infected cells display a Ly-6G-positive staining. Surprisingly, infected cells expressing the MHCII and CD11c markers are seldom observed, suggesting that infected cells are neither MHCII high expressing-myeloid cells ($MHCII^+$) nor dendritic cells ($CD11c^+$ $MHCII^+$). However, an explanation could be that *Brucella* is known to reduce the expression of MHCII (Barrionuevo P. *et al.*, 2007), preventing us to detect the MHCII- expressing macrophages with the MHCII marker. In the future, other makers could be used to identify the infected cells such as CD11b and F4/80 macrophage markers.

In the draining lymph nodes, due to the very low CFU level observed at 2 hours and 1 days, infected cells are only detectable from 3 days p.i.. These cells are rarely $Ly\text{-}6G^+$ but 50 % of infected cells appear to be $CD11c^+$ cells (dendritic cells) and 50 % $MHCII^+$ (MHCII expressing

cells), suggesting that the infected dendritic cells could migrate from lesion to draining lymph node and help to the dissemination of the bacteria. Other markers could be used as for the lesion, as the antibody specific of B cells such as B220/CD45R. Indeed, it has been shown that *Brucella* is able to infect these cells (R. Goenka *et al.*, 2012).

It is important to note that the counting of infected cells in lesion and draining lymph node is based on the overlap of mCherry signal expressed by bacteria and the cell surface marker. As our frozen tissue sections are 5 µm thick, it is possible that some bacteria are not really inside the cells, but just in overlapping with cells. In this case, the percentage of positive infected cells should be lowered. To be sure that bacteria are inside the cell, the visualization and the counting of infected cells of the stained lesions and draining lymph nodes must be confirmed by confocal microscopy analysis.

Preliminary histological and flow cytometric data show that monocytes are also already recruited at 3 and 7 days p.i. in the footpad lesion. These time points correspond to the start of the decrease of the bacterial load in the lesion and the decrease of the swelling of the footpad. Because we know that a population of monocyte is CCR2-positive (C-C chemokine receptor type 2) and that this cytokine allows the infiltration of monocytes from bone marrow to blood (C. Shi and E.G. Pamer, 2011), we have compared the ability of WT and $CCR2^{-/-}$ mice to control ID *Brucella* infection. In absence of CCR2, the recruitment of monocytes and the decrease of bacterial load give a delayed pattern compared to the WT mice, confirming the role of CCR2 in the recruitment of monocytes and suggesting a direct role of monocytes in the control of bacteria.

Following ID infection, *Brucella* is already detected in the spleen at 2 hours p.i., suggesting a rapid dissemination of bacteria via the blood. We know from previous works that *Brucella* is present in the blood after an IP (M.-A. Vitry *et al.*, 2014) but not after an IN infection, in which bacteria invade the spleen only 1 week p.i. (D. Hanot Mambres *et al.*, in reviewing). In order to confirm the presence of bacteria in blood, the bacterial load in the blood has been studied. As expected, we have detected *Brucella* in the blood after IP, but also after ID infection. CFU level is approximately 10-fold lower after an ID infection than through an IP infection. This difference of CFU could be due to the different dose received by mice. Indeed, $4x10^4$ bacteria are injected in IP whereas about $5x10^3$ CFU are injected in ID (CFU in the lesion at 2 hours p.i.). The detection of bacteria in the blood after two hours p.i. could suggest a destruction of tissue due to the injection of 20 µL in the skin, as the increase of the thick of the dermis suggest it, and so a direct contact with blood.
In the intra-peritoneal mode of infection, it has been shown that *B. melitensis* invades the erythrocytes *in vivo* but do not replicate inside (M.-A. Vitry *et al.*, 2014), suggesting that it could be the same for the ID model, although other experiments need to be performed to confirm this issue. Finding *Brucella* in blood cells from 3 hours p.i. gives support to the idea of an intracellular protection, preventing therefore the antibodies to detect the bacteria.
We will discuss about the role of the antibodies hereafter.

2 Characterization of immune response following primary ID infection

Brucella is an intracellular pathogen. Classically, the response to fight this type of pathogen is dominated by IFN-γ-mediated T_H1 response. Study of the *Brucella* IP infectious model has confirmed this vision (R. Copin *et al.*, 2007). However, following IN infection, the lung has

been shown to control the bacterial population via both T_H1- and T_H17-mediated immune responses. In addition, $\gamma\delta TCR^+$ T cells seem to play an important role in the early control of bacterial growth in lung (D. Hanot Mambres *et al.*, in reviewing). To identify the sub-class of T helper controlling *Brucella* growth following ID infection, we have compared the course of infection in mice deficient for IFN-γR, the receptor of the main cytokine produced during a T_H1 response, and for IL-17RA, the receptor of IL-17A, an interleukin produced during a T_H17 response. Our results suggest that a deficiency in IFN-γR has a huge impact on the bacterial load present in lesion at 3, 7 and 14 days p.i., in the draining lymph node at 7 and 14 days p.i., and in the spleen at 7 days p.i.. On the contrary, the deficiency in IL-17RA does not seem to have a significant impact on the control of bacteria. This experiment must be reproduced to confirm that IL-17RA has indeed no impact to control bacteria. The images of the lesion at 14 days p.i. show the importance of IFN-γ. Indeed, IFN-γ could be a modulator of hematopoiesis, and without IFN-γ, the precursors could be differentiated into neutrophils and not into monocytes (MacNamara *et al.*, 2011). In agreement with this, in the lesion of IFN-$\gamma R^{-/-}$ mice, a recruitment of neutrophils was observed (A. Lison's master thesis), that could correlate with the necrosis observed at the lesion site. Collectively, these results suggest an important role of IFN-γ in the activation and recruitment of monocytes, confirming the data of A. Lison's master thesis.

We were also interested at identifying the signalling pathway leading to IFN-γ production. Possible pathways are via IL-27/STAT-1/T-bet or IL-12/STAT-4/T-bet, leading us to compare the course of infection in WT, STAT-$1^{-/-}$, T-$bet^{-/-}$ and IL-$12p35^{-/-}$ mice. Our results show a very important impact on CFU and survival when mice are deficient for STAT-1, suggesting that the production of the protecting-IFN-γ could be STAT-1-dependent. Concerning the T-bet pathway, several experiments suggest that it is not the main way leading to IFN-γ production. As far as IL-12p35 is concerned, the experiment has been made at a unique time point. We observed an increase of CFU of less than 1 log, but other experiments must be performed to improve our conclusions about the IL-12/STAT-4/T-bet pathway. Surprisingly, the production of IFN-γ could bypass T-bet. However, it could be possible that IFN-γ promoter is directly activated by STAT-1, without the implication of T-bet (Y. Sun *et al.*, 2010). This could explain why the STAT-1 deficiency is the only deficiency to have a huge impact on the bacterial load. Flow cytometric analysis must be performed on cells from deficient mice in order to confirm the involvement of each pathway on IFN-γ production.

3 Identification of lymphocyte cells critically involved in the control of primary and secondary *Brucella* infection

3.1 Primary immune response following ID infection

Primary response against *Brucella* has been analyzed in details by numerous research groups in IP model: the role of $CD4^+$ T cells appears indispensable to control infection, via the production of IFN-γ and thus the induction of iNOS production by the infected cells. $CD8^+$ T cells and B cells (M.-A. Vitry *et al.*, 2012) do not seem to play a crucial role to fight against *Brucella* in the spleen. Indeed, the deficient mice for TAP1 and MuMT present the same bacterial load than WT mice. $\gamma\delta TCR^{-/-}$ mice display an enhanced susceptibility at one week post-infection (JA. Skyberg *et al.*, 2011). In the IN model, the T_H17 response associated with $\gamma\delta TCR^+$ T cells seem to play an important role in the early control (5 days p.i.) of lung infection. Later, the control

of infection in lung, spleen and liver is mediated by T_H1 response, via $CD4^+$ T cells and the production of IFN-γ. As in the IP model, B cells do not seem indispensable to control IN infection.

In our ID infectious model, although $CD8^+$ T cells seem to help to the response in the lesion at 14 days p.i., $CD4^+$ T cells appear indispensable to control *Brucella* growth in footpad lesion and draining lymph node. In the spleen, $CD4^+$ T cells and $CD8^+$ T cells seem both able to compensate each other to control bacteria at later times p.i.. On the contrary, $\gamma\delta TCR^+$ T cells appear dispensable for the response against *Brucella*. Indeed, in the three organs, we observed a statistically significant difference of bacterial load between $CD3^{-/-}$ and $\alpha\beta TCR^{-/-}$ mice. This could suggest that another $CD3^+$ T lymphocyte population could be involved in the control of primary response when $\alpha\beta TCR^+$ T cells are not present. This population could be the $\gamma\delta TCR^+$ T cells. Skin constitutes a particular environment that is characterized by specialized cell populations such as Langerhans cells or dendritic epidermal T cells (DETC) expressing $\gamma\delta TCR^+$ on their surface (Sumaria N. *et al.*, 2011). In naive wild type mice, DETC are the major T cell populations present in the basal layer of epidermis and represent 50 % of dermal T cells. During *Staphylococcus aureus* infection, it has been shown that these cells secrete chemokines that allow neutrophils recruitment (MacLeod A. S. et Havran W; L, 2011) and cytokines such as IFN-γ or TNF-α (Vantourout P. and Hayday A., 2013). In *Leishmania major* cutaneous infectious model, an increase of 20-30 % of $\gamma\delta TCR^+$ T cells has been described during infection (Nylen *et al.*, 2012), suggesting an active role of this T cells subpopulation.
The fact that DETC population is found in mice, but not in humans or sheep/goat, can be a limitation of this model. Indeed, if a particular response against *Brucella* is mediated by DETC in mice, it will not be possible to extrapolate this response to goat and sheep cases. The study could be realized with the specific host but for practical and management reasons, mice stay the most used model.
In the primary infection, preliminary data suggest also that B cells do not play a role in the control of ID infection, despite the fact that *Brucella*-specific antibodies are detected in the blood of mice from 6 days p.i. (IgM) to 50 days p.i. (IgG).

3.2 Secondary immune response following ID infection

Concerning the secondary response in the IP model, both humoral and cellular immunities are indispensable. Indeed, $MuMT^{-/-}$ and CD4 T $cells^{-/-}$ mice do not develop a protective immune memory. After IN infection, the $CD3^{-/-}$ mice and the $\alpha\beta$ $TCR^{-/-}$ mice are not protected against secondary infection, suggesting that both $CD8^+$ and $CD4^+$ T cells established a memory immunity and compensate each other.
In the ID model, an interesting result is about the absence of significant difference between the control footpad from immunized mice and the immunized footpad from immunized mice. This result suggests that there is an absence of local control (peripheral memory) at the footpad. However, a significant difference (1 log) is observed between the CFU level detected in the lesion and draining lymph node from primary infected mice and in the lesion and draining lymph node from immunized mice, suggesting that these latter have indeed acquired a protective memory. Following challenge, the CFU in the spleen from immunized mice display a 4 log reduction when compared to control mice. Two hypotheses are possible: (i) bacteria are not present in the spleen because they are eliminated in blood by specific antibodies before getting in the spleen or (ii) the spleen displays a very active immunity and locally eliminates the bacteria during a second infection. To test these hypotheses, we could realize a flow cytometric analysis on spleen to try to detect IFN-γ production. Its detection could suggest

Mice	Intra-peritoneal	Intra-nasal	Intra-dermal
WT	R	R	R
$CD3^{-/-}$	/	S	S
$\gamma\delta TCR^{-/-}$	/	R	R
$\alpha\beta TCR^{-/-}$	/	S	R
$CD4^{-/-}$	S	R	R
$CD8^{-/-}$	/	R	R
$MuMT^{-/-}$	S	R	S

Table 6: WT and different deficient mice and their ability to control bacteria during a secondary infection in the IP, IN and ID models

Comparison of the different mice models of infection in their response to the secondary infection. In IP, CD4 T cells and B cells seem important, in the IN model, αβTCR T cells (CD4 and CD8 T cells) seem playing a role in the control of secondary infection and compensate each other. Finally, in the ID model, CD3 T cells (αβTCR and γδTCR) and B cells seem indispensable.
R (resistant), S (sensible), in green: cell populations playing a role in the secondary infection.

	Intra-peritoneal	Intra-nasal	Intra-dermal
Primary immune response	T_H1 (role of $CD4^+$ T cells with IL-12 and IFN-γ) B cells not involved	T_H17 (role of IL-17 and $\gamma\delta TCR^+$ - 5 days p.i.) and then T_H1 (role of $CD4^+$ T cells with IL-12 and IFN- γ) B cells not involved	In the lesion and the dLN: $CD4^+$ T cells. In the spleen: $\alpha\beta TCR^+$ T cells ($CD4^+$ and $CD8^+$ T cells) B cells not involved
Blood infection?	Yes, from 10 minutes	No detected	Yes, at least from 2 hours
Secondary immune response	$CD4^+$ T cells and B cells	$\alpha\beta TCR^+$ T cells ($CD4^+$ and $CD8^+$ T cells) Compensation of T_H1 and T_H17 responses	In the lesion: $CD4^+$ T cells and B cells In the spleen: $CD3^+$ T cells ($\gamma\delta TCR^+$ and $\alpha\beta TCR^+$ T cells); and B cells

Table 7: Comparison of intra-peritoneal, intra-nasal and intra-dermal models

Comparison of the primary immune response, infection of the blood and secondary immune response for the intra-peritoneal, intra-nasal and intra-dermal models.

an active response in the spleen during secondary infection.

Among lymphocytes deficient mice, only the $CD3^{-/-}$ and $MuMT^{-/-}$ mice appear unable to control the challenge in the spleen. These data suggest that all $\alpha\beta TCR^+$ ($CD4^+$ and $CD8^+$ T cells) and $\gamma\delta TCR^+$ memory cells play a redundant role and could compensate each other when a population is absent. The **table 6** summarizes the response of the three models of infection during a secondary response and demonstrates the importance of the infection route to study the memory response against *Brucella* infection.

It seems that antibodies play a crucial role in the models where bacteria invade massively the blood, as it is the case for the IP and ID models. In IN model, bacteria probably use the blood as an invasive road in small amounts and the cellular immunity is probably sufficient to fight bacteria. On the contrary, when bacteria pass rapidly in blood after IP and ID infection, the cellular immunity could be saturated and insufficient to control infection in absence of humoral immunity. We have analyzed by ELISA the sera from WT, $CD3^{-/-}$, $MHCII^{-/-}$ and $\alpha\beta TCR^{-/-}$ mice harvested just before the challenge to detect the presence of *Brucella*-specific antibodies. We observe that IgG1 and IgG2a isotypes are completely absent when mice are deficient for $CD4^+$ $TCR\alpha\beta^+$ T cells. This result is no surprising since it is known that the production of these antibodies are mainly thymo-dependent. At the opposite, mice deficient for CD3, MHCII and $\alpha\beta TCR$ lose partially IgM and IgG3 isotypes, as expected by their production that is partially independent of T cells. These results suggest that the use of T cells deficient mice will lead to a partial deficiency for some antibodies which are produced in a T-dependent manner. That suggests that when mice do not control the infection, this may be due to T cells deficiency, but also due to the B cells deficiency.

All together, our data permits to conclude that both humoral and cellular immunities are required for the control of the secondary infection.

The **table 7** compares the intra-peritoneal and intra-nasal models, completed by the data that our results suggest after intra-dermal infection.

Conclusion and perspectives

CONCLUSION

In this master thesis, we have observed that following ID inoculation in the footpad of C57BL/6 mice, *B. melitensis* bacteria actively replicate in the dermis. At 72 hours p.i., the peak of swelling and of bacterial load is reached in the primary lesion. We are not able to identify the precise phenotype of the main infected cell populations in lesion. Indeed, only a weak fraction of infected cells seems to be neutrophils (Ly-6G$^+$), mature monocytes (MHC-II$^+$) or dendritic cells (CD11c$^+$ MHCII$^+$). In contrast, in the draining lymph node, 50 % of infected cells appear to be MHCII$^+$ CD11c$^+$ cells, suggesting that these cells could be dendritic cells.

The control of ID *Brucella* infection seems mainly dependent of the IFN-γ-mediated T_H1 response due to our observation that the deficiency of IFN-γR leads to uncontrolled bacterial growth and formation of necrotic lesion. IFN-γ appears to be produced in a STAT-1-dependent way but in a T-bet independent way. Indeed, only STAT-1 deficiency induces a phenotype similar to IFN-γR deficiency.

In the primary infection, as demonstrated by the comparison of mice deficient for lymphocytes subsets, CD4$^+$ T cells seem to be the main lymphocyte population involved in the control of *Brucella melitensis* in lesion and the draining lymph node. In the spleen, CD4$^+$ T cells and CD8$^+$ T cells could compensate each other to control the infection. Despite the detection of *Brucella* specific antibodies, B cells do not seem to play an indispensable role during the primary infection in lesion, draining lymph node and spleen. In striking contrast, in a secondary infection, B cells appear indispensable to control *Brucella* in the lesion and in the spleen. In this last organ, we observed that both αβTCR$^+$ T cells and γδTCR$^+$ T cells can able to eliminate *Brucella*.

PERSPECTIVES

Reproduction of the experiments performed once

The first perspectives should be to reproduce the experiments that we have been realized only one time, for example the ELISA tests or the stainings of dLN. Indeed, due to the low number of collected images, we cannot conclude that our countings are representative of all infected cells in popliteal lymph node. MuMT deficient mice must also be tested a second time.

Further analysis of the phenotype of infected cells with other cell specific markers

The staining with the F4/80 marker must be performed in lesion in order to verify if the infected cells are monocyte/macrophages with a weak expression of MHCII. In addition, an analysis with the confocal microscopy could allow to confirm that stained cells are really infected or if it is just an overlap between stained cells and *Brucella*. In the dLN, a staining for B cells could be tested.

Identification of the cellular source of IFN-γ

Other perspectives for our work include the investigation of specific sources of IFN-γ in skin and dLN by flow cytometric analysis and specific IFN-γ intracellular staining. Indeed, previous data from the A. Lison's master thesis suggest that Natural killers (NK) are the primary source of

IFN-γ secretion in dLN of wild type mice, this function being then taken over by T populations ($CD4^+$ T cells mainly). Identification of IFN-γ origin in skin would help us to unravel the role of T cells populations in the control of *Brucella* growth. Flow cytometric analysis would be completed by a fluorescent microscopic analysis of skin tissue in order to characterize the location and the phenotype of IFN-γ-producing T cells and infected cells.

Investigation about NO, an effector mechanism of T_H1 response

IFN-γ is well known to induce the iNOS enzyme that produces NO. This latter is known to be one of the main effector mechanism of the T_H1 response. It could be interesting to study the impact of the iNOS deficiency during ID *Brucella* infection.

Further investigation of the T cells populations involved in the control of *Brucella* infection

We found a significant difference in the CFU level between $CD3^{-/-}$ and $\alpha\beta TCR^{-/-}$ mice after a primary infection in three organs, suggesting that $\gamma\delta TCR^+$ T cells could cooperate with $\alpha\beta TCR^+$ T cells to control bacterial growth. After a second infection, $\alpha\beta TCR^+$ T cells and $\gamma\delta TCR^+$ T cells could also to compensate each other. In order to test these hypotheses, we plan to develop double deficient mice for both $\alpha\beta TCR^+$ and $\gamma\delta TCR^+$ T cells by breeding and to subsequently test whether these mice display a susceptibility similar to $CD3^{-/-}$ mice in the first infection and to observe if these double deficient mice are susceptible during the secondary infection. If it is the case, that would confirm the compensations between both populations during the secondary infection.

Development of other cutaneous mice model?

The last perspective could be the development of a model of infection in the ear of mice. The goal would be to induce a slight wound in the skin of the outer ear, and drop off a "drop" containing *Brucella melitensis*. This model could have several advantages such as the mode of infection that would be more physiological. Indeed, the deposition of a drop on a skin lesion would allow to understand how *Brucella* spreads and enters in the body. In our current model, the dissemination is distorted by the injection with a needle. Then, because the skin of the outer ear is very thin, we could follow in real time the cell cycle of the bacteria (cell multiplication and infection) and local cellular recruitment of immune cells by placing the anesthetized infected mice under a fluorescent inverted microscope. This technique is called "Intra-vital" microscopy and has been applied with success to the study of several experimental models of infection. In addition, this model has ethical benefits because the outer skin of the ear can be studied without discomfort to the animal and it will not be necessary to euthanize animals.

Materials and methods

MATERIALS AND METHODS

1 Materials

1.1 Bacterial strain

The strain of *Brucella* used in our experiment is *Brucella melitensis* 16 M (biotype 1, ATCC 23456). This smooth strain is naturally resistant to nalidixic acid (Nal^R). Based on this *B. melitensis* 16M strain, a genetically modified strain was engineered to constitutively express a red fluorescent protein (mCherry). This mCherry strain is used during *in vitro* and *in vivo* infections for visualization of the bacteria by fluorescence microscopy (R. Copin *et al.*, 2012). This second strain is both resistant to kanamycin (Kan^R) and to nalidixic acid (Nal^R). *B. melitensis* is stored at -80 °C in 30 % glycerol solution.

1.2 Mice of experiments

During our experiments, the mice used are wild type (WT) C57BL/6 mice and immune-deficient mice $^{(-/-)}$ for CD3, αβTCR, γδTCR, TAP1, MHCII, MuMT, IFN-γR, CCR2-, STAT-1, T-bet, IL-17RA and IL-12p35.

CD3$^{-/-}$ are mice devoid of all T lymphocytes;
αβTCR$^{-/-}$ are mice deficient for T cells with a T Cell Receptor (TCR) composed of an alpha and a beta chains (95 % of cases);
γδTCR$^{-/-}$ are mice deficient for T cells with a TCR composed of a gamma and delta chains (5 % of cases);
MHCII$^{-/-}$ are mice unable to present peptides and to select $CD4^+$ T cells differentiation, these mice are thus devoid of $CD4^+$ T cells;
TAP1$^{-/-}$ are mice unable to load peptides in the MHCI of antigen-presenting cells (APC) and to select $CD8^+$ T cells differentiation, these mice are thus devoid of $CD8^+$ T cells;
MuMT$^{-/-}$ are mice devoid of all B lymphocytes;
STAT-1$^{-/-}$ are mice deficient for STAT-1, activated by IL-27 to produce IFN-γ. These mice cannot produce IFN-γ by this pathway;
Il-12p35$^{-/-}$ are mice deficient for the IL-12p35 subunit of IL-12 cytokine and are thus unable to produce IFN-γ by the STAT-4 pathway;
T-bet$^{-/-}$ are mice deficient for T-bet, a transcription factor that controls the expression of IFN-γ. These mice are unable to produce IFN-γ by this pathway;
IFN-γR$^{-/-}$ are mice deficient for the receptor of IFN-γ present at the surface of infected cells and that is involved in the induction of effector mechanisms and the activation of monocytes. Mice deficient for this receptor are unable to induce effector mechanism such as iNOS to fight *Brucella*;
IL-17RA$^{-/-}$ are mice deficient for the receptor of IL-17, a cytokine released by a T_H17 response. These mice have thus a failure in the T_H17 response;
CCR2$^{-/-}$ are mice deficient for this receptor and attract monocytes with delay time.

Some of deficient mice have been tested by flow cytometry (see Appendix).

1.3 Ethics statements

Mice are aged from 6 to 12 weeks at the time of infection. At least 8 mice per condition were used for statistical relevance. The breeding of these different mice is performed at the IBMM (Institut de Biologie et Médecine Moléculaires), which is a conventional animal facility attached to the ULB (Université Libre de Bruxelles). This breeding is in accordance with the ethic's rules of ULB and respects the European legislation (directive 86/609/EEC) and the Belgian law (Royal Decree on the Protection of Experimental Animals of 6th April 2010). The complete protocol has been approved by the Animal Welfare Committee of the University of Namur (Belgium).

1.4 Medium, products and solutions

1.4.1 2 YT agar: a rich medium for *Brucella* growth

Composition	Concentration
Liquid LB Mix[15]	20 g/L
Yeast Extract	5 g/L
Casein hydrolyzate (peptone)	6 g/L
Agar (for solid medium only)	1 g/L

These powders are mixed in a stock from which 44 g are taken to be dissolved in 1 L of bi-distilled water to prepare the 2 YT agar medium. The medium is sterilized by autoclave (20 minutes at 121 °C) before using.
Kanamycin can be added to the medium to prevent contaminations.

1.4.2 PBS X10 (Phosphate Buffer Saline)

Composition	Concentration
NaCl	80 g/L
KCl	2 g/L
Na_2HPO_4	11.5 g/L
KH_2PO_4	2.4 g/L

These components are dissolved in bi-distillated water under agitation. Adjust the pH to 7-7.4 and store at room temperature (RT).

1.4.3 PBS-Triton-X100: solution to lyse cells

Composition	Quantity
PBS X1	500 mL
Triton-X100	500 µL

Watch out for the viscosity of the Triton. This solution is used to lyse cells in order to have access to their content. It is notably used to evaluate the bacterial load. This solution has to be autoclaved before using and store at RT.

[15] Liquid LB Mix is composed of peptone (10g/L), Yeast Extract (5g/L) and sodium chloride (5g/L)

1.4.4 FACS buffer

Composition	Quantity/Concentration
PBS X1	500 mL
BSA (Bovin Serum Albumin)	2 g/L (0.5 %)
NaN_3	0.2 g/L (0.02 %)

An agitation during 30 minutes allows a complete dissolution.
This solution must not be autoclaved.

1.4.5 Sucrose solution (20 %): used to dehydrate organs before freezing

Composition	Quantity
PBS 1X	100 mL
Sucrose (saccharose)	20 g

1.4.6 Blocking solution

Composition	Quantity
PBS 1X	50 mL
Blocking reagent	0.5 g

This solution is aimed to block the aspecific sites during the stainings for histology. Heat and stir thoroughly for complete dissolution, then adjust pH to 7-7.4. Conserved at 4 °C for maximum 10 days.

1.4.7 Paraformaldehyde (PFA - 4 %)

- Add 4 g of paraformaldehyde to 50 mL of bi-distilled H_2O, under agitation
- Heat the solution at 70 °C
- Add a few drops of NaOH (1 M) to facilitate the complete dissolution
- The solution is cooled on ice
- Add 10 mL of PBS 10X
- Adjust the pH of solution between 7-7.4
- Add water to a final volume of 100 mL
- The solution is filtrated through pores of 0.22 µM
- The solution is aliquoted in 15 mL-tubes (Falcon)
- Conserve the Falcon at -20 °C

The concentration of PFA depends on the experiment: 1 % to fix cells during a flow cytometric analysis, 2 % to fix organs before freezing in histology.

Be careful: PFA is a toxic compound and it is important to handle it under a chemical hood, with gloves and mask.

1.4.8 DNase/Collagenase

Composition	Quantity
RPMI	10 mL
DNase	100 µL
Collagenase	1 mL

The collagenase D is a powder and needs to be resuspended in RPMI. The volume of RPMI to add is calculated in function of enzymatic activity (noted on the bottle). The solution is filtered and aliquoted in 1 mL-Eppendorfs and conserved at -20 °C.

$$\boxed{(\text{Act.} \times 750\ \text{mL} \times 500\ \text{mg}) / 4000\ \text{mg} = \text{volume (mL)}}$$

The DNase is also in the state of a powder and is resuspended in NaCl (0.15 M) to reach a final solution of 10 mg/mL. The solution is aliquoted in 1 mL-Eppendorfs and conserved at - 20 °C.

1.4.9 Products references

Product	Use	Firm	References
Mix LB liquid	Culture medium (see above)	Luria Bertani	22700-041
DNase I	DNA degradation	Sigma	D45131VL
Collagenase	Collagen degradation	Roche Applied Science	11088866001
2.4G2	Fc receptor of rat anti-mouse	BD Pharmingen	553142
Permwash (saponin-based buffer)	Permeabilization of cell membranes	BD Biosciences	51-2091KZ
RPMI 1640	Medium	Life Technologies Laboratories	52400-025
Tissue-Tek OCT (Optimal Cutting Temperature)	Freezing medium	Sakura	1119300006
Blocking reagent	Block the aspecific sites during stainings	Boeringer	11096176001
Triton X100	Lyse cells	Sigma-Aldrich	UN3082
Fluoro-Gel medium	Cover-slides for histology	Electron microscopy Sciences	1785-10

2 Methods

2.1 *Brucella melitensis* strain streaking

- One week prior the infection of mice, the strain is taken from the stock solution conserved at - 80 °C and is streaked on 2 YT agar medium plate
- The plate is incubated at 37 °C for 5-6 days

2.2 Liquid culture

- Twenty hours before the infection, a liquid culture is prepared (10 mL of liquid 2 YT medium) from a 2 YT plate of *B. melitensis* to reach an optical density OD_{600nm} equal to 1 (= 3.10^9 bacteria/mL). At this absorbance, *Brucella* are at the end of the exponential growth phase
- A liquid medium will be the control (without bacteria)
- The liquid culture and the control are incubated overnight at 37 °C under agitation

2.3 Preparation of infectious dose

- The day of infection, measure the optical density $OD_{600\ nm}$. The liquid medium without bacteria is considered as the blank
- Wash 2 times the liquid culture with RPMI (10 mL): 10 minutes at 3,500 rpm, 4 °C
- After the second wash, add 10 mL of RPMI, resuspend and measure at $OD_{600\ nm}$
- The dilution factor is calculated to establish the desired infectious dose ($2x10^6$ bacteria/mL for intra-dermal infection). A $OD_{600\ nm}$ equal to 1 would correspond to $3x10^9$ bacteria/mL. The dilution factor and the amount of bacterial suspension to add to RPMI are calculated through the following equations:

$$(OD \times 3.10^9) / (\text{dose wanted/mL}) =$$
$$D\ Vtot / D = Vbs$$
$$Vtot = Vbs + VRPMI$$

D: dilution factor
Vtot: total volume
Vbs: volume of bacterial solution
VRPMI: Volume of RPMI

- A control of the infectious dose is realized by plating serial dilutions of the inoculum on 2 YT agar medium

2.4 Infection of mice

Mice are infected by injection of approximatively 20 µL of the prepared infectious dose ($2x10^6$ bacteria/mL) at the foodpad. The swelling confirms the injection of suspension.

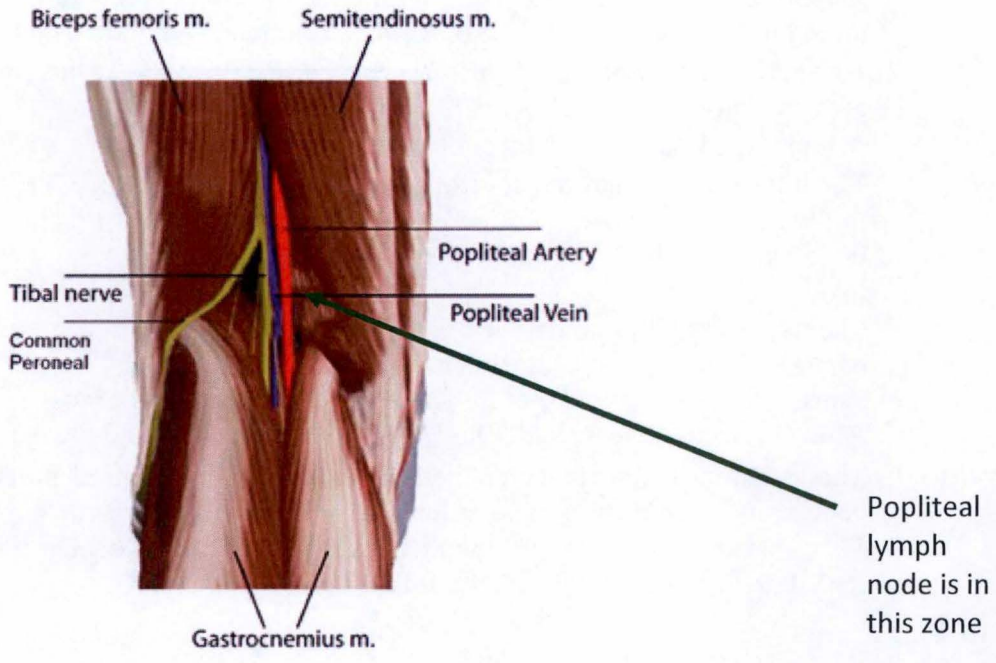


Figure 44: Location of the popliteal lymph node

The popliteal lymph node is found at the back of the lower limbs (in the knee gap). It is between the semi-membranous, biceps femoris and gastrocnemius muscles.

2.5 Euthanasia of mice and dissection

Mice are euthanized by cervical dislocation at different times post-infection;

- Before dissection, disinfect the tools used (scalpel, scissors and pliers of dissection) by alcohol 70 %
- Mice are immersed in alcohol 70 % for sterilization

Here, the organs harvested are: the lesion (the foodpad), the popliteal lymph node (draining lymph node) and the spleen.

- For the lesion, take the mouse by the foot
- With the scalpel, cut through the footpad (at the base), parallel to the footpad, and pull up the incision until the fingers
- The popliteal lymph node is placed at the back of the lower limbs (in the knee gap). It is between the semi-membranous, biceps femoris and gastrocnemius muscles (**figure 44**)
- Cut and separate the skin behind the knee and remove the ganglion using pliers
- Finally, to harvest the spleen, place the mouse on the right side, the spleen being on the left one. Cut the skin and the peritoneum with scissors and take the spleen with tweezers

These different organs can be used for:

- evaluation of the bacterial load in different organs by CFU (see below)
- flow cytometric analysis to analyze and characterize the immune cells populations
- immunofluorescence microscopy to characterize the infected cells and the recruitment of cells
- etc.

2.6 Evaluation of bacterial load (colony forming units)

2.6.1 Principle

The evaluation of the colony forming units (CFU) is aimed to determine the number of bacteria alive presents in an infected organ. This technique is based on the number of bacteria able to form a new colony at different times post-infection, in different organs.

2.6.2 Method

- The different organs (lesion, popliteal lymph node and spleen) are harvested (see 2.5)
- Place the different organs in a sterile plastic bag
- Grind the organs in the plastic bag (with the plug of a 50 mL-Falcon)
- Suspend and homogenize it in 1 mL of PBS/0.1 % Triton X100
- Serial dilutions are realized if necessary in RPMI to get a countable number
- Plate 100 µL of the suspension on 2 YT agar medium
- Incube the plate five days at 37 °C before counting the CFU

Marker	Canal	Dilution	Firm
DAPI	Alexa Fluo 355	1/1000	Sigma-Aldrich
Phalloidin	Alexa Fluor 488	1/100	Invitrogen
Anti-CD11c	Alexa Fluor 647 (APC)	1 /200	eBiosciences
Anti-MHCII	Alexa Fluor 647 (APC)	1/200	eBiosciences
GR1 (anti-Ly-6G)	Alexa Fluor 647 (APC)	1/200	eBiosciences

Table 8: Table of markers and their characteristics

Table of the different markers used during the immunohistofluorescence, their canal, the dilution used and the firm providing the specific marker.

2.7 Preparation of tissues for analysis by immunohistology

2.7.1 Principle

Immunohistology is a method used to visualize different markers of the tissues, or types of cells via stainings. The method is composed of 3 stages:

- Freezing
- Section realization
- Stainings

2.7.2 Method

FREEZING

- Take the different organs (see 2.5)
- Fix the organs in PFA 2 % during 2 hours at room temperature (RT)
- Wash 2 times with PBS 1X
- Incubate the organs in a solution of PBS-Sucrose 20 % overnight at 4 °C to dehydrate organs and thus avoid their bursting during freezing
- Place the organs in Tissue-Tek OCT cupules (Sakura), containing paraffin
- Freeze with liquid nitrogen

SECTIONS REALIZATION

- Remove the Tissue-Tek OCT of the organ
- Realized sections of 5 µM via the cryostat at – 20 °C
- Place the section on superfrost slides (3/slides)
- Conserve the slides at – 20 °C

STAININGS

- Rehydrate the organs in PBS 1X during 5 minutes
- Wipe the edges of the slide with a paper
- Block the non-specific sites with blocking reagent (PBS-BR 1 %, Boeringer)
- Incubate for 20 minutes
- Wash slides in PBS 1X to remove the excess of blocking reagent
- Wipe the edges of the slides with a paper
- Add the antibodies, diluted in blocking reagent (**Table 8**)
- Incube overnight at 4 °C
- Wash the slides in 3 different baths of PBS 1X to remove the excess of antibodies
- Place the cover-slides with the mounting medium called Fluoro-Gel
- Let it dry for 2 hours

The observation is optimal 3 or 4 days after the staining. The microscope is an inverted fluorescence microscope (Axiovert 200, Zeiss), provided with a high resolution monochrome camera (AxioCam HR, Zeiss).

2.8 Blood sampling

Blood is collected from mice with 75 µL-heparinized capillaries (Hirshmann – ref 9100275). A small piece of mice tail (less than 2 mm) is cut and the blood enters in the capillary by

capillarity. One capillary is collected and then plated on 2 YT agar medium containing kanamycin to count CFU present in blood (see 2.6 for CFU realization). Two capillaries are collected to realized ELISA test (see 2.9). For that, the serum is collected after centrifugation (10,000 rpm for 10 minutes) and then conserved at - 20 °C.

2.9 ELISA test

2.9.1 Principle

An ELISA test (enzyme-linked immunosorbent assay) is a test to identify a substance (usually an antigen) using antibodies and color modifications. The plates are coated with heat-killed (HK) *Brucellae melitensis* and the antigens present in the serum to test (the antibodies anti-*Brucellae*) can link these HK *Brucellae*. The antigens are revealed via an anti-isotype of these antigens. Here, the detection of IgM, IgG1, IgG2a and IgG3 has been tested with the following anti-isotype: anti-IgM (Sigma), LO-MG1-13 HRPO, LO-MG2a-9 HRPO[16], LO-MG3-13 HRPO (LO-IMEX).

2.9.2 Method

DAY 1: 96 wells NUNC 69620 plates coating:

- Add 50 µL/well of HK *Brucella melitensis* solution (concentration of 10^9 CFU/mL in PBS, to diluted to a final concentration of 10^7 CFU/mL)
- Shake delicately the plate to evacuate the air bubbles
- Incubate overnight at 4 °C with Parafilm recovering the plate

DAY 2: Saturation of non-specific sites, test ELISA and revelation:

- Flick the plate
- Add 200 µL/well of casein hydrolyzate diluted in PBS (3.65 g/100 mL) to block the non-specific sites
- Incube for 2 hours at RT
- Flick the plate
- Add 50 µL/well of serums to test and perform the following controls:
    - Positive test: IgG3 of *Brucella:* 12B12 (50 µL/well)
    - Negative tests: nothing and serum of naive mice, diluted 30X (50 µL/well)
  - ➢ Realize 6 serial dilutions (3 to 3) in casein hydrolyzate
  - ➢ Realize the dilutions in another plate with conical wells
  - ➢ Start the first dilution at 30X
  - ➢ Optional: add gentamycin (1/1000) if it exists a risk of contamination by *Brucella*
- Incubate for 2 hours with Parafilm and shake at 200 rpm at RT
- Wash the wells 4 times with PBS
- Add 50 µL/well of antibodies anti-tested serum (detection antibodies - for example: anti-IgG, anti IgG3, etc.), diluted in casein hydrolyzate
- Incubate 1 hour at RT with Parafilm and in darkness with shaking
- Flick and wash 4 times the plate with PBS
- Add 100 µL/well of TMB substrate mix[17] (2 solutions need to be mixed in a 50/50 ratio)

[16] C57BL/6 mice do not have IgG2a, but IgG2c. This antibody cross recognizes IgG2a and IgG2c.

[17] Let the Tetramethylbenzidine (TMB) reach room temperature before using it.

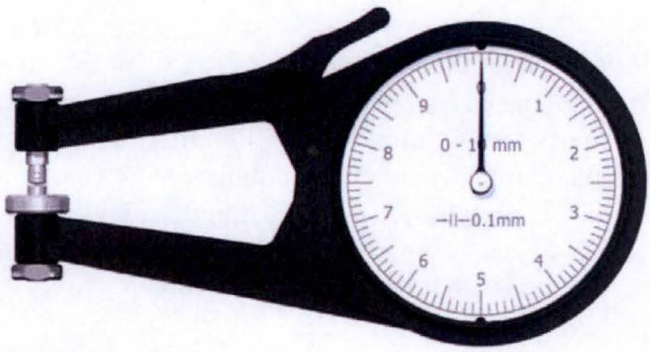


Figure 45: Picture of the « Vernier » tool

The Vernier is the tool used to measure thickness of the lesion to evaluate the swelling after infection of mice.

- Incubate the plate in the darkness during the revelation at RT for 15 minutes. A blue color should appear
- Stop the reaction by adding 50 µL/well of H_2SO_4 (2N). The blue staining should become yellow
- Read the absorbance of the plate at 450 nm (specific for TMB)

2.10 Mice immunization and challenge

A second infection of mice allows to study the memory response

- On day 0, infect mice as described above with *Brucella melitensis* 16M WT by ID with a dose of $2x10^6$ CFU/mL in RPMI as described in 2.3
- After 35 days, mice are treated with antibiotics (see 2.11) to clear the first infection
- After resting for an additional 3 weeks, mice are challenged by ID with the same dose of *B. melitensis* 16M-mCherry
- At selected times post-infection, mice were bled or sacrificed by cervical dislocation and CFU counting were realized

2.11 Antibiotic treatment

Antibiotic treatment was administered to control and infected mice for 15 days. The oral treatment is prepared daily and given in the drinking water. It is a combination of rifampycin (5 µL/mL) and streptomycin (3.75 mg/mL). An additional IP treatment was given to the more susceptible deficient mice. It consisted of four injections of streptomycin (300 mg/kg) at the same period than the oral treatment.

2.12 Measure of lesion size

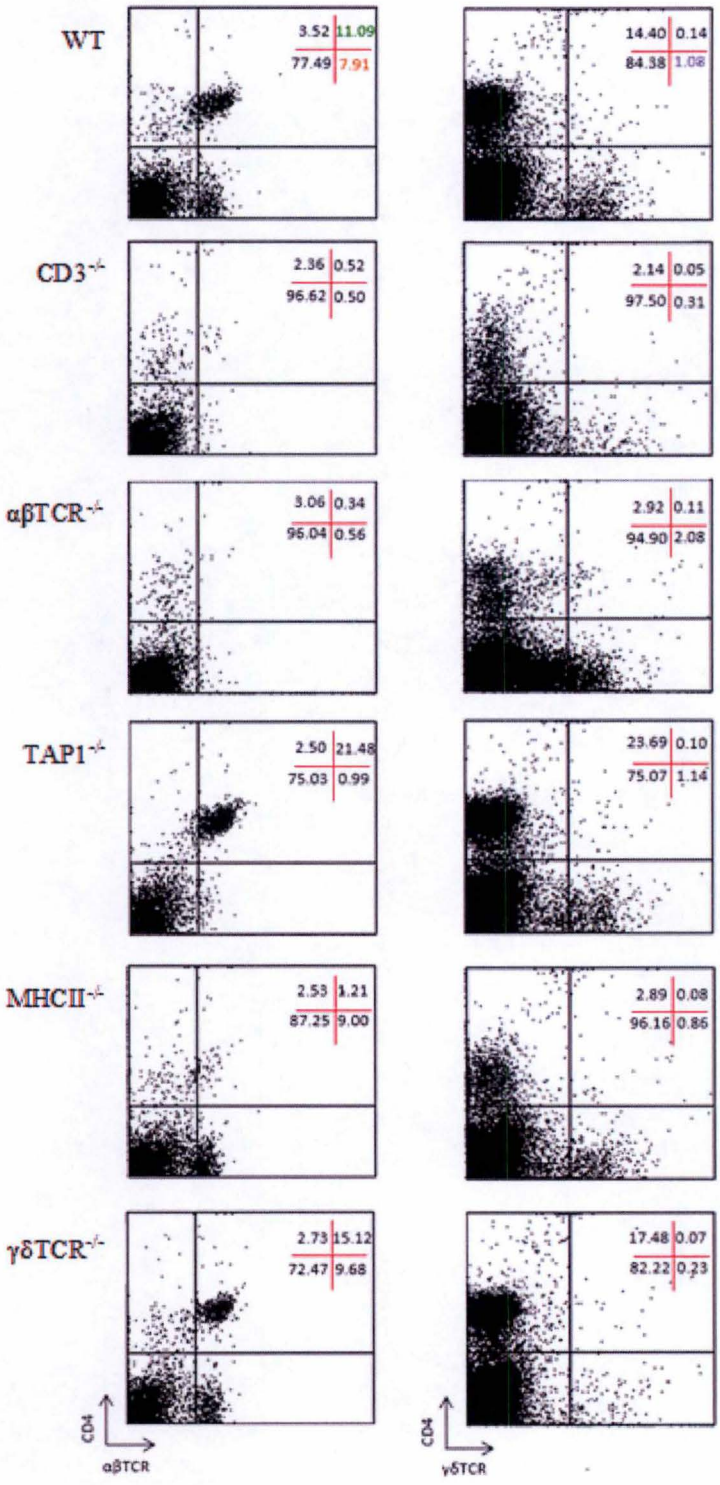
In some experiments, the size of the lesion at the footpad is measured to compare the swelling between a non-infected and an infected footpad, or between different deficient mice. The size of the lesion is measured via a tool called « Vernier » (**figure 45**). The footpad is set between two clamps, the spacing depending on the thickness of the footpad. This spacing will give us the measurement of the lesion.

2.13 Statistical analysis

The Wilcoxon-Mann-Whitney U test provided by the GraphPad Prism software is used to statistically analyze our results. Each group of knockout (KO) mice was compared to the wild type mice. Each group to each other is also compared when it is required and the results are noted by stars. Values of $p < 0.05$ are considered to represent a significant difference: * $p < 0.05$, ** $p < 0.01$, *** $p < 0.001$ and **** $p < 0.0001$, ns (non significant).

Appendix

APPENDIX


WT
3.52 11.09
77.49 7.91
14.40 0.14
84.38 1.08
CD3-/-
2.36 0.52
96.62 0.50
2.14 0.05
97.50 0.31
αβTCR-/-
3.06 0.34
96.04 0.56
2.92 0.11
94.90 2.08
TAP1-/-
2.50 21.48
75.03 0.99
23.69 0.10
75.07 1.14
MHCII-/-
2.53 1.21
87.25 9.00
2.89 0.08
96.16 0.86
γδTCR-/-
2.73 15.12
72.47 9.68
17.48 0.07
82.22 0.23
CD4
αβTCR
CD4
γδTCR

Flow cytometric analysis of splenic T cells populations of WT and deficient C57BL/6 mice

Spleen of naive WT and deficient ($CD3^{-/-}$, $\alpha\beta TCR^{-/-}$, $TAP1^{-/-}$, $MHCII^{-/-}$ and $\gamma\delta TCR^{-/-}$) C57BL/6 mice have been harvested and analyzed by flow cytometry.
Green, orange and purple correspond to $CD4^+$, $CD8^+$ and $\gamma\delta TCR^+$ T cells, respectively.
*The percentage of each quadrant is indicated in the top right corner.

Method: Flow cytometric analysis

After dissection of lesions, draining lymph nodes and spleen of mice, the organs are homogenized and incubated with Collagenase-D/DNAse (400 Mandl units/mL; 1 mL of Collagenase D and 1 mL of DNAse (Sigma-aldrich Chimie SARL, Lyon, France) in 8 mL of RPMI) at 37 °C and 5 % of CO_2 for 30 minutes. Then, cells are filtered (through pores of 72 µm), centrifugated and finally incubated with RPMI containing 2.4G2 (a rat anti-mouse Fc receptor; American Type Culture Collection) and rat serum for 20 minutes. After washing, cells are treated with a solution of FACS buffer (PBS with BSA 0.1 % containing the antibodies (Abs; 200 µL) for the staining. Two sets of different stainings are used in this case: either fluorescein isothiocyanate (FITC) anti-αβTCR (BD Biosciences) and allophycocyanin (APC) anti-CD4 (BD Biosciences) or phycoerythrin (PE) anti-γδTCR (BD Biosciences) and APC anti- CD4. Cells are fixed with paraformaldehyde 1 % (PFA) and finally treated with Permwach (BD Biosciences) to lyse erythrocytes. Cells are suspended in PFA and transferred into the specific tubes for the FACS. The apparatus used for the analysis is a "Calibur cytofluorometer".

Flow cytometric analysis of splenic T cells populations of WT and deficient C57BL/6 mice

Spleen of naive WT and deficient ($CD3^{-/-}$, $\alpha\beta TCR^{-/-}$, $TAP1^{-/-}$, $MHCII^{-/-}$ and $\gamma\delta TCR^{-/-}$) C57BL/6 mice have been harvested and analyzed by flow cytometry.
Green, orange and purple correspond to $CD4^+$, $CD8^+$ and $\gamma\delta TCR^+$ T cells, respectively.
*The percentage of each quadrant is indicated in the top right corner.

Method: Flow cytometric analysis

After dissection of lesions, draining lymph nodes and spleen of mice, the organs are homogenized and incubated with Collagenase-D/DNAse (400 Mandl units/mL; 1 mL of Collagenase D and 1 mL of DNAse (Sigma-aldrich Chimie SARL, Lyon, France) in 8 mL of RPMI) at 37 °C and 5 % of CO_2 for 30 minutes. Then, cells are filtered (through pores of 72 µm), centrifugated and finally incubated with RPMI containing 2.4G2 (a rat anti-mouse Fc receptor; American Type Culture Collection) and rat serum for 20 minutes. After washing, cells are treated with a solution of FACS buffer (PBS with BSA 0.1 % containing the antibodies (Abs; 200 µL) for the staining. Two sets of different stainings are used in this case: either fluorescein isothiocyanate (FITC) anti-αβTCR (BD Biosciences) and allophycocyanin (APC) anti-CD4 (BD Biosciences) or phycoerythrin (PE) anti-γδTCR (BD Biosciences) and APC anti- CD4. Cells are fixed with paraformaldehyde 1 % (PFA) and finally treated with Permwach (BD Biosciences) to lyse erythrocytes. Cells are suspended in PFA and transferred into the specific tubes for the FACS. The apparatus used for the analysis is a "Calibur cytofluorometer".

References

REFERENCES

Akcali C., Savas L., Baba M., Turunc T. Seckin (2007). Cutaneous manifestations in brucellosis: a prospective study. *Advences in Therapy*.

Akira, S., Uematsu, S., & Takeuchi, O. (2006). Pathogen recognition and innate immunity. *Cell*, *124*(4), 783–801.

Atluri, V. L., Xavier, M. N., de Jong, M. F., den Hartigh, A. B., & Tsolis, R. M. (2011). Species with Their Hosts. *Annual Review of Microbiology*, *65*(1), 523–541.

Archambaud C, Salcedo SP, Lelouard H, Devilard E, de Bovis B, Van Rooijen N, Gorvel JP, Malissen B. (2010) Contrasting roles of macrophages and dendritic cells in controlling initial pulmonary *Brucella* infection. *Eur J Immunol*. 2010 Dec;40(12):3458-71.

Ariza J., Servitje O., Pallarés R., Fernandez P., Rufi G., Peyri J., Gudiol F. (1989). *Arch Dermatol.* 125(3) :380-383.

Baldwin, C. L., & Parent, M. (2002). Fundamentals of host immune response against *Brucella abortus*: What the mouse model has revealed about control of infection. *Veterinary Microbiology*, *90*(1-4), 367–382.

Barnes, P. J. (2008). Immunology of asthma and chronic obstructive pulmonary disease. *Nature Reviews Immunology*, *8*(3), 183–192.

Barrionuevo, P., Cassataro, J., Delpino, M. V., Zwerdling, A., Pasquevich, K. a, García Samartino, C., … Giambartolomei, G. H. (2008). *Brucella abortus* inhibits major histocompatibility complex class II expression and antigen processing through interleukin-6 secretion via Toll-like receptor 2. *Infection and Immunity*, *76*(1), 250–62.

Batista, F. D., & Harwood, N. E. (2009). The who, how and where of antigen presentation to B cells. *Nature Reviews Immunology*, *9*(1), 15–27.

Behar SM., Porcelli SA. (2007). CD-1-restricted T cells in host defense to infectious diseases. *Curr. Top. Microbiol. Immunol.* 314 :215-50.

Biron, C. a. (2010). Expansion, maintenance, and memory in NK and T cells during viral infections: responding to pressures for defense and regulation. *PLoS Pathogens*, *6*(3), e1000816.

Bold TD., Ernst JD. (2008). Who benefits from granumomas, *Mycobacteria* or host? *Cell.* 136(1) :17-19.

Bottero, V., Withoff, S., & Verma, I. M. (2006). NF-kappaB and the regulation of hematopoiesis. *Cell Death and Differentiation*, *13*(5), 785–97.

Boyman, O., Létourneau, S., Krieg, C., & Sprent, J. (2009). Homeostatic proliferation and survival of naive and memory T cells. *European Journal of Immunology*, *39*(8), 2088–2094.

Brumell, J. H. (2012). *Brucella* "hitches a ride" with autophagy. *Cell Host and Microbe*, *11*(1), 2–4.

Capasso, L. (2002). Bacteria in Two-millennia-old Cheese, and Related Epizoonoses in Roman Populations. *Journal of Infection*, *45*(2), 122–127.

Celli, J. (2015). The changing nature of the *Brucella*-containing vacuole. *Cellular Microbiology*, *17*(7), 951–958.

Conde-Álvarez, R., Arce-Gorvel, V., Iriarte, M., Manček-Keber, M., Barquero-Calvo, E., Palacios-Chaves, L., … Gorvel, J.-P. (2012). The Lipopolysaccharide Core of *Brucella abortus* Acts as a Shield Against Innate Immunity Recognition. *PLoS Pathogens*, *8*(5), e1002675.

Copin, R., De Baetselier, P., Carlier, Y., Letesson, J.-J., & Muraille, E. (2007). MyD88-dependent activation of B220-CD11b+LY-6C+ dendritic cells during *Brucella melitensis* infection. *Journal of Immunology (Baltimore, Md.: 1950)*, *178*(8), 5182–5191.

Copin, R., Vitry, M. A., Hanot Mambres, D., Machelart, A., de Trez, C., Vanderwinden, J. M., … Muraille, E. (2012). In situ microscopy analysis reveals local innate immune response developed around *Brucella* infected cells in resistant and susceptible mice. *PLoS Pathogens*, *8*(3).

Corbel MJ. (1995). Brucellosis: an overview. *Maltese Medical Journal.* 7:7-8

Cutler, S. J., Whatmore, a. M., & Commander, N. J. (2005). Brucellosis - New aspects of an old disease. *Journal of Applied Microbiology*, *98*(6), 1270–1281.

D'Anastasio, R., Zipfel, B., Moggi-Cecchi, J., Stanyon, R., & Capasso, L. (2009). Possible brucellosis in an early hominin skeleton from sterkfontein, South Africa. *PloS One*, *4*(7), e6439.

De Figueiredo, P., Ficht, T. a., Rice-Ficht, A., Rossetti, C. a., & Adams, L. G. (2015). Pathogenesis and Immunobiology of Brucellosis. *The American Journal of Pathology*, *185*(6), 1–13.

Doganay, M., & Aygen, B. (2003). Human brucellosis: an overview. *International Journal of Infectious Diseases*, *7*(3), 173–182.

Eisenberg, T., Hamann, H.-P., Kaim, U., Schlez, K., Seeger, H., Schauerte, N., … Zschöck, M. (2012). Isolation of potentially novel *Brucella spp.* from frogs. *Applied and Environmental Microbiology*, *78*(10), 3753–5.

Ewalt, D. R., Payeur, J. B., Martin, B. M., Cummins, D. R., & Miller, W. G. (1994). Characteristics of a *Brucella* species from a bottlenose dolphin (Tursiops truncatus). *Journal of Veterinary Diagnostic Investigation*, *6*(4), 448–452.

Ficht TA., Kahl-McDonagh MM., Arenas-Galboa AL., Rice-Ficht AC. (2009). Brucellosis: the case for live, attenuated vaccines. *Vaccine*.

Forestier, C., Moreno, E., Pizarro-Cerda, J., & Gorvel, J. P. (1999). Lysosomal accumulation and recycling of lipopolysaccharide to the cell surface of murine macrophages, an *in vitro* and *in vivo* study. *Journal of Immunology (Baltimore, Md.: 1950)*, *162*(11), 6784–6791.

Galińska, E. M., & Zagórski, J. (2013). Brucellosis in humans--etiology, diagnostics, clinical forms. *Annals of Agricultural and Environmental Medicine: AAEM*, *20*(2), 233–8.

Gascoigne, N. R. J. (2008). Do T cells need endogenous peptides for activation? *Nature Reviews. Immunology*, *8*(11), 895–900.

Gawkrodger D., Arden-Jones M. (2012). Dermatology, an illustrated colour text. Fifthedition. *Churchill Livingstone Elsevier*. p.2-11.

Goenka, R., Guirnalda, P. D., Black, S. J., & Baldwin, C. L. (2012). B Lymphocytes provide an infection niche for intracellular bacterium *Brucella abortus*. *The Journal of Infectious Diseases*, *206*(1), 91–8.

Grillá, M. J., Blasco, J. M., Gorvel, J. P., Moriyán, I., & Moreno, E. (2012). What have we learned from brucellosis in the mouse model? *Veterinary Research*, *43*(1), 1–35.

Haake A. Scott G.A., Holbrook KA. (2000). The biology of the skin. Parthenon Publishing. p. 15-39.

Hanot Mambres, D., Machelart, A., Vanderwinden, J.-M., De Trez, C., Ryffel, B., Letesson, J.-J., & Muraille, E. (2015). In Situ Characterization of Splenic *Brucella melitensis.* Reservoir Cells during the Chronic Phase of Infection in Susceptible Mice. *Plos One*, *10*(9), e0137835.

Holling, T. M., Schooten, E., & Van Den Elsen, P. J. (2004). Function and regulation of MHC class II molecules in T-lymphocytes: Of mice and men. *Human Immunology*, *65*(4), 282–290.

Iannello, A., Debbeche, O., Samarani, S., & Ahmad, A. (2008). Antiviral NK cell responses in HIV infection: II. viral strategies for evasion and lessons for immunotherapy and vaccination. *Journal of Leukocyte Biology*, *84*(1), 27–49.

Janeway C., Travers P., Walport M., Shlomchik M. (2010). Immunobiology. 5th ed. p.3, p.21-23, p.174, p. 59-74, p. 210-215.

Jefferson, J. J., Leung, C. L., & Liem, R. K. H. (2004). Plakins- Goliaths That Link Cell Junctions and the Cytoskeleton, *5*(July), 542–553.

Kalia V., Sarkar D. Gourley TS, Rouse BT, Ahmed R. (2006). Differentiation of memory B and T cells. *Curr Opin Immunol*. Jun;18(3):255-64.

Kamiya, S., Owaki, T., Morishima, N., Fukai, F., Mizuguchi, J., & Yoshimoto, T. (2004). An indispensable role for STAT1 in IL-27-induced T-bet expression but not proliferation of naive $CD4^+$ T cells. *Journal of Immunology (Baltimore, Md.: 1950)*, *173*(6), 3871–3877.

Karaali Z., Baysal B., Porturogly S., Kendir M. (2011). Cutaneous manifestations in brucellosis. *Indian J. Dermatol.* 56(3) :339-340

Kittelberger, R., Hilbink, F., Hansen, M. F., Penrose, M., Lisle, G. W. De, Letesson, J., ... Schurig, G. (1995). and Yersinia enterocolitica 0 : 9 I Immunoblot analysis of the antibody response to *Brucella* protein antigens in bovine brucellosis. *Animal Research*, *47*, 257–270.

Klein, L., Hinterberger, M., Wirnsberger, G., & Kyewski, B. (2009). Antigen presentation in the thymus for positive selection and central tolerance induction. *Nature Reviews Immunology*, *9*(12), 833–844.

Ko, J., & Splitter, G. a. (2003). Molecular Host-Pathogen Interaction in Brucellosis: Current Understanding and Future Approaches to Vaccine Development for Mice and Humans Molecular Host-Pathogen Interaction in Brucellosis : Current Understanding and Future Approaches to Vaccine Develop, *16*(1), 65–78.

Kobayashi, K. S., & van den Elsen, P. J. (2012). NLRC5: a key regulator of MHC class I-dependent immune responses. *Nature Reviews. Immunology*, *12*(12), 813–20.

Kobayashi, Y. (2010). The regulatory role of nitric oxide in proinflammatory cytokine expression during the induction and resolution of inflammation. *Journal of Leukocyte Biology*, *88*(6), 1157–62.

Kono, H. & Rock, K. L. (2008). How dying cells alert the immune system to danger. *Nat Rev Immunol* 8, 279- 289.

Linden, S. K., Sutton, P., Karlsson, N. G., Korolik, V., & McGuckin, M. a. (2008). Mucins in the mucosal barrier to infection. *Mucosal Immunology*, *1*(3), 183–197.

Lison Aurore's master thesis (2015). Développement d'un modèle murin d'infection cutanée par *B. melitensis.*

McLay, J., Leonard, E., Petersen, S., Shapiro, D., Greenspan, N. S., Schreiber, J. R., & Igg, A. (2002). γ3 Gene-Disrupted Mice Selectively Deficient in the Dominant IgG Subclass Made to Bacterial Polysaccharides. II. Increased Susceptibility to Fatal Pneumococcal Sepsis Due to Absence of Anti-Polysaccharide IgG3 Is Corrected by Induction of Anti-Polysacchar. *The Journal of Immunology*, *168* (7), 3437–3443.

MacLeod, A. S., & Havran, W. L. (2011). Functions of skin-resident γδ T cells. *Cellular and Molecular Life Sciences*, *68*(14), 2399–2408.

MacNamara K.C., Oduro K., Martin O., Jones D.D., McLaughlin M., Kyunghee C., Borjesson D.L. Winslow G.M. (2011) Infectioon-induced myelopoiesis during intracellular bacterial infection is critically dependent on IFN-γ signaling., *The journal of immunology*, 2011, 186;1032-1043.

Mantur, B. G., Mangalgi, S. S., & Mulimani, M. (1996). *Brucella melitensis*, a sexually transmissible agent? *Lancet*, *347*(9017), 1763.

Matsuuchi, L., & Gold, M. R. (2001). New views of BCR structure and organization. *Current Opinion in Immunology*, *13*(3), 270–277.

Medical, H., & East, C. (2011). B 29, 1855, *. *Singapore Medical Journal*, *52*(3), 138–139.

Miller, L. S., & Modlin, R. L. (2007). Human Keratinocyte Toll-like Receptors Promote Distinct Immune Responses. *Journal of Investigative Dermatology*, *127*(2), 262–263.

Moreno, E., & Moriyó, I. (2006). The Genus *Brucella*.

Moser, M., & Leo, O. (2010). Key concepts in immunology. Vaccine, 28(SUPPL. 3), 2–13.

Murphy, E. a., Sathiyaseelan, J., Parent, M. a., Zou, B., & Baldwin, C. L. (2001). Interferon-γ is crucial for surviving a *Brucella abortus* infection in both resistant C57BL/6 and susceptible BALB/c mice. *Immunology*, *103*(4), 511–518.

Mutolo MJ., Jenny LL., Bszek AR., Fenton TW., Foran DR. (2012). Osteological and molecular identification of brucellosis in ancient Butrint, Albania. *Am. Journal of Physical Anthropology.*

Nestle, F. O., Di Meglio, P., Qin, J.-Z., & Nickoloff, B. J. (2009). Skin immune sentinels in health and disease. *Nature Reviews. Immunology*, *9*(10), 679–691.

Neta, A. V. C., Mol, J. P. S., Xavier, M. N., Paixão, T. a., Lage, A. P., & Santos, R. L. (2010). Pathogenesis of bovine brucellosis. *Veterinary Journal*, *184*(2), 146–155.

Nylén, S., & Eidsmo, L. (2012). Tissue damage and immunity in cutaneous leishmaniasis. *Parasite Immunology*, *34*(12), 551–561.

Oliveira, S. C., Soeurt, N., & Splitter, G. (2002). Molecular and cellular interactions between *Brucella abortus* antigens and host immune responses. *Vet Microbiol*, *90*(1-4), 417–424.

Pappas, G., Papadimitriou, P., Akritidis, N., Christou, L., & Tsianos, E. V. (2006). The new global map of human brucellosis. *The Lancet Infectious Diseases*, *6*(2), 91–99.

Pasparakis, M., Haase, I., & Nestle, F. O. (2014). Mechanisms regulating skin immunity and inflammation. *Nature Reviews Immunology*, *14*(5), 289–301.

Pierce, S. K., & Liu, W. (2010). The tipping points in the initiation of B cell signalling:how small changes make big differences. *Nature Reviews Immunology*, *10*(11), 767–777.

Roop, R. M., Bellaire, B. H., Valderas, M. W., & Cardelli, J. a. (2004). Adaptation of the *Brucellae* to their intracellular niche. *Molecular Microbiology*, *52*(3), 621–630.

Rubinstein, L. J., García-ojeda, P. a, Jennings, H. J., Stein, K. E., & Michon, F. (1998). Murine Immune Responses to Neisseria meningitidis Group C Capsular Polysaccharide and a Thymus-Dependent Toxoid Conjugate Vaccine Murine Immune Responses to Neisseria meningitidis Group C Capsular Polysaccharide and a Thymus-Dependent *Toxoid Conjugate Vac*, *66*(11), 5450–5456.

Salcedo, S. P., Marchesini, M. I., Degos, C., Terwagne, M., Von Bargen, K., Lepidi, H., ... Gorvel, J.-P. (2013). BtpB, a novel *Brucella* TIR-containing effector protein with immune modulatory functions. *Frontiers in Cellular and Infection Microbiology*, *3*(July),28.

Scholz, H. C., Nöckler, K., Llner, C. G., Bahn, P., Vergnaud, G., Tomaso, H., ... De, B. K. (2010). *Brucella inopinata* sp. nov., isolated from a breast implant infection. *International Journal of Systematic and Evolutionary Microbiology*, *60*(09), 801–808.

Schultz, K. T., & Grieder, F. (1987). Structure and function of the immune system. *Toxicologic Pathology*, *15*(3), 262–4.

Seleem, M. N., Boyle, S. M., & Sriranganathan, N. (2010). Brucellosis: A re-emerging zoonosis. *Veterinary Microbiology*, *140*(3-4), 392–398.

Shi, C., & Pamer, E. G. (2011). Monocyte recruitment during infection and inflammation. *Nature Reviews. Immunology*, *11*(11), 762–74.

Shortman, K., & Naik, S. H. (2007). Steady-state and inflammatory dendritic-cell development. *Nature Reviews. Immunology*, *7*(1), 19–30.

Skyberg, J. a, Thornburg, T., Rollins, M., Huarte, E., Jutila, M. a, & Pascual, D. W. (2011). Murine and bovine γδ T cells enhance innate immunity against *Brucella abortus* infections. *PloS One*, *6*(7), e21978.

Spang, a, Tub, T., Marschall, L. G., Joshi, H. C., Ahmad, F. J., Li, Q., ... Amos. (2000). The molecular basis of T helper 1 and T helper 2 cell differentiation. *Cell*, *10*(December), 542–550.

Starr, T., Ng, T. W., Wehrly, T. D., Knodler, L. a., & Celli, J. (2008). *Brucella* intracellular replication requires trafficking through the late endosomal/lysosomal compartment. *Traffic*, *9*(5), 678–694.

Sumaria, N., Roediger, B., Ng, L. G., Qin, J., Pinto, R., Cavanagh, L. L., ... Weninger, W. (2011). Cutaneous immunosurveillance by self-renewing dermal gamma/delta T cells. *The Journal of Experimental Medicine*, *208*(3), 505–518.

Sun, J. C., & Lanier, L. L. (2011). NK cell development, homeostasis and function: parallels with $CD8^+$ T cells. *Nature Reviews. Immunology*, *11*(10), 645–57.

Sun, Y., Wu, X.-X., Yin, Y., Gong, F.-Y., Shen, Y., Cai, T.-T., ... Xu, Q. (2010). Novel immunomodulatory properties of cirsilineol through selective inhibition of IFN-gamma signaling in a murine model of inflammatory bowel disease. *Biochemical Pharmacology*, *79*(2), 229–38.

Suraud, V., Jacques, I., Olivier, M., & Guilloteau, L. a. (2008). Acute infection by conjunctival route with *Brucella melitensis* induces IgG^+ cells and IFN-γ producing cells in peripheral and mucosal lymph nodes in sheep. *Microbes and Infection*, *10*(12-13), 1370–1378.

Swain, S. L., McKinstry, K. K., & Strutt, T. M. (2012). Expanding roles for $CD4^+$ T cells in immunity to viruses. *Nature Reviews Immunology*, *12*(2), 136–148.

Szabo, S. J., Kim, S. T., Costa, G. L., Zhang, X., Fathman, C. G., Glimcher, L. H., & Carolina, S. (2000). A Novel Transcription Factor, T-bet, Directs Th1 Lineage Commitment. *Cell*, *100*(1), 655–669.

Takeuchi, O., & Akira, S. (2010). Pattern Recognition Receptors and Inflammation. *Cell*, *140*(6), 805–820.

Terwagne, M., Ferooz, J., Rolán, H. G., Sun, Y., Atluri, V., Xavier, M. N., … Tsolis, R. M. (2014). Innate immune recongnition of flagellin limits systemic persistence of *Brucella*. *Cell Microbiol.* *15*(6), 942–960.

Trombetta, E. S. (2003). Activation of Lysosomal Function During Dendritic CellMaturation. *Science*, *299*(5611), 1400–1403.

Underhill, D. M., & Goodridge, H. S. (2012). Information processing during phagocytosis. *Nature Reviews Immunology*, *12*(7), 492–502.

Vantourout, P., & Hayday, A. (2013). Six-of-the-best: unique contributions of γδ T cells to immunology. *Nature Reviews. Immunology*, *13*(2), 88–100.

Vitry, M. A., Trez, C. De, Goriely, S., Dumoutier, L., Akira, S., Ryffel, B., … Muraille, E. (2012). Crucial role of gamma interferon-producing $CD4^+$ Th1 cells but dispensable function of $CD8^+$ T cell, B cell, Th2, and Th17 responses in the control of *Brucella melitensis* infection in mice. *Infection and Immunity*, *80*(12), 4271–4280.

Vitry, M.-A., Hanot Mambres, D., De Trez, C., Akira, S., Ryffel, B., Letesson, J.-J., & Muraille, E. (2014). Humoral Immunity and CD4+ Th1 Cells Are Both Necessary for a Fully Protective Immune Response upon Secondary Infection with *Brucella melitensis*. *Journal of Immunology (Baltimore, Md.: 1950)*, *192*(8), 3740–52.

Weynants, V., Walravens, K., Didembourg, C., Flanagan, P., Godfroid, J., & Letesson, J. J. (1998). Quantitative assessment by flow cytometry of T-lymphocytes producing antigen- specific γ-interferon in *Brucella* immune cattle. *Veterinary Immunology and Immunopathology*, *66*(3-4), 309–320.

Whatmore, A. M., Davison, N., Cloeckaert, A., Al Dahouk, S., Zygmunt, M. S., Brew, S. D., … Schlabritz-Loutsevitch, N. E. (2014). *Brucella papionis* sp. nov., isolated from baboons (*Papio spp.*). *International Journal of Systematic and Evolutionary Microbiology*, *64*(Pt 12), 4120–8.

Witherden, D. a, Ramirez, K., & Havran, W. L. (2014). Multiple receptor-ligand interactions direct tissue-resident γδ T cell activation. *Frontiers in Immunology*, *5*(November), 1–5.

Wucherpfennig, K. W., Gagnon, E., Call, M. J., Huseby, E. S., & Call, M. E. (2010). Structural biology of the T-cell receptor: insights into receptor assembly, ligand recognition, and initiation of signaling. *Cold Spring Harbor Perspectives in Biology*, *2*(4), 1–14.

Zhan, Y., & Cheers, C. (1993). Endogenous gamma interferon mediates resistance to *Brucella abortus* infection. *Infection and Immunity*, *61*(11), 4899–4901.